

THESIS FOR THE DEGREE OF DOCTOR OF PHILOSOPHY

in

MACHINE AND VEHICLE SYSTEMS

Head kinematics in car–pedestrian crashes

The influence of sliding, spine bending, elbow and shoulder impacts

RUTH PAAS



Division of Vehicle Safety

Department of Applied Mechanics

CHALMERS UNIVERSITY OF TECHNOLOGY

Gothenburg, Sweden, 2015

Head kinematics in car–pedestrian crashes
The influence of sliding, spine bending, elbow and shoulder impacts

RUTH PAAS
ISBN 978-91-7597-293-0

© RUTH PAAS, 2015

Doktorsavhandlingar vid Chalmers tekniska högskola
Ny serie nr 2015: 3974
ISSN: 0346-718X

Department of Applied Mechanics
Chalmers University of Technology
SE-412 96 Gothenburg
Sweden
Telephone +46 (0)31 7721000

Cover: Elbow impact in a car–pedestrian simulation (Chapter 4). Image: Ruth Paas

Printed by Chalmers Reproservice
Gothenburg, Sweden, 2015

HEAD KINEMATICS IN CAR-PEDESTRIAN CRASHES

THE INFLUENCE OF SLIDING, SPINE BENDING, ELBOW AND SHOULDER IMPACTS

RUTH PAAS

Division of Vehicle Safety, Department of Applied Mechanics
Chalmers University of Technology

Abstract

In vehicle-pedestrian crashes, head injuries account for an overwhelming percentage of all severe and fatal injuries. These injuries are caused by the linear acceleration and rotation of the head. To mitigate head injuries, tools such as Human Body Models (HBMs) are used in the development and evaluation of pedestrian safety systems. The tools need to be compared with experimental data to evaluate their biofidelity. Previous studies regarding full-scale pedestrian experiments with post-mortem human subjects (PMHSs) have mainly provided two-dimensional linear trajectories and injuries. Six-dimensional linear and angular whole-body kinematics from full-scale pedestrian experiments are scarce. Detailed data on the subject's anthropometry and initial body posture would increase the quality of simulations but are rarely published.

The main aim of this thesis is to quantify six-dimensional head translational and rotational kinematics in car-pedestrian crashes prior to head impact against the vehicle. This aim is pursued by means of PMHS testing and Finite Element (FE) simulations with the Total Human Model for Safety (THUMS) version 4.0. The PMHS data are generated to provide HBM evaluation data and to investigate how pedestrian anthropometry and minor differences in initial stance influence head and upper body kinematics in car-pedestrian crashes. Additional aims are to evaluate THUMS in pure shoulder impacts and on a full-scale level, and to provide full-scale experimental data and pragmatic HBM scaling methods to industry and academia.

Six-dimensional kinematics of the head, spine, pelvis and shoulders were quantified in five new full-scale pedestrian PMHS experiments with a small sedan. Varying anthropometry and minor variations in initial posture influenced pelvic sliding over the bonnet and ipsilateral upper arm responses, which in turn influenced head kinematics. THUMS was generally biofidelic although the arm abduction and the neck stiffness should be improved. In full-scale simulations, the best pragmatic scaling method was to use two scaling factors to adjust height and weight, and to translate THUMS to adjust pelvis height.

Overall, the findings in this thesis increase the knowledge on how pedestrian upper-body 6DOF kinematics influence head kinematics. They highlight the importance of elbow and shoulder impacts and will thereby contribute to increase the quality of testing and simulating. Adding new inspiration for novel pedestrian safety systems, this work will contribute to decreasing pedestrian fatalities and mitigating pedestrian injuries.

KEYWORDS: pedestrian, kinematics, head, shoulder, spine, PMHS, Human Body Model, THUMS

Acknowledgements

They say that a PhD candidate is ready to defend the thesis when she has dreamt twice about killing her supervisor. Johan, I'm sorry to say that over the years, I have killed you three times in my dreams. I am deeply, deeply grateful for all your moral and technical support that you never ceased to provide. Thank you for always pushing me close to but not over the edge, and for lifting me up when I was on the ground. And special thanks for all the joking around!

For all the additional support, I am very thankful to my other supervisors, Jonas Östh, Karin Brolin and Jikuang Yang. Thank you for the fruitful discussions and support along the way.

All support from the project partners in current and previous projects was much appreciated. Personally, but also as representatives of their companies and universities within our projects, I thank Bengt Pipkorn at Autoliv Research, Lotta Jakobsson at Volvo Car Corporation, Mats Lindkvist at Umeå University, and Peter Halldin at KTH Royal Institute of Technology.

Without the research team and lab staff at IFSTTAR Marseille, this thesis would not have been possible. Catherine Masson and Pierre-Jean Arnoux, I am very grateful that you invited me to participate in your experiments and for supporting me with the implementation of all my ideas.

To the UVa folks and JARI researchers, I am very thankful for all your support and great advice. The study visit at UVa was one of my highlights, thank you so much for inviting me.

Funding for this work has been provided by SAFER – Vehicle and Traffic Safety Centre at Chalmers, Sweden, and by VINNOVA – Swedish Governmental Agency for Innovation Systems through the *Fordonsstrategisk Forskning och Innovation* (FFI) – Vehicle and Traffic Safety research programme. Project partners were Autoliv Research AB, Volvo Car Corporation, KTH Royal Institute of Technology, and Umeå University.

My colleagues and friends at SAFER and at the divisions of Vehicle Safety and VEAS, thank you so much for providing such a wonderful atmosphere. It is a pleasure working with you!

Jóna och Isabelle, jag är så jätteglad att jag fick träffa och jobba ihop med er. Utan er hade det inte alls varit lika roligt! Tack så jättemycket för all stöd och råd, jag vet inte vad jag hade gjort utan er. Ruben, Giulio, Lisa och hela gänget, tack för roliga fikapauser, kväller och helger!

Ohne meine Familie und Freunde hätte ich es nie so weit geschafft. Tag und Nacht wart ihr immer für mich da, habt mit mir gelacht und geweint, euch für mich gefreut und meine Sorgen mit mir geteilt und in all den Jahren immer hinter mir gestanden. Ich bin euch unendlich dankbar für all eure Liebe und Unterstützung.

Göteborg, November 2015

Table of Contents

Acknowledgements.....	v
List of Appended Papers.....	viii
1 Introduction to Pedestrian Crashes.....	1
1.1 Epidemiology.....	1
1.2 Countermeasures	5
1.3 Kinematics	5
1.4 Head Injury Mechanisms and Injury Criteria.....	7
1.5 Biomechanical Tests	8
1.5.1 Full-scale Experiments.....	8
1.5.2 Shoulder Impact Experiments.....	11
1.6 Accident Data for Dummy and HBM Evaluation.....	12
1.7 Human Body Models and other Test Tools	12
1.7.1 The Total Human Model for Safety (THUMS).....	14
1.7.2 Positioning, Scaling and Morphing.....	14
1.8 Summary: Status of Pedestrian Safety.....	16
2 Aims	17
3 Summary Of Papers.....	18
3.1 Full-scale PMHS experiments	18
3.2 Elbow and Shoulder Impact Epidemiology.....	19
3.3 Shoulder impacts	19
3.4 Full-scale simulations	21
4 Addendum: Head injury criteria in full-scale THUMS and head impactor simulations	23
4.1 Introduction	23
4.2 Methods	23
4.2.1 Simulations	23
4.2.2 Data analysis.....	25
4.3 Results.....	26
4.4 Discussion.....	28
5 General Discussion	30
5.1 Methods and Analyses in the PMHS experiments	30
5.2 Experimental Data in HBM Evaluations	31
5.3 PMHS vs. Volunteers Data in HBM Evaluations	33
5.4 Prevalence of Elbow and Shoulder Impacts	33

5.5	Simulation Results.....	34
5.5.1	Shoulder Impact Simulations	35
5.5.2	Full-body Simulations.....	37
5.6	Implications for HBM Development and Physical Testing.....	38
5.7	Implications for Safety Systems	40
5.8	Contributions	41
6	Conclusions	42
7	Future Work	43
References		44
Appendix		54
Appendix A: Anatomy and Physiology	54	
Appendix A1: Shoulder Anatomy and Physiology	54	
Appendix A2: Spine Anatomy and Physiology.....	55	
Appendix B: Crash Test Dummies and Impactors	56	
Appendix C: Three-Dimensional Rotations.....	56	
Appendix D: Head Injury Criteria and their Injury Risk Curves	57	
Appendix D1: HIC	58	
Appendix D2: RIC.....	58	
Appendix D3: GAMBIT	59	
Appendix D4: HIP	59	
Appendix D5: BrIC.....	59	
Appendix D6: BITS and RVCI.....	60	
Appendix E: Additional Results from the Addendum	61	
Appendix F: Initial Neck Lateral Bending away from the Vehicle	62	

List of Appended Papers

Paper I

Paas R, Davidsson J, Masson C, Sander U, Brolin K, Yang JK (2012) *Pedestrian Shoulder and Spine Kinematics in Full-Scale PMHS Tests for Human Body Model Evaluation*, Proceedings of IRCOBI Conference, Dublin, Ireland, 730-750.

Division of work between authors: Paas and Davidsson developed the outline of this study. Masson conducted the new PMHS test with the help of Paas and Davidsson. Davidsson and Paas designed and assembled additional instrumentation and data recordings. Sander provided the accident data. Paas analysed and presented all data included in the paper. The paper was written by Paas with the help of Davidsson, and was reviewed by all authors.

Paper II

Paas R, Masson C, Davidsson J (2015) Head boundary conditions in pedestrian crashes with passenger cars: six-degrees-of-freedom post-mortem human subject responses, *International Journal of Crashworthiness*, 20:6, 547-559, DOI 10.1080/13588265.2015.1060731.

Division of work between authors: Paas developed the outline of this study with support from Davidsson. Masson conducted the PMHS tests with the help of Paas and Davidsson. Davidsson and Paas designed and assembled additional instrumentation and data recordings. Paas analysed and presented all data included in the paper. The paper was written by Paas and reviewed by all authors.

Paper III

Paas R, Davidsson J, Brolin K (2015) Head Kinematics and Shoulder Biomechanics in Shoulder Impacts Similar to Pedestrian Crashes—A THUMS Study, *Traffic Injury Prevention*, 16:5, 498-506, DOI: 10.1080/15389588.2014.968778.

Division of work between authors: Paas developed the outline of this study with support from Brolin and Davidsson. Paas re-analysed data from previous experiments and produced all simulation results. Brolin provided support with simulation questions. The paper was written by Paas and reviewed by all authors.

Paper IV

Paas R, Östh J, Davidsson J (2015) Which Pragmatic Finite Element Human Body Model Scaling Technique Can Most Accurately Predict Head Impact Conditions in Pedestrian–Car Crashes?, Proceedings of IRCOBI Conference, Lyon, France.

Division of work between authors: Paas made the outline of this study and conducted all simulations. The vehicle model used in this study was developed by Paas. Validation experiments for the vehicle model were carried out by Autoliv as well as by Chalmers students under the supervision of Davidsson. Paas analysed and presented all data included in the paper. The paper was written by Paas and reviewed by all authors.

Conference Presentations of the Included Work

Paas R, Davidsson J, Masson C, Sander U, Brolin K, Yang JK *Pedestrian Shoulder and Spine Kinematics in Full-Scale PMHS Tests for Human Body Model Evaluation*, IRCOBI Conference, Dublin, Ireland, 2012

Paas R, Östh J, Davidsson J *Which Pragmatic Finite Element Human Body Model Scaling Technique Can Most Accurately Predict Head Impact Conditions in Pedestrian–Car Crashes?* IRCOBI Conference, Lyon, France, 2015

Nomenclature

AIS	Abbreviated Injury Scale
Anthropometry	Individual or statistical measurements of the human body as a whole, or of parts of the human body, e.g., total height, total mass or body part dimensions. If used in a statistical context, anthropometry is subject to variations over time.
APROSYS	Advanced Protection Systems—a European Integrated Project within the 6th Framework program
Biofidelity	Human likeness
BLE	Bonnet leading edge as defined by EEVC 98
C1 – C7	Cervical vertebrae
CIREN database	Crash Injury Research Engineering Network database
CG	Centre of Gravity
DOF	Degrees of Freedom
EEVC	European Experimental Vehicles Committee
Euro-NCAP	European New Car Assessment Programme
FE	Finite Element
Full-scale	In this context, full-scale experiments or simulations refer to complete pedestrian tests or simulations where the whole human body is engaged as opposed to component tests
GIDAS database	German In-Depth Accident Study database
HBM	Human Body Model
HIC	Head Injury Criterion
In-crash phase	Time period between first contact and final resting position of the crash opponents
IRTAD	International Traffic Safety Data and Analysis Group
L1 - L5	Lumbar vertebrae
Mortality rate	Number of deaths in a particular population. Here: death risk for any given pedestrian casualty
NASS database	National Automotive Sampling System database
NHTSA	National Highway Traffic Safety Administration
PCDS database	Pedestrian Crash Data Study database
PMHS	Post Mortem Human Subject, human cadaver
Primary impact	Vehicle–pedestrian crash from first contact until the time of head impact
RTFs	Road traffic fatalities
Scuttle panel	The plastic part between the bonnet and the windscreens (cowl screen)
SD	Standard Deviation
Secondary impact	Pedestrian–ground impact from first contact until final resting position
T1 – T12	Thoracic vertebrae
TBI	Traumatic brain injury
Throw distance	Horizontal distance of the pedestrian CG between initial position immediately before impact and final position on the ground

THUMS	Total Human Model for Safety, developed by TOYOTA MOTOR CORPORATION in cooperation with Toyota Central R&D Labs Inc.
VRU	Vulnerable Road Users, here defined as pedestrians, cyclists and motorised two-wheelers
WAD	Wrap Around Distance, length measurement from the ground to the impact location of any specific body part on a vehicle, as defined by EEVC 98. WAD is mostly used for the head but can also be defined for other body parts.

In this thesis, unless specified otherwise, the term pedestrian is defined as in WHO (2013b), page 3: “*A pedestrian is any person who is travelling by walking for at least part of his or her journey. In addition to the ordinary form of walking, a pedestrian may be using various modifications and aids to walking such as wheelchairs, motorized scooters, walkers, canes, skateboards, and roller blades. The person may carry items of varying quantities, held in hands, strapped on the back, placed on the head, balanced on shoulders, or pushed/pulled along. A person is also considered a pedestrian when running, jogging, hiking, or when sitting or lying down in the roadway.*”

Anatomical directions

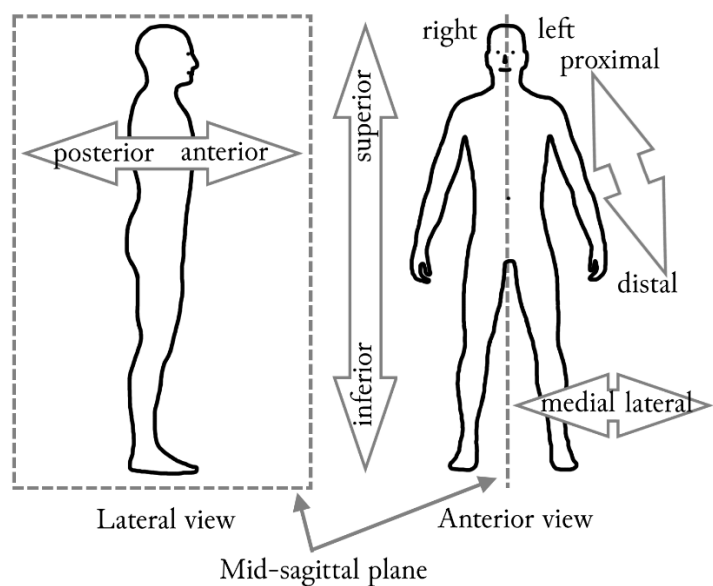


Figure 0.1: Anatomical terms of direction and mid-sagittal plane (modified from Wikimedia Commons 2014)

1

Introduction to Pedestrian Crashes

Pedestrians account for 22% of all road traffic fatalities world-wide with more than 270 000 fatalities each year (WHO 2013b). Between 1970 and 1993, the number of pedestrian fatalities generally decreased in high-income countries (OECD 1998). Although, today, pedestrian crashes are more frequent in low-income than in high-income countries (WHO 2013b), between 2009 and 2012 the number of pedestrian fatalities increased slightly in middle- and high-income countries (IRTAD 2014). A study by the National Highway Traffic Safety Administration (NHTSA) concluded that the fatality risk in pedestrian crashes has increased (Chang 2008). Considering the rising number of pedestrian fatalities and the increased fatality risk in these crashes, considerable effort is required to further reduce pedestrian fatalities and injuries.

To reduce road traffic fatalities and mitigate injuries resulting from road traffic crashes, the World Health Organization (WHO) has defined five pillars guiding road safety activities: *road safety management, safer roads and mobility, safer vehicles, safer road users and post-crash response* (WHO 2013a). Similarly, the Haddon Matrix (Haddon 1980) separates host, agent and environment factors in three time phases: pre-crash, in-crash and post-crash. In addition, not only each factor but also interactions between the various factors contribute to the injury outcome in a crash (WHO 2006). The pedestrian injury risk in the in-crash phase greatly depends on the host–agent (pedestrian–vehicle) and the host–environment interaction (pedestrian–ground). To analyse the complex vehicle–pedestrian interaction and further diminish pedestrian fatality and injury risk during the crash, a thorough understanding of real-life crashes, current countermeasures as well as pedestrian kinematics and injury mechanisms is required.

This chapter provides an overview over state-of-the-art research in pedestrian safety, focusing on the in-crash phase during pedestrian collisions with passenger cars. Pedestrian accident statistics show the most common crash scenarios and reveal that the most seriously injured body region is the head. Countermeasures currently on the market mitigate pedestrian injuries to a certain extent although these safety systems do not necessarily prevent all injury types. To explain this gap in safety technology and to explain the injury mechanisms and injury criteria, pedestrian kinematics during car–pedestrian impacts are analysed with a focus on the upper body and head. Data sources for investigating kinematics and injuries as well as for Human Body Model evaluation are presented, and tools to further study the biomechanics in car–pedestrian crashes are introduced.

1.1 Epidemiology

In the past, by analysing accident databases, numerous studies have been conducted to statistically investigate real-life pedestrian crashes. In-depth crash reconstructions are vital for the understanding of pedestrian biomechanics and injury patterns. When attempting to improve pedestrian safety through experiments or simulations, accident statistics aid in focussing on the relevant crash conditions in terms of e.g. vehicle speed and braking behaviour, pedestrian posture and pedestrian avoidance manoeuvres. The inclusion criteria for the populations in the statistics presented in this section are listed in Table 1.1.

The majority of pedestrians involved in crashes (71–79%) were standing upright and moving across the road (Maki et al. 2003a). Most pedestrians (65%) were walking when impacted while

20% were running (Hardy 2009). Walking speeds generally varied between 0.9 and 1.7 m/s (Simms and Wood 2009). The percentage of pedestrians struck laterally varied between 65% (Hardy 2009) and 89% (Simms and Wood 2009). Most pedestrians (60%) did not display any avoidance manoeuvre such as jumping or turning away (Jarrett and Saul 1998).

Table 1.1: Populations of pedestrians included in various studies. Simms and Wood (2009) does not appear in this list since they provide a review of other studies. (*) The number of pedestrians included in their statistics is unknown. (**) Abbreviated Injury Scale (AAAM 2005). (***) Severe Traumatic Brain Injury.

Reference	Complete study			Used for this section		
	n	Injury level	Age	n	Injury level	Age
Arregui-Dalmases et al. (2010)	10341	hospitalised	all		(complete data set)	
Badea-Romero and Lenard (2013)	273	AIS (**) 0+	all	70	head injury or impact	all
Fildes et al. (2004)	> 2100	AIS1+	all		(complete data set)	
Fredriksson et al. (2010)	1030	AIS1+	all	50	AIS3+	adult
Hardy (2009)	330974+	AIS0+	all	NA (*)	AIS0+	all
Harruff et al. (1998)	217	fatal	all		(complete data set)	
Jarrett and Saul (1998)	< 300	AIS0+	all		(complete data set)	
Lau et al. (1998)	369	fatal	all		(complete data set)	
Leijdesdorff et al. (2014)	154	sTBI (***)	all		(complete data set)	
Maki et al. (2003a)	4416	AIS1+	13+		(complete data set)	
Mizuno (2005)	1605	AIS0+	all	NA (*)	AIS2+	all
Otte (1999)	762	AIS1+	all		(complete data set)	
Rosén and Sander (2009)	490	AIS1+	15+		(complete data set)	
Yao et al. (2008)	120	AIS1+	all	77	AIS2+ head	all

The vehicles involved in pedestrian crashes were mainly (66–82%) passenger cars (Hardy 2009). Most pedestrians (60–77%) were struck by the vehicle front (Hardy 2009). Half of all pedestrian crashes occurred at vehicle speeds below 25 km/h (Simms and Wood 2009), 70% at 40 km/h or less (Otte 1999) and 90% below 50 km/h (Simms and Wood 2009). Injury severity generally increased with increasing vehicle speed (Rosén and Sander 2009). More specifically, above 40 km/h to 50 km/h, the injury severity increased rapidly with speed (Fildes et al. 2004, Rosén and Sander 2009, Simms and Wood 2009). Braking reduces impact speed from first contact to head impact and introduces braking pitch, thus changing the head impact location height on the car. Hardy (2009) found that one third of all drivers did not brake whilst 30% braked hard. Jarrett and Saul (1998) reported braking in 43% whereas they found no driver avoidance (no braking or steering) in 40% of their cases. In almost half of the cases in which the pedestrian was hit laterally the vehicle was in a straight line of motion (Jarrett and Saul 1998).

Head injuries are the main cause of death in pedestrian crashes (Lau et al. 1998, Hardy 2009). Non-fatal head injuries can cause long-term medical impairment (Olver et al. 1996). Figure 1.1 compares injury statistics from two pedestrian crash studies (Lau et al. 1998, Mizuno 2005).

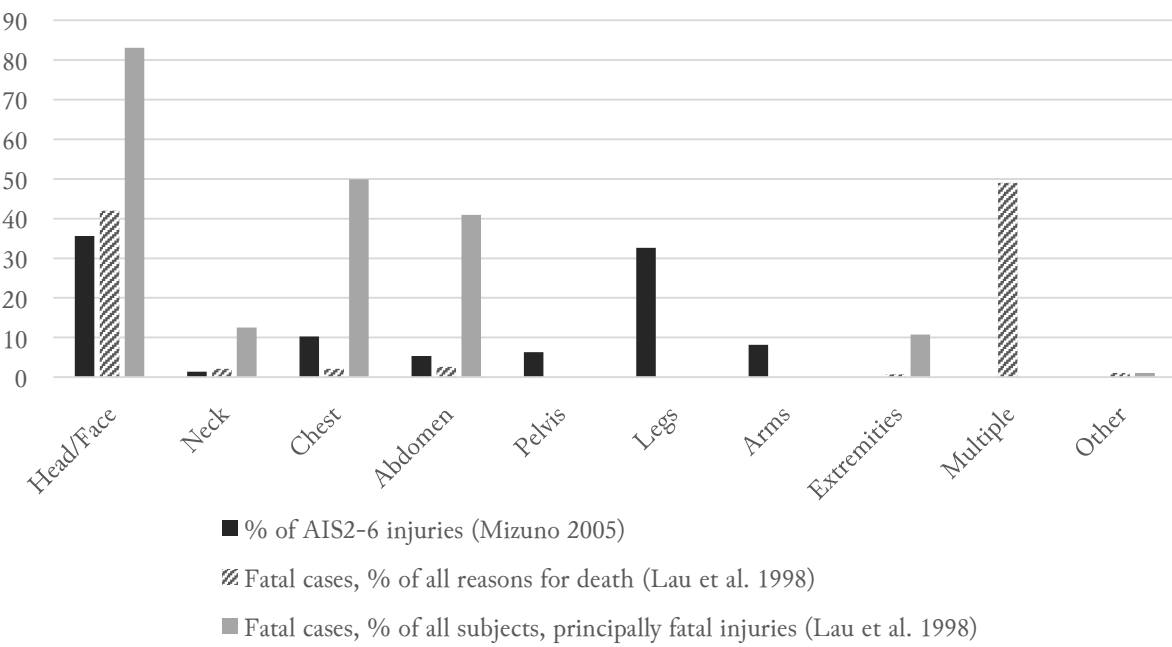


Figure 1.1: Injury frequency distribution per body region for different injury severities. The black and striped bar groups each add up to 100%. For the light grey bars, multiple nominations were possible for each injury that would have been fatal even if it had been the only injury sustained by a subject.

The black bars in Figure 1.1 show that, apart from minor injuries such as skin abrasions, defined on the Abbreviated Injury Scale (AIS) as 1 (AAAM 2005), the head and legs are the body parts most frequently injured in pedestrian crashes. The striped bars show which body part was affected in the main cause of death. It is important to note that *multiple injuries* are listed as an additional item in this group. Among the single body parts, head injuries are most likely to be the main cause of fatalities. In contrast, the legs account for a relatively large portion of all injuries (black bars), but represent only a low percentage of causes of death (striped bars). The light grey bars show how many of the deceased pedestrians had suffered a principally fatal injury in each body region, i.e., an injury that would likely have led to death even if it would have been the only injury sustained. Thus, the striped bars represent only one injury per subject as the main cause of death, whereas the light grey bars include every injury that would have led to death independent of any other injuries. While Figure 1.1 clearly shows that although head injuries are the major cause of pedestrian fatalities, chest and abdominal injuries must be also addressed as they are frequent among the fatally injured. In the chest, abdomen, neck and extremities, the principally fatal injuries (light grey) exceed the percent of injuries identified as responsible for a fatality (striped) by far. As an example, chest injuries were determined to be the primary cause of death in 2% of the cases while 50% of the fatally injured pedestrians sustained chest injuries that would have been principally fatal. This divergence can only be explained if most of the principally fatal chest injuries (light grey) are included in *multiple injuries* (striped). Principally fatal injuries in the chest, abdomen, neck and extremities thus appear to be most common when multiple injuries were determined to be the cause of death. Thus, head injuries still remain the main focus in pedestrian crashes although chest and abdominal injuries should also be considered in the future.

Among life-threatening head injuries in pedestrians, brain (intracranial) injuries are most common, followed by skull fractures (Harruff et al. 1998, Arregui-Dalmases et al. 2010,

Leijdesdorff et al. 2014). In 154 pedestrians with severe traumatic brain injury (sTBI, AIS 3+), 337 injuries were intracranial (89% cerebrum, 64% hemorrhage, 52% contusion, multiple injuries per pedestrian possible) and 149 were skull fractures (Leijdesdorff et al. 2014). In 217 fatally injured pedestrians, 228 intracranial injuries were observed of which 120 were cerebral contusions / lacerations, 42 were brainstem / midbrain contusions / lacerations and 66 were subdural haematomae, and 150 skull fractures (Harruff et al. 1998). While skull fractures occur due to linear acceleration of the head during direct impact, brain injuries occur due to linear or angular motion, or a combination thereof (Holbourn 1943, Hirsch and Ommaya 1970, Gennarelli et al. 1971, Gennarelli et al. 1972, Ono et al. 1980, Ommaya 1995). Whether head rotation in pedestrians without contact is excessive enough to cause brain injuries still remains to be established.

Several studies investigated the distribution of head-impact locations on the car (Figure 1.2). For adults, the windscreen area has been identified to be the most common site of head impact when a head–vehicle impact occurs (Mizuno 2005, Yao et al. 2008, Fredriksson et al. 2010, Badea-Romero and Lenard 2013). For children, the head most commonly impacts the bonnet (Yao et al. 2006). Excluding the bumper, bonnet leading edge (BLE) and bonnet, almost two thirds of AIS 3+ head injuries were caused by structural parts in the outer region of the windscreen (Fredriksson et al. 2010), indicating that it is not the windscreen itself, but the stiff parts in the windscreen region—such as the A-pillars and the dashboard—that are most hazardous to the head.

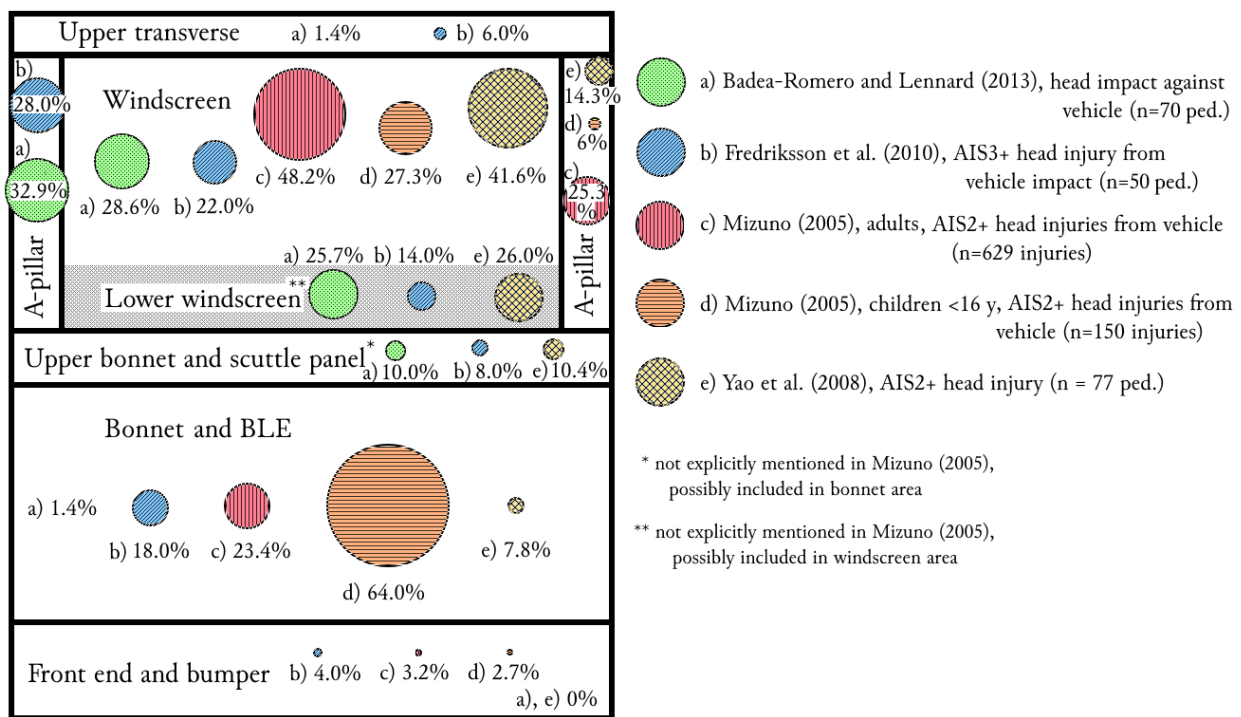


Figure 1.2: Distribution of head-impact locations on a standardised car front in various studies.

Based on the accident statistics reviewed in this section, a standard scenario can be established for car–pedestrian crashes: A pedestrian in an upright position is hit laterally by the mid-part of a passenger vehicle front while walking and without attempting avoidance, with car speeds generally being below 50 km/h. The review in this section also shows that head injuries are the most common life-threatening injuries in car–pedestrian crashes, and that brain injuries are more frequent than skull fractures. Stiff structures around the windscreen appear to be the most

beneficial areas for installing countermeasures which mitigate the consequences of a head–vehicle impact.

1.2 Countermeasures

To date, state-of-the-art pedestrian passive safety countermeasures available on the market include reduced stiffness of the bumper, BLE, bonnet, A-pillars and the upper windscreens frame (Schuster 2006, Longhitano 2009, Lindman et al. 2010). Increasing the space for deformation between bonnet and the components below such as the battery has increased pedestrian safety. Further increases of space for deformation and reduction of stiffness have been accomplished by introducing active bonnets that are raised automatically in case of a pedestrian impact, as well as air bags on the outside of the car, especially in the bonnet rear end and A-pillar regions (Paye 2002, Maki et al. 2003b, Jakobsson et al. 2013). All of these countermeasures aim at reducing vehicle stiffness and thereby mitigating direct impact injuries. In addition, vehicle front geometry has the potential to contribute to pedestrian safety by changing pedestrian kinematics in a way that reduces injury risk from a biomechanical perspective: Reducing the space between the lower vehicle front and the ground by lowering the front end or by adding structures such as a secondary bumper or an external airbag prevents the feet from being dragged underneath the car and reduces lateral knee loading (Pipkorn et al. 2007, Thollon et al. 2007). Lowering the BLE and smoothing its curvature reduces pelvic injuries by allowing the pelvis to slide over it (Kallieris and Schmidt 1988). Similar approaches for mitigating head injury risk, by e.g. reducing head rotation prior to head–vehicle impact, have not yet, to the best knowledge of the author, been developed.

Advances in active safety have enabled vehicles to detect pedestrians and brake autonomously, providing the potential to help avoiding pedestrian accidents or mitigate the consequences (Lindman et al. 2010). However, due to mechanical limitations in braking capabilities, limitations in pedestrian detection by sensors and limitations in prediction of pedestrian behaviour, active safety is not expected to be able to prevent all pedestrian accidents in the near future. Reducing pedestrian fatalities and injuries through passive safety is still necessary, and will continue to be an important contributor to pedestrian safety even in the future. Although statistics indicate that earlier pedestrian protection measures have already provided significant benefits—annual pedestrian fatalities in Europe have been reduced from about 13 000 to about 6 000 between 1980 and 2000 (Breen 2002)—pedestrian crashes remain a major health issue (WHO 2013a). Further reduction of fatalities and mitigation of injuries must be realized, especially since this decrease in the number of fatalities has recently levelled off (IRTAD 2014).

1.3 Kinematics

Typical pedestrian in-crash kinematics have been reported in many studies based on post-mortem human subjects (PMHS) and pedestrian dummy experiments, e.g., in Simms and Wood (2009). Since the kinematics are important for further reduction of injuries, a short summary of pedestrian PMHS kinematics is provided in this section. Typical kinematics are also shown in Figure 1.3.

In the standard scenario, the first contact between vehicle and pedestrian takes place between the bumper and the legs, the main source of leg injuries in crashes with passenger cars (Longhitano et al. 2005). In this phase, an initial rotation around the longitudinal axis of the pedestrian is

initiated. The direction and amount of this rotation depends mainly on whether the ipsilateral leg is forward or rearward as this determines the lever arm and the orientation of the pelvis prior to impact (Forman et al. 2015a).

Some milliseconds after vehicle–leg contact, the BLE impacts either the pelvic region (sedan type car), the upper leg (sports car or tall pedestrian) or the thorax (sport utility vehicle type car or child pedestrian), making the BLE another main source of leg injuries (Longhitano et al. 2005). Up to this impact, due to inertia the upper torso and head are usually still upright. As the vehicle continues its path and partly drags the pelvis with it, the torso begins to rotate towards the vehicle. The arms do not naturally follow this motion since inertia and gravity keep the upper arms vertical (Ishikawa et al. 1993). This sequence of events in some cases makes the car impact the pedestrian's elbow, upper arm and/or shoulder, e.g., if the upper body rotation around the longitudinal axis is small.

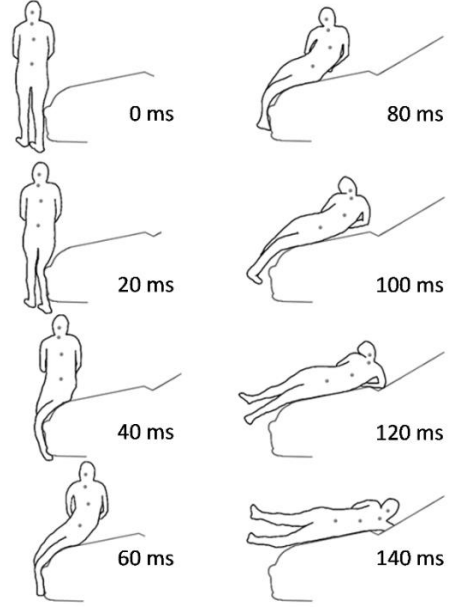


Figure 1.3: Typical pedestrian kinematics (adapted from Paas et al. 2012)

As with the upper arm, the head does not immediately follow the motion of the torso. While the torso falls down towards the car, inertia causes the head to lag behind this motion until the neck finally drags the head towards the car, followed by head impact against the vehicle. After the phase from first vehicle–pedestrian contact to head–vehicle contact (primary impact) follows either a flight phase, a phase of the pedestrian being carried on the bonnet, or a sliding or rolling off phase (Simms and Wood 2009). Which of these occurs depends largely on vehicle shape, speed and braking (Hamacher et al. 2012). Subsequently, the pedestrian hits the ground (secondary impact) and continues to slide on or roll over the ground until reaching the resting position, with the risk of further impacting structures on or near the road (tertiary impact). The percentage of injuries sustained during vehicle and ground impact reported in literature varies (Figure 1.4), although in all studies most injuries were attributed to vehicle impact.

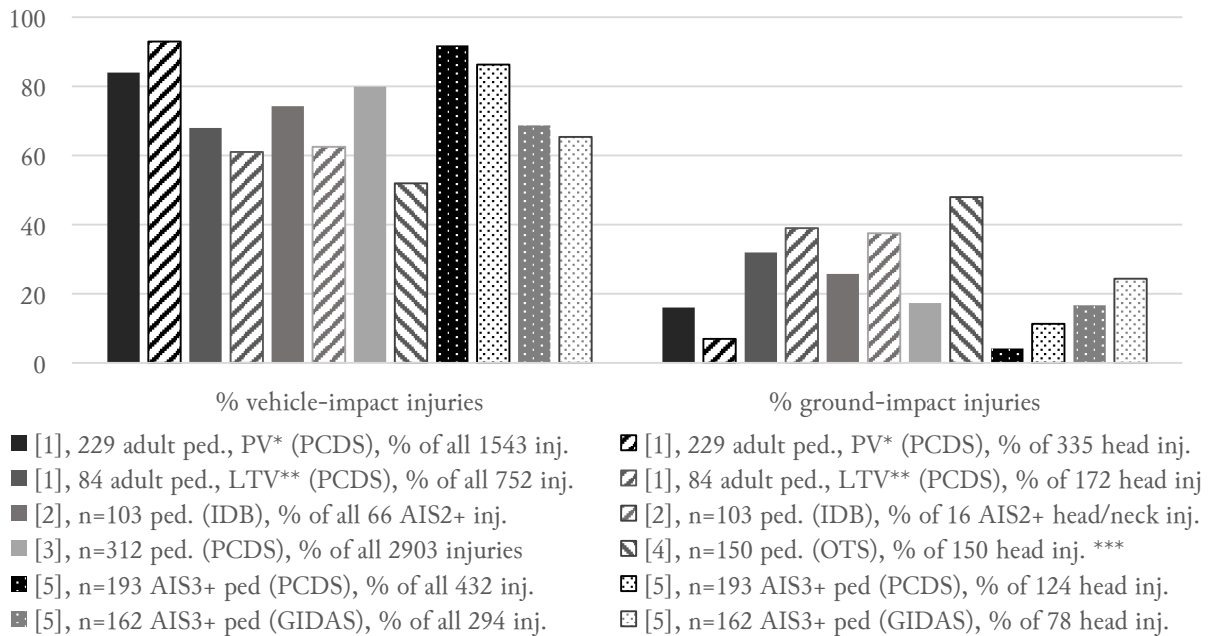


Figure 1.4: Percentage of vehicle-impact (left) vs. ground-impact (right) injuries. Solid filled bars and dotted dark-background bars (left legend side) indicate injuries to all body parts, striped and dotted light-background bars (right legend side) indicate head injuries. References: [1] Roudsari et al. (2005), [2] Öman et al. (2015), [3] Zhang et al. (2008), [4] Badea-Romero and Lenard (2013), [5] Mallory et al. (2012). Notes: * Passenger Vehicles (PV), ** Light Truck Vehicles (LTV), *** only one head injury per pedestrian was considered. Databases: Pedestrian Crash Data Study (PCDS, US police-reported cases), Injury Database (IDB, Swedish cases, here: non-fatal cases only), On-the-Spot (OTS, UK police-reported cases), German In-Depth Accident Study (GIDAS, German police-reported cases).

Although two-dimensional kinematics during vehicle impact have been recorded in many studies, the variability between different tests is large (Thollon et al. 2007, Subit et al. 2008). Contributing to this variability are different test setups, subject anthropometries and different vehicle geometries (Subit et al. 2008). Nevertheless, only few studies have published detailed subject anthropometries, and three-dimensional rotations still remain to be quantified. As detailed in Section 1.1, brain injuries are the dominant type of head injuries. Brain injuries can be caused by linear acceleration or by head rotation, as detailed in Section 1.4.

1.4 Head Injury Mechanisms and Injury Criteria

When the head hits the vehicle, skull fractures and brain injuries can occur due to linear acceleration and rotation (Section 1.1). Since the head linear acceleration is highest during impact, current pedestrian passive safety systems for the head aim mainly at reducing vehicle stiffness (Section 1.2). However, brain injury might also occur in the phase between pelvis and head impact due to the head lag and catching up motion (Section 1.3) although the amount of this rotation has not yet been quantified. This type of motion causes head rotation and thus relative motion between the skull and brain which is known to cause traumatic brain injury (TBI, Holbourn 1943).

Head injury criteria can be divided into global and local criteria. These are described in detail in Chapter 4 and Appendix D. In short, the most often used global Head Injury Criterion (HIC) takes only head linear acceleration during a certain time interval into account (Versace 1971). More

recent global criteria focus on head angular velocity, e.g., the Brain Injury Criterion (BrIC, Takhounts et al. 2013), or on head angular acceleration, e.g., the Head Impact Power (HIP, Newman et al. 2000) or the Brain Injury Threshold Surface (BITS, Antona-Makoshi et al. 2015). These studies indicate that head rotation is receiving increasing attention in traffic injury research.

1.5 Biomechanical Tests

Biomechanical tests on component and full-scale level are important to improve the understanding of pedestrian kinematics and injuries as well as for the evaluation of test tools. In the past, full-scale PMHS tests have often been carried out to improve the understanding of injury mechanisms. To date, ethical concerns would restrict biomechanical tests that are not suitable for development and evaluation of test tools such as crash test dummies, impactors and human body models (Section 1.7). These test tools are required for detailed crash reconstructions and safety system evaluation. In the future, once fully validated, the test tools might replace biomechanical tests.

1.5.1 Full-scale Experiments

Extensive full-scale pedestrian experimental testing began in the 1970s when attention was brought to the increasing number of fatalities and injuries involving pedestrians in accidents with motor vehicles. Kramer et al. (1973) investigated lower leg fracture mechanisms in pedestrian impacts. Pritz et al. (1975) was one of the first studies to focus on the whole body in which the influence of vehicle design on pedestrian injury was examined. At the time, they believed that car–pedestrian contacts were mainly responsible for severe leg and pelvic injuries while it was predominantly the pedestrian–ground impact that caused severe head and arm injuries (Pritz et al. 1975). This differs from today's understanding, which might partly be due to vehicle front shapes being different at that time, and to the study being predominantly focussed on leg and pelvic injuries. Investigating a lowered vehicle front end profile, the study highlighted that the overall effectiveness of this countermeasure would depend on its effect on upper body and head injuries: both lowering and softening the vehicle front end tended to increase head velocity. In addition, they discovered that the peak head velocity was higher than the velocity of the bonnet in all experimental tests and that this peak occurred before head impact during a “whipping, rotation motion about the upper body that suggests a potential for neck injuries” (Pritz et al. 1975). Krieger et al. (1976) studied pedestrian kinematics in detail, focussing on leg and head acceleration but describing body rotation as well. They concluded that pedestrian crashes lead to “a wide variety of complex (pedestrian) motions”. Based on the HIC, the risk of injury was higher in head–bonnet impact than in head–ground impact, and that “dummy and cadaver response to almost identical impacts were quite different” (Krieger et al. 1976). An early mathematical pedestrian model was introduced by Ashton et al. (1983), a study in which reconstructions of several real-life accidents were attempted using dummy testing, PMHS testing, and a mathematical model. One of their findings was that, contrary to the findings of Pritz et al. (1975), lowering the vehicle front end reduced head impact velocity. They also noted the difficulties in reproducing specific events due to the complexity of the pedestrian kinematics, as well as considerable differences between dummy and PMHS responses. Other notable early full-scale pedestrian PMHS tests have been conducted by Césari et al. (1980), Farisse et al. (1981), Cavallero et al. (1983), Brun-Cassan et al. (1984), Kallieris and Schmidt (1988), and Ishikawa et al. (1993), to name just a few.

In order to investigate advances in vehicle designs aimed at protecting pedestrians, Schroeder et al. (1999) studied the kinematics and injuries of six PMHSs that had been impacted by two different vehicles. They concluded that while a lower vehicle front end was found to reduce leg injuries, head impact against the vehicle remained an issue to be addressed. During the loading of the pedestrian onto the bonnet, the spine was elongated. They hypothesised that this elongation would have contributed to the spine injuries discovered in the subjects in subsequent autopsies.

Kerrigan et al. (2005a), (2005b) and (2007) investigated the kinematics of PMHSs and the Polar-II dummy in impacts against two different mid-size sedan cars and an SUV in an attempt to establish kinematic corridors by scaling time, as well as the trajectories for each body segment. One of their findings was that the PMHSs generally showed longer Wrap Around Distances (WADs) than the dummy, and which they attributed partly to the PMHSs' tendency to slide more over the bonnet than the dummy, and partly to the lack of muscle tension in the PMHSs. The main reasons for a greater lateral bending stiffness in the dummy compared with the PMHSs appear to have been dummy durability and previous dummy component design (Akiyama et al. 2001) although it can also be argued that due to muscle tension, living humans probably have a greater lateral bending stiffness than PMHSs. While the PMHSs' heads lagged behind the upper torso during the upper body rotation over the bonnet towards the vehicle, the head lag was not as pronounced in the dummy, which Kerrigan et al. (2005b) attributed to a greater neck bending stiffness in the dummy compared with the PMHSs.

Subit et al. (2008) studied the kinematics and injuries of four PMHSs, where two short and two tall subjects were impacted by a small city car and a mid-sized sedan. The study focused on the pelvis and upper body kinematics, which were found to depend on subject size and vehicle front geometry. For the tall subjects, the amount of sliding over the bonnet was larger than for the short subjects. In contrast, the shorter subjects displayed a considerable change in pelvis kinematics around the time of pelvis contact. Subsequently, around the time of head impact, the shorter subjects displayed a higher amount of overall lateral bending than did the taller subjects, and a higher HIC score was measured for the shorter subjects for each of the vehicles. Post-test autopsies revealed that the subjects impacted by the small city car sustained more rib fractures than the subjects impacted by the mid-sized sedan. All four subjects sustained spinal fractures, either to the vertebral body (three subjects) or the vertebral processes only (one subject).

The head velocity peak was consistently found to occur before head impact in all examined recent studies which have investigated head velocity curves (Schroeder et al. 1999, Kerrigan et al. 2005a, Kerrigan et al. 2005b). The head lagging behind the upper torso during rotation over the bonnet was seen in all these studies and with all investigated vehicle front geometries; though increased neck stiffness appeared to considerably reduce this effect. In order to reduce variability, the hands were attached to each other in most of the studies. Substantial elbow impacts were seen in two of the three tests in Schroeder et al. (1999) while the upper arm was restrained in the third test. Shoulder impacts occurred in all three tests. Both elbow and shoulder impact occurred in the one PMHS test where video snapshots were displayed in Kerrigan et al. (2005a) and in Kerrigan et al. (2005b), respectively, although the hands were tied together in their experiments. In the four experiments carried out in Subit et al. (2008), communication with the authors revealed that all four test subjects impacted the vehicle with the shoulder while only one subject displayed a

considerable elbow impact, i.e., elbow impact in which a notable amount of energy can be expected to be transferred into the upper body.

Normalising kinematics and trajectories of pedestrian PMHS experiments has been attempted in several studies. Traditional normalisation methods based on momentum transfer in single impacts (Mertz 1984, Viano 1989) require calculation of the effective mass in the impact and thus cannot be applied to full-scale pedestrian experiments in which multiple impacts occur. Normalisation methods based on the total body mass (Eppinger et al. 1999) do not take into account the subject's height. Since subject height is known to affect pedestrian trajectories, such mass-based normalisation methods are of limited value for pedestrian kinematics. In a normalisation method developed specifically for pedestrian kinematics (Kerrigan et al. 2005b, Kerrigan et al. 2007), scaling factors were calculated from the height of body parts in the initial positions of the subjects. These scaling factors were then used to scale the horizontal and vertical linear displacements of each body part. Nevertheless, the authors themselves noted that their method was not sufficient when applied to experiments with a different vehicle front (Kerrigan et al. 2007). Similarly, Ontario et al. (2008) attempted to scale trajectories of different-size pedestrian dummies to average male dummy trajectories and found non-linear dummy kinematics which traditional dimensional normalisation methods could not take into account. In later studies, body part trajectories were instead normalised using the vertical distance between the ipsilateral knee to the body part (Forman et al. 2015a, Yanaoka et al. in press). However, the number of subjects was limited to three in Forman et al. (2015a) and only one vehicle was used. Thus, their method has not yet been finally validated.

Two studies have attempted to develop normalised trajectory corridors (SAE J2868 2010, Forman et al. 2015a). In both studies, three full-scale PMHS experiments formed the basis for corridor development, and all six subjects had their hands bound together. In SAE J2868 (2010), the tests from Kerrigan et al. (2005a) were used and in these the PMHSs were struck by a Honda Civic year model 2004. In contrast, in Forman et al. (2015a), a generic buck was used to strike the PMHSs. Both studies first normalised the trajectories of each body part. In SAE J2868 (2010), the normalisation method of Kerrigan et al. (2005b)—which normalised according to body part heights—was adopted. In Forman et al. (2015a), the vertical distance from the knee was used instead. In both studies, after the normalisation of the individual trajectories of each body part of all three PMHSs, the average of each body part's normalised trajectory was calculated before constructing the corridors. The corridors were then calculated from the average trajectories of each body part using a percentage of the accumulated path length of each trajectory at each point in time. For the head and spine, the upper bounds of the corridors were set to +5% and the lower bounds to -10% of the trajectory path lengths. For the pelvis, the upper bound percentage was +10%, and the lower bound percentage was -5%. The total corridor width of 15% of the trajectory path length was chosen with the aim that not all dummies would fit into the corridors, but fitting a dummy into the corridor was deemed possible with existing technology. However, none of the two studies specified how well a dummy or HBM should match the corridors in order to be considered biofidelic. Although not published in their study, Forman et al. (2015a) recorded out-of-plane motions as well. In addition, they reported detailed subject anthropometry and initial stance. Thus, the individual trajectories are highly valuable for HBM evaluations.

1.5.2 Shoulder Impact Experiments

As detailed in Section 1.3, pedestrians in the standard scenario may impact a striking vehicle with their shoulder. However, the influence of shoulder impacts on head kinematics in pedestrian crashes is largely unknown. Shoulder impacts have in the past mostly been studied in relation to side impacts, with car occupant responses in impacts with the side interior of the vehicle such as the door or the B pillar being in focus. All shoulder impact experiments existing to date, to the best knowledge of the author, have been conducted with seated subjects. These experiments can be divided into two categories. In the first category relatively small surface impactors were used, most often directed against the glenohumeral (GH) joint (e.g., Bolte et al. 2000, Thollon 2001, Marth 2002, Bolte et al. 2003, Compigne et al. 2004, Ono et al. 2005, Subit et al. 2010). In the second category, larger impactors that additionally directly engage other body parts, such as the thorax or the pelvis were used (e.g., Cavanaugh et al. 1990, Irwin et al. 1993, Koh et al. 2001). To study the influence of shoulder impacts on head kinematics in pedestrian crashes, both these categories are of interest. However, when evaluating the shoulder of an HBM well-defined conditions and impacts locally restricted to the shoulder would be preferred for biofidelity assessment.

In a number of pure shoulder impact studies, the arm was not supported or the authors did not mention any arm support. In these impacts, the shoulder might have been in a more inferior position than would be expected in a living human, thus resulting in a more inferior impact and load path. In order to establish an injury risk distribution, Bolte et al. (2000) investigated shoulder response and injuries of eleven PMHSs hit by a 23 kg padded impactor at velocities between 3.5 and 7 m/s. Almost half (41%) of the impacts caused a distal clavicle fracture, and 63% of the impacts resulted in a loose sternoclavicular joint. Compigne et al. (2004) subjected seven PMHSs to lateral and oblique ($\pm 15^\circ$) impacts at 1.5 m/s and purely lateral impacts at 3, 4, and 6 m/s with a rigid 23.4 kg impactor. Similarly to Bolte et al. (2003), they found greater mobility in the shoulder when the impact was lateral or anterior-oblique than when it was posterior-oblique. The authors of both studies attributed this to the scapula sliding over the rib cage.

Bolte et al. (2003) conducted 14 shoulder impacts against PMHSs with a 23 kg padded impactor at velocities of 4.4 (12 tests) and 7 m/s (2 tests) in lateral, 15° anterior-oblique and 30° anterior-oblique impact directions while supporting the upper arms. Oblique loading resulted in greater shoulder deflections than lateral loading which was attributed to the scapula sliding posteriorly over the thorax. Regarding bone injuries, only one distal clavicle fracture occurred and one subject sustained four rib fractures. The reduced number of injuries compared with Bolte et al. (2000) was attributed to reduced impact severities below the injury threshold.

Ono et al. (2005) subjected eight volunteers to lateral and $\pm 15^\circ$ oblique impacts with an 8.5 kg rigid impactor and pre-defined load curve, calibrated with a Hybrid III dummy to maximum contact forces of 400, 500, and 600 N. The volunteers were asked to relax their muscles in one set of tests and to tense them in a second set. Corridors were established for impact load, head, T1 and pelvis accelerations, neck force and moment, shoulder deflection, as well as head, T1, and head relative to T1 rotation angles. The maximum head acceleration did not change considerably when comparing relaxed and tensed volunteers, but after 150 ms the maximum lateral head displacement of the average tensed volunteer was approximately double that of the average relaxed volunteer. Shoulder deflection was reduced by 20% for the tensed compared with the relaxed volunteers. The

maximum neck moment around the anterior-posterior axis (where the main head rotation occurred) was reduced by 24% for the tensed compared with the relaxed volunteers. Differences in head/neck/torso responses were also found in different impact directions and this was attributed “to the difference in shoulder anatomical shape or structure” (Ono et al. 2005). The shoulder medial motion was limited in the posterior impact compared with the lateral and antero-lateral impact, well in agreement with the findings of the studies named earlier in this section.

1.6 Accident Data for Dummy and HBM Evaluation

As described in Section 1.1, in-depth accident data is valuable for the understanding of real-life pedestrian crashes in terms of the biomechanics, injury patterns and boundary conditions such as e.g. vehicle type, speed, steering and braking, pedestrian age, stature and walking speed. These are typical variables recorded in accident databases such as the German In-Depth Accident Study (GIDAS) database (Otte et al. 2003), the PCDS (Jarrett and Saul 1998), and the Advanced Protection Systems (APROSYS) database (Carter et al. 2008).

Detailed in-depth pedestrian accident reconstruction is complex and may lead to varying results based on the information available to the investigators and the techniques used for reconstruction (Depriester et al. 2005, Brach 2015). Depriester et al. (2005) compared the results of several accident reconstruction methods. To assess the quality of these methods, they used two real-life accidents that had previously been reconstructed in depth. Most methods either calculated vehicle impact speed from the throw distance, or determined both vehicle impact speed and throw distance in an iterative process. The quality of vehicle impact speed prediction varied, and the ranges of the predicted speeds were rather large. In addition, two of the methods could not be applied to one of the cases as this crash did not meet the methods’ requirements. The impact locations of body parts on the vehicle could, to a large extent, be matched by their simulation models. Using these simulation methods, an understanding of pedestrian kinematics could be gained. Matching body parts to impact locations may not always be feasible although it was possible in the above two cases.

However, whether accident data can be used to validate the detailed kinematics of pedestrian test tools is questionable. Traditional in-depth accident reconstruction utilises test tools to study the pedestrian’s behaviour immediately prior to the crash. To study exact pedestrian in-crash kinematics test tools such as HBMs are required. Using the opposite approach of validating the kinematics of these test tools with accident reconstructions may have limited value. However, a multi-level approach utilizing accident reconstruction, biomechanical tests both on component and on full-scale level, crash test dummies, HBMs, physics, anatomy and physiology is likely to provide the best possible solution to increase knowledge about pedestrian kinematics.

1.7 Human Body Models and other Test Tools

In the present thesis, test tools are defined as physical or numerical representations the whole human body or of human body parts used to assess the injury risks of vehicles as well as the potential benefits of safety systems for vehicle–pedestrian crashes. Some of these test tools are pedestrian crash test dummies, leg, upper leg and head impactors, and numerical HBMs.

Pedestrian crash test dummies and impactors used to improve pedestrian safety are presented in Appendix B. To date, two main pedestrian dummies have been developed: the Polar-II along

with the updated Polar-III (Akiyama et al. 1999, Akiyama et al. 2001) as well as the Hybrid-III pedestrian dummy (Humanetics Innovative Solutions 2013). Sub-system impactors for pedestrian safety used in Euro NCAP today consist of adult and child head impactors, upper leg and lower leg impactors (Euro NCAP 2014a). Physical crash test dummies and sub-system impactors are designed to be tested with actual vehicles. In this sense, dummies and impactors may represent a more realistic assessment of the actual vehicle than numerical simulations, which require a numerical vehicle model. However, both dummies and impactors are themselves highly simplified models of actual humans, which may lead to injury assessments that differ from those obtained in PMHS tests (Kerrigan et al. 2005b, Kerrigan et al. 2008). Additionally, safety systems should protect a large range of the population, which can more easily be represented by HBMs, while anthropometric changes to a dummy are more difficult to introduce. Therefore, HBMs are invaluable tools for pedestrian safety system development and evaluation.

Since HBMs are relatively easy to adjust and modify they can be used to study many different impact conditions without causing physical damage to real vehicles, crash test dummies or PMHSs. Due to the complexity of pedestrian crashes adjustability is especially important. Thus HBMs are suitable tools for variation studies and preparation of physical tests during the early stages of product development by car manufacturers. Recent HBMs provide increasing levels of detail including detailed inner organs and/or advanced brain models (Kleiven 2007, TMC 2011, Sahoo et al. 2014). When properly validated, such HBMs can be used to develop detailed injury criteria.

Until recently, two main approaches to human body modelling have been available for use in the in-crash phase: the multibody (MB) and the FE method. As both have different advantages and shortcomings (Wismans et al. 2005), combined MB/FE modelling has been developed as a third option. MB models are usually composed of rigid body ellipsoids and planes with a point mass in their centres of gravity and with inertial properties assigned to them. These bodies are connected by joints with a lumped parameter joint stiffness, simulating the interaction between bones, muscles and ligaments. Contact and penetration characteristics are approximated by idealised functions. This approach allows for low computation time. The level of detail in MB models is lower than in FE models, and their tissue-level injury prediction capabilities are limited.

In contrast, FE models consist of deformable elements and can be used to predict injury based on tissue level criteria by calculating variables such as stress, strain, and strain rate. The FE method allows for modelling of complex geometries and using advanced material laws, and provides a high level of detail. With FE models, the load path through the human body during an impact can be quantified at tissue level. Therefore, FE models for pedestrian impacts must be validated both in terms of kinematics and at the tissue level.

The three categories of pedestrian FE models that currently exist are impactor models, dummy models and human models. The human models can be further divided into models of body parts (component models) and full-body HBMs. To date, several pedestrian FE full-body HBMs have been developed and refined. The Total Human Model for Safety (THUMS) pedestrian model is a commercially available full-body FE model developed jointly by Toyota Motor Corporation and Toyota Central R & D Labs Inc. (Watanabe et al. 2011). The THUMS model was developed for the FE software LS-Dyna (LSTC Inc. 2014a) and the current version 4 consists of approximately 2 000 000 elements (TMC 2011). Other existing full-body pedestrian FE models are the simplified

pedestrian GHBMC models (ELEMANCE 2015), the pedestrian HUMOS2-model developed during the EC-funded HUMOS1 and HUMOS2 projects (Vezin and Verriest 2005), the H-model developed by the ESI group (Haug et al. 2004), the JAMA pedestrian model (Sugimoto and Yamazaki 2005), the in-house pedestrian models developed by several car manufacturers, and the NHTSA pedestrian model (Mizuno 2003). However, these models were not available on the market when the work for this thesis was initiated.

1.7.1 The Total Human Model for Safety (THUMS)

The main releases of THUMS that have so far been made available are version 1, launched in the year 2000, version 3, launched in 2006, and the latest, version 4, launched in 2010. A number of studies have attempted to evaluate the biofidelity of THUMS version 1 (e.g., Maeno and Hasegawa 2001, Iwamoto et al. 2002, Chawla et al. 2005, Pipkorn and Mroz 2009). In comparison with earlier versions of THUMS version 4 has a refined mesh, includes internal organs and more solid-element muscles that provide damping in an impact.

The THUMS pedestrian version 4 has been developed using new computed tomography (CT) scans although the head model of version 3 was re-used with a refined mesh (TMC 2011). A certain amount of full-scale and component level evaluation was conducted by Shigeta et al. (2009), Watanabe et al. (2011) and Watanabe et al. (2012). In the full-scale evaluations, THUMS body dimensions and total mass were adjusted to match those of the subjects. Full-scale kinematics were evaluated against three PMHS tests comprising a sedan, an SUV and a minivan (Watanabe et al. 2012). Two-dimensional linear displacements of the head centre of gravity, T1, L5/S1, the knees, and the heels were shown to generally match the PMHS results. However, the head WADs of THUMS were up to 10 cm lower than those in any PMHS test. At the component level, Shigeta et al. (2009), Watanabe et al. (2011) and Watanabe et al. (2012) evaluated impact responses of the head and neck in frontal and lateral impacts, head rotation with respect to brain kinematics and injuries, direct impact against the head, chest responses in several frontal and lateral impact conditions, frontal abdominal impact responses, lateral impact and four-point bending responses of the knee, as well as static three-point bending and dynamic compression responses of the humerus. To the best of the author's knowledge, other validation studies of the THUMS 4.0 pedestrian were not available in the literature, although many studies have used various THUMS versions as a validated tool to, e.g., study real-life crashes.

1.7.2 Positioning, Scaling and Morphing

To accurately replicate real-life crashes or full-scale experiments for model evaluation and safety system development, HBMs must replicate the initial posture and anthropometry of the pedestrian or test subject. This can be achieved through positioning, scaling and/or morphing of the HBM.

In the context of this thesis, positioning an HBM according to a crash or test means to bring the HBM into a position and orientation relative the vehicle and to adjust the body posture, i.e. the angle of body parts relative to each other and to the ground, so that they match those of the pedestrian in the related crash or test. To position FE HBMs, two main techniques are available, geometric positioning and positioning through simulations. In geometric positioning, the whole body or body parts are shifted or rotated in a pre-processor prior to a simulation. For whole-body

positioning relative to the vehicle this technique is fast and efficient. However, when adjusting the body posture with geometric positioning the axes of rotation have to be determined manually and usually remain constant throughout the process, which may not lead to physiologically accurate postures. In addition, soft tissues become deformed which may distort the elements in the HBM and lead to numerical instabilities (Desai et al. 2012). To mitigate these issues, HBMs can also be positioned through simulations in which body parts are gradually pushed or pulled into the desired body posture. Although more time consuming than geometric positioning, positioning through simulation generally allows for physiologically more accurate positioning, and reduces the risk of severe element distortion since the loads are applied gradually. However, element distortion cannot be completely eliminated and manual mesh adjustment may be required (Jani et al. 2009a). To mitigate these issues and to reduce the amount of time spent on positioning, several studies have since attempted to develop positioning tools (Jani et al. 2009b, Desai et al. 2012). However, to date these tools still require manual input of the joint rotation axes, and they yield meshes of limited quality at large posture changes (Desai et al. 2012). In addition, attempts are being made to simplify the positioning of FE HBMs with the aid of newly developed personalisation tools (PIPER 2015).

Scaling is one of the methods used to adjust anthropometric measurements of an HBM to those of a pedestrian or a test subject. To scale an HBM, one or more scaling factors in different directions can be applied to the model as a whole or to body parts. If the body as a whole is scaled, some of the pedestrian's or test subject's body proportions might not be captured. If body parts are scaled independently, some mesh refinements may be required to restore node connectivity. Still, scaling is a relatively fast process and requires less anthropometric measurements than morphing, as described below.

Morphing is currently the most accurate method of matching the anthropometry of an HBM to that of a pedestrian or a test subject. To the best knowledge of the author, no study has yet investigated if morphed HBMs predict pedestrian kinematics better than scaled HBMs. However, the technique of morphing has been applied in both model development and application. In model development, the original HUMOS2 mesh obtained from a single individual was morphed to represent a mid-sized male, a large male and a small female (Serre et al. 2006). To study the effects of obesity in frontal crashes, Shi et al. (2015) developed a morphing technique to represent an obese occupant and applied this technique to the seated THUMS 4 occupant model. One of the issues with morphing came to light in their study. Although they attempted to match the morphed model anthropometries with those of experimental subjects from a previous study, CT images of the experimental subjects were not available. To obtain target geometries for obese subjects, Shi et al. (2015) consequently used a combination of statistical analysis of 400 landmarks on the ribcage and generic outer body shapes (Reed and Parkinson 2008) for the torso. The new inner organ geometries were estimated from the new ribcage and outer body shapes. Additional fat tissue was modelled as subcutaneous fat; no fat tissue was added within the abdomen. The upper and lower extremity geometries were estimated using the Generator of Body Data (GEBOD) programme (Cheng et al. 1996). The complexity of defining target geometries in Shi et al. (2015) highlights the complexity of the morphing process and its need of large quantities of anthropometric data.

1.8 Summary: Status of Pedestrian Safety

The ultimate goal of developing pedestrian safety systems is to reduce vehicle–pedestrian crashes and, when a crash cannot be avoided, to mitigate pedestrian injuries. Since it is likely that vehicle–pedestrian crashes cannot all be avoided with any of the current systems, pedestrian injuries should be mitigated for the whole variety of pedestrian anthropometries and for all crash scenarios.

Pedestrian in-crash safety is still immature compared with occupant in-crash safety, despite more than 40 years of research. Among the reasons for this lack of knowledge are the facts that pedestrian kinematics are complex, experimental data are limited, and crash data cannot generally provide detailed information on pedestrian kinematics.

Detailed experimental full-scale pedestrian PMHS data publicly available to date are mainly limited to two-dimensional trajectories in crashes with less than ten modern passenger car fronts. The vehicle speed at which these experiments are conducted is usually 40 km/h, and the first contact is in the front centre region of the car. As detailed in Section 1.1, most pedestrians are impacted by the vehicle front. In addition, most car–pedestrian crashes occur at or below 40 km/h whereas the risk of severe injuries increased rapidly at and above this speed which makes this particular testing speed a compromise between crash frequency and injury risk. Prior to starting the work for this thesis, the author could not find any publicly available experimental 3D translational pedestrian kinematics or any rotational kinematics apart from resultant rotational head acceleration. However, a recent study indicated that rotationally induced TBI injury thresholds are directionally dependent (Takhounts et al. 2013). Experimental kinematics following the head–vehicle impact have, to the best knowledge of the author, not been published either. Thus, the kinematics during flight phase and secondary (ground) impact are largely unknown. Detailed experimental pedestrian kinematics from impacts with other areas of a vehicle such as the front corners or the vehicle rear side and kinematics in crashes with other vehicle geometries (e.g., busses, trucks) have not been published, to the best knowledge of the author. Another severe limitation of the experimental pedestrian data available today is that the initial pedestrian posture and anthropometry have not been reported in detail.

Due to these shortcomings of experimental data, an obvious issue is that none of the tools mentioned in Section 1.6 can be validated thoroughly in terms of kinematics that have not been recorded in an experimental setup.

2 Aims

This thesis contributes to the ultimate goal of improving pedestrian safety. The main aim is to quantify six-dimensional head translational and rotational kinematics in passenger-car–pedestrian crashes prior to head impact against the vehicle by means of PMHS testing and FE simulations. The PMHS data are generated to provide HBM evaluation data and to investigate how pedestrian anthropometry and minor differences in initial stance influence upper body kinematics in passenger-car–pedestrian crashes. Head kinematics are examined with focus on the influence of pelvic sliding over the bonnet, spine bending, and elbow and shoulder impacts against the vehicle for pedestrians with varying anthropometries. Additional aims are to evaluate an HBM on a full-scale level and to provide full-scale experimental data and pragmatic HBM scaling methods to industry and academia.

3 Summary Of Papers

This chapter summarises the papers in the thematic sections: full-scale PMHS experiments, elbow and shoulder impact epidemiology in real-life crashes, shoulder impacts, and full-scale pedestrian HBM-evaluations. To contribute to the long-term aim of reducing pedestrian head injuries, an Addendum (Chapter 4) explores whether full-scale pedestrian simulations could add information on head injury risk due to head rotation which is not currently covered by consumer ratings.

3.1 Full-scale PMHS experiments

In Papers I and II, five new full-scale pedestrian PMHS experiments were conducted and three previous experiments were re-analysed in order to investigate how pelvic sliding, spine bending, and elbow and shoulder impacts influence head kinematics in vehicle-pedestrian full-scale experiments as well as to provide new 6 degrees-of-freedom (DOF) data for HBM evaluation.

All subjects were impacted laterally in a walking posture by a small sedan. The vehicle velocity was 30 km/h in one test and 40 km/h in the seven other tests. In all experiments, high-speed cameras filmed the subjects from their posterior side, recording the kinematics of the head, spine, pelvis and scapulae and providing new 6DOF data (see Paper II, Appendix C3 for all 6DOF data).

Figure 3.1 displays typical PMHS kinematics. In summary, the head kinematics were altered by pelvic sliding over the bonnet, spine bending, upper arm and shoulder response. Compared with one experiment in which sliding was virtually non-existent, the sliding increased the maximum horizontal head velocity component towards the vehicle. Both spine lateral bending and especially neck lateral bending increased the head velocity prior to head impact to levels above the initial vehicle velocity. Compared with subjects that did not experience considerable arm support, substantial upper arm support reduced head linear velocity relative to the vehicle prior to as well as during head impact, and also initiated head rotation towards the vehicle, reducing head peak angular velocity.

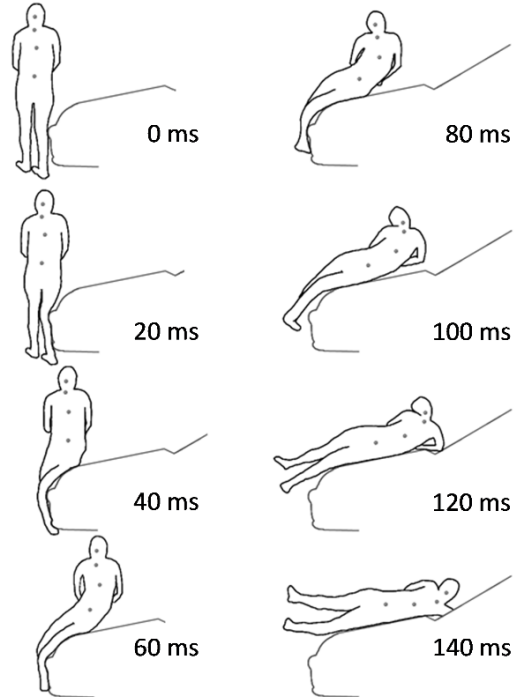


Figure 3.1: Typical PMHS kinematics

Although head injuries from linear and angular acceleration were most likely to occur during head impact against the vehicle, a risk of mild TBI during head rotation prior to impact was identified. All subjects exceeded angular velocity and acceleration thresholds for cerebral concussion prior to head impact while the head rotated towards the vehicle. The subject experiencing the highest rotational acceleration did not display considerable arm support after

elbow impact. The lack of arm support contributed to the head rotating towards the vehicle comparatively late which caused high head angular accelerations in the coronal plane.

3.2 Elbow and Shoulder Impact Epidemiology

An epidemiological study was included in Paper I to determine the frequencies of elbow and shoulder impacts in real-life crashes in the context of impact conditions and crash severity.

The German In-Depth Accident Study (GIDAS) database was queried for typical pedestrian crashes between the years 1999 and 2011. Since the cases were not weighted, a slight bias towards severe cases was present. Crash severity, pedestrian size and orientation at the time of impact as well as head WADs were examined in view of the frequencies of elbow and shoulder impacts.

The total number of pedestrians included was 1 212 of which 164 were injured with MAIS3+. Figure 3.2 shows the occurrence of elbow, shoulder and head impacts in cases where any body part was injured with MAIS3+, and it can be seen that most pedestrians do not experience elbow or shoulder impacts. Elbow and shoulder impacts appeared to occur more frequently in higher severity impacts, although the car speed differences were not statistically significant. As elbow and shoulder impacts might not leave any indentations at low car speeds, underreporting of these impacts was likely. The pedestrian's orientation and size did not considerably change the frequencies of elbow and shoulder impacts, and the frequencies were not correlated with head WAD.

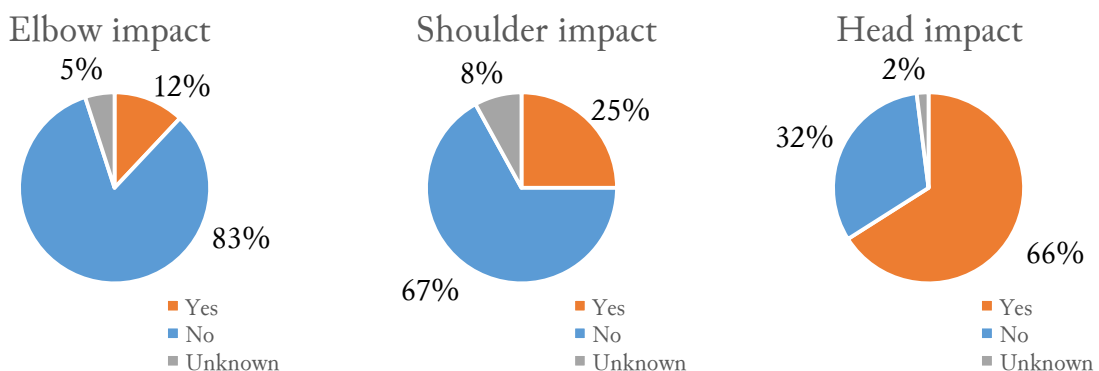


Figure 3.2: Frequencies of elbow, shoulder and head impacts in n=162 MAIS3+ cases.

3.3 Shoulder impacts

The influence of shoulder impacts on pedestrian head kinematics were further investigated in Paper III. Previous shoulder impact experiments with relaxed and tensed volunteers as well as with PMHSs were reanalysed and simulated with THUMS version 4. Since the impact conditions in full-scale pedestrian experiments deviated from those in pure shoulder impact experiments (Figure 3.3), a parameter variation study was simulated to examine the influence of the impact angle, impactor orientation and shoulder posture on the head kinematics.

The head and spine kinematics of THUMS generally compared better with the tensed rather than with the relaxed volunteers. The THUMS spine was slightly less curved and moved less overall than the average tensed volunteer spine, a combination which resulted in a close match of the head kinematics of THUMS and the tensed volunteers (Figure 3.4). Head twist and spine stiffness were greater in THUMS than in the volunteers.

In the shoulder impacts similar to pedestrian–vehicle shoulder impacts, lateral linear head displacements were sensitive to shoulder posture, impact direction and impactor orientation. Changing the impact direction and/or impactor orientation from lateral to supero-lateral tended to decrease the lateral linear head displacements. Elevated shoulder postures increased the lateral linear head displacements compared with neutral shoulder postures. The THUMS shoulder responded as would be expected from functional biomechanics.

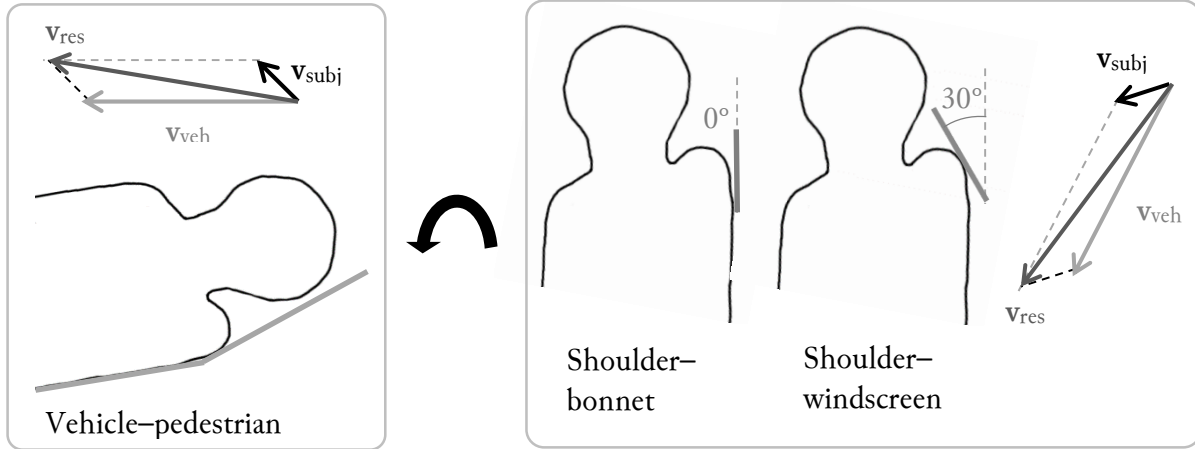


Figure 3.3: Typical shoulder impact conditions in vehicle–pedestrian impacts, here: subject PM01 in Paper II. Left: stationary image of the resultant velocity (v_{res}) of a vehicle (v_{veh}) and a falling pedestrian (v_{subj}). Right: turning the image to mimic a shoulder impactor experiment with pedestrian-like impact configurations: The shoulder is in an elevated position. The impactor orientation changes depending on whether the shoulder impacts the bonnet or the windscreen. The impact direction is in the direction of the resultant velocity (v_{res}), i.e., from supero-lateral.

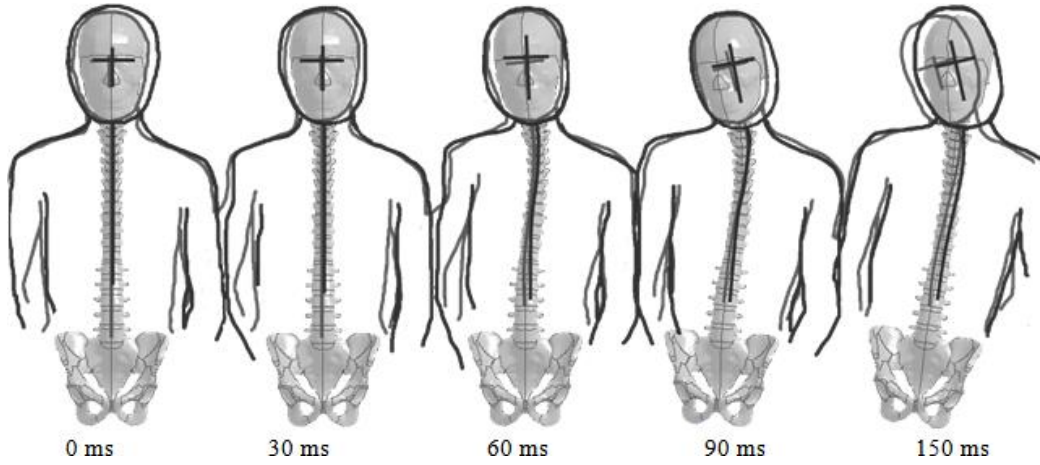


Figure 3.4: Head and spine kinematics in THUMS (light grey) as well as relaxed (black) and tensed (dark grey) volunteers

The timing of the onset of head movement after shoulder impacts is crucial for pedestrian head injury risk. Future pedestrian safety systems might increase the time span between shoulder and head impacts, e.g., through introduction of larger and thicker pedestrian airbags or through further raising the pedestrian pop-up bonnet. Such countermeasures are expected to be beneficial not only

through earlier reduction of head–vehicle velocity difference, but also by decreasing vehicle stiffness and thus providing increased safety for smaller than average pedestrians and mitigating thoracic injuries. The head peak angular velocity is generally not expected to increase when such systems are introduced. As Paper II has shown, supporting the upper torso leads to an early start of head rotation towards the vehicle, which contributes to reducing rotation-induced brain injuries.

3.4 Full-scale simulations

Varying anthropometries influence pedestrian kinematics in HBM biofidelity evaluations and pedestrian safety system evaluations. Therefore, in Paper IV, six pragmatic HBM scaling techniques were assessed regarding their ability to replicate the head impact conditions in the full-scale PMHS experiments in Paper II. To enable this assessment, an FE model of the vehicle used in the experiments was created and validated using impactor test data. THUMS version 4 was positioned according to each experiment and then translated and scaled in six different ways (Figure 3.5). In total, the five experiments combined with the six techniques resulted in 30 simulations.

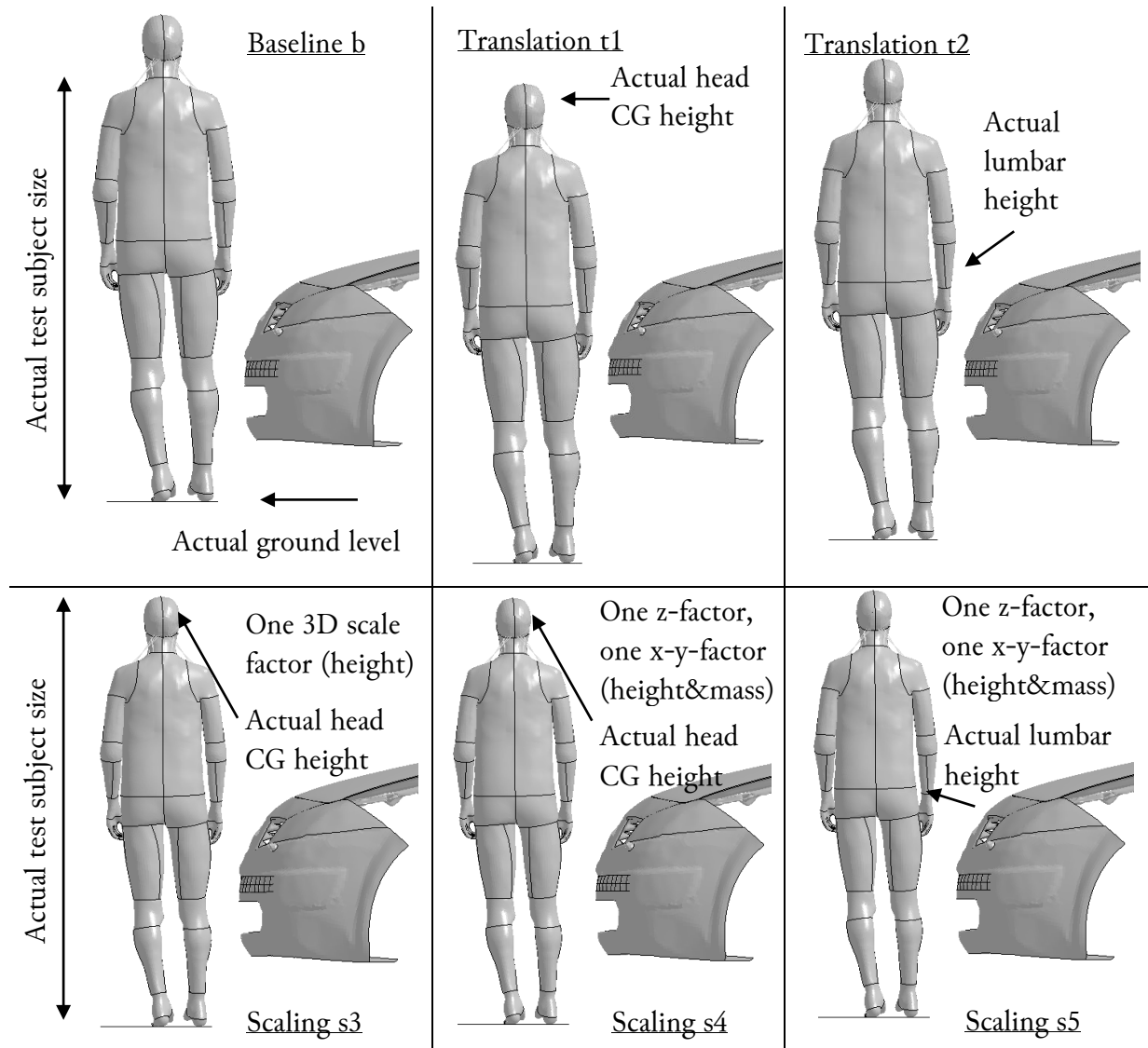


Figure 3.5: The six scaling techniques from top left to bottom right: baseline (b), translation 1 (t1), translation 2 (t2), scaling 3 (s3), scaling 4 (s4) and scaling 5 (s5)

The head impact location was matched best when applying scaling method s5 although all translation and scaling methods (excluding the baseline method) yielded high scores of over 95% for the head WAD. A larger spread in ratings was observed for head impact velocities where the method s5 scored considerably higher than the other methods. Using the best-rated method s5, THUMS generally showed biofidelic responses and was numerically stable in most simulations. Reproducing the upper arm response was crucial for accurate reproduction of the head impact conditions. However, some responses observed in the PMHS experiments were not replicated by THUMS. In the experiments the head rotated away from the vehicle, starting approximately 50 ms after first contact. Such head rotation was not replicated by THUMS, indicating that the THUMS neck was stiffer in lateral bending than the necks of the PMHSs. Upper arm abduction influenced the support of the upper body, and thus head kinematics, after elbow impact. In two of the five experiments, upper arm abduction at the time of elbow impact exceeded 70°, but the maximum upper arm abduction measured in THUMS was 49°. Thus, suggested biofidelity improvements for THUMS include slightly softening the neck and facilitating larger upper arm abduction.

4

Addendum: Head injury criteria in full-scale THUMS and head impactor simulations

4.1

Introduction

To assess the risk of pedestrian head injury for different vehicles, to date, consumer ratings such as Euro NCAP test vehicles with head impactors. These impactors represent a human head and are instrumented with three-axial accelerometers which measure linear acceleration during impact against the vehicle (Euro NCAP 2014a). From the resultant linear acceleration, the HIC₁₅ is calculated. In Euro NCAP, multiple areas on the bonnet, lower windscreens and A-pillars are tested at an impactor speed of 40 km/h and an angle to ground level of 65° (Euro NCAP 2014a).

The current head impactor is limited in its ability to measure head rotation. Before impact, the impactor follows a ballistic curve (Euro NCAP 2014a) whereas full-scale tests show head rotation during this time span (Schroeder et al. 1999, Kerrigan et al. 2005a, Kerrigan et al. 2005b). Current test methods thus do not take into account head rotation although head rotation has been shown to cause TBI (Holbourn 1943, Gennarelli et al. 1972, Melvin and Weber 1985).

Previous studies have compared HIC₁₅ measured in full-scale pedestrian PMHS experiments with that measured in head impactor experiments on a sedan (Kerrigan et al. 2008) or in dummies with a sedan and an SUV (Kerrigan et al. 2009, Kerrigan et al. 2012). Compared with the impactor experiments, higher HIC values and lower head impact speeds were measured in the PMHSs. Compared with the dummies, in the sedan impact, the PMHSs and the dummy displayed generally similar HIC values, and the PMHSs displayed considerably higher averaged angular accelerations than the dummy. Head Injury Criteria (IC) other than the HIC that take angular kinematics into account have, to the best of the author's knowledge, not yet been compared in impactor and full-scale pedestrian test setups.

The main aim of this Addendum is to investigate, in a pilot study, whether full-scale simulations with THUMS could provide more information on head Injury Risk (IR) than head impactor simulations. Five global head ICs are used to study the IR. A secondary aim is to investigate if measuring head impactor rotation, without changing the impact test setup, could provide a benefit for head IR assessment.

4.2

Methods

4.2.1

Simulations

A total of 24 FE simulations were carried out. In one series of 12 simulations, THUMS pedestrian version 4.0 was impacted by a vehicle. In the other series, a head impactor was shot against a vehicle according to Euro NCAP test procedure. LS-Dyna R7.1.1 MPP (LSTC Inc. 2014a) was used for all simulations and LS-Prepost version 4.2 (LSTC Inc. 2014b) was used as a pre-processor. All simulations were run at least until the point of deepest head intrusion into the vehicle model. In all simulations, three-axial linear velocity and acceleration as well as three-axial angular velocity and acceleration of the head were measured.

The vehicle model consisted of the front of an early Volvo S80 model (Figure 4.1). It included all outside parts up to the upper transverse between the A-pillars as well as all parts under the bonnet and the suspension. A deformable windscreen was modelled based on the smeared modelling technique in Timmel et al. (2007) where two coincident shell layers with a bilinear elasto-plastic material model and the same thickness (3.93 mm) were used to obtain bending stiffness of a 3-layered laminated glass composite. In the windscreen model, the layer mimicking the glass had a Young's modulus of 125 GPa, adjusted for the modelling technique as described in Timmel et al. (2007), a yield stress of 50 MPa, and was allowed to erode at a plastic strain of 0.001. The layer mimicking the PVB had an adjusted Young's modulus of 15 GPa and a yield stress of 0.03 MPa, and no failure criterion was defined. A validation of the whole vehicle model for pedestrian crashes was carried out in-house, but not published. To account for the missing mid and rear section, additional mass was added in the vehicle centre of gravity.

THUMS was first positioned as in simulation PM01 in Paper IV where the right, ipsilateral leg was forward and the left, contralateral leg was rearward of the THUMS centre of gravity (Figure 4.1). Both arms were moved slightly forward to reduce the influence of elbow impacts. THUMS was then mirrored to add an additional stance in which the ipsilateral leg was rearward. The original AM50 model was used to simulate an American male of average height and mass. The positioned AM50 model was also scaled to a 95th percentile male (AM95) and a 5th percentile female (AF05) by using one scaling factor in the z-direction for the height and one factor in the x-y-plane to adjust the mass. Two vehicle speeds were used for the vehicle-THUMS simulations, 30 km/h and 40 km/h. THUMS was impacted by the centre of the vehicle. Braking was not simulated. Gravity was set to 9.81 m/s². The friction coefficients between THUMS and the vehicle as well as between THUMS and the ground were set to 0.5 and 0.7. Combining two stances, three model sizes and two vehicle velocities, 12 vehicle-THUMS simulations were carried out.



Figure 4.1: Simulation setup for AM50 in the vehicle-THUMS simulations

The head impactor model consisted of a viscoelastic hollow sphere with an outer diameter of 165 mm and a thickness of 23 mm with a rigid end plate (Figure 4.2). Inside the hollow sphere was a smaller rigid hollow sphere for stabilisation purposes. The total mass of the head impactor was 4.8 kg. For all impactor-vehicle simulations, the impact direction was 65° relative to the ground surface, according to the Euro NCAP test procedures for the adult head impactor (Euro NCAP 2014a). The head impactor speed was 40 and 30 km/h. The impactor was aligned such that it impacted the vehicle in the same locations as the THUMS head in the vehicle-THUMS simulations. Gravity and friction were also the same as in the vehicle-THUMS simulations. This resulted in 12 impactor-vehicle simulations.

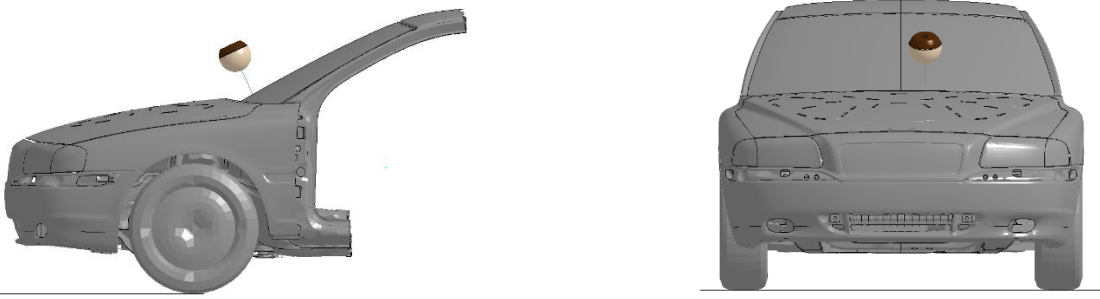


Figure 4.2: Simulation setup in the impactor–vehicle simulations

The masses and inertial properties of all head models used compared with human heads are presented in Table 4.1.

Table 4.1: Masses and inertial properties of all head models used compared with human heads. The coordinate system for the inertial properties is according to SAE (1994), and the impactor was rotated accordingly such that the different models were comparable.

	THUMS AM50	scaled THUMS AM95	scaled THUMS AF05	head impactor	human head, average (Plaga et al. 2005)
Mass (kg)	4.1	5.6	2.7	4.8	3.3
I_{xx} (kg/cm ²)	137.596	226.638	66.706	120.385	109.43
I_{yy} (kg/cm ²)	192.588	328.817	91.551	124.972	148.44
I_{zz} (kg/cm ²)	192.779	304.073	78.960	120.385	135.88

4.2.2 Data analysis

The following five global head ICs were analysed:

- 1) the HIC₁₅ and HIC₃₆ (Versace 1971, Eppinger et al. 1999), calculated from resultant linear acceleration,
- 2) the brain rotational injury criterion (BrIC) (Takhounts et al. 2013), calculated from three-dimensional angular velocities,
- 3) the generalized acceleration model for brain injury threshold (GAMBIT)(Newman 1986), calculated from resultant linear and resultant angular accelerations,
- 4) the head impact power (HIP) (Newman et al. 2000), calculated from three-dimensional linear and angular accelerations, and
- 5) the rotational injury criterion (RIC) (Kimpala and Iwamoto 2012), calculated from resultant angular accelerations.

From each IC, the AIS 2+ head IR was calculated for each of the 24 simulations. For the BrIC, two injury risks were calculated from two risk curves based on previous evaluations of maximum principal strain (MPS) and cumulative strain damage measure (CSDM). Detailed information on the head ICs and the calculation of head IRs is provided in Appendix D. All data was post-processed with Matlab R2012b (Mathworks 2012). The IRs of the two stances used were averaged.

4.3 Results

All simulations terminated without numerical instabilities. Head impact velocities and raw values of all calculated ICs can be found in Appendix E.

Visual analysis of the simulations revealed that AF05 head always impacted the bonnet, the AM50 the lower end of the windscreens or upper part of the bonnet, and the AM95 in the lower third of the windscreens. The head impact was generally further upwards on the vehicle for the 40 km/h compared with their equivalent 30 km/h cases. For the AM50 and the AM95, this resulted in the head impacting stiffer structures in the 30 km/h than in the 40 km/h cases—the AM50 impacted the upper bonnet edge instead of the lower windscreens and the AM95 impacted lower on the windscreens with a subsequent head–dashboard impact.

For a given impact speed, the ICs generally decreased with increasing subject height (Figure 4.3). For a given subject height, the ICs generally decreased with decreasing impact speed. For HIC, the results from the impactor simulations were reasonably similar to the THUMS simulation results. For the purely rotational IC, BrIC and RIC, there was no correlation between THUMS and impactor simulation results. GAMBIT and HIP generally followed the HIC trends. BrIC also showed less sensitivity to impact speed than any other criterion. Comparing HIC₁₅ and BrIC, although the trends were generally similar, a reduction of HIC₁₅ did not relate to an equally large reduction of BrIC. Also, the HIC₁₅ showed a larger spread around the average than the BrIC. The largest spread around the average was observed for the RIC.

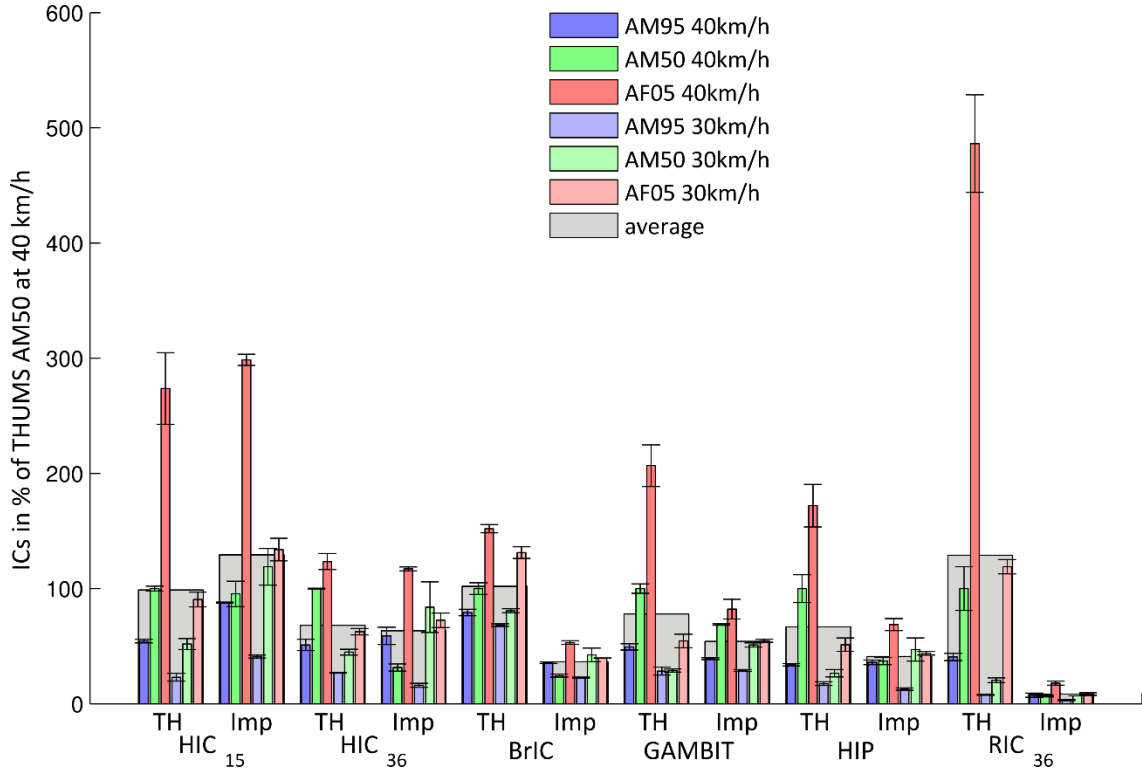


Figure 4.3: ICs in percent of the THUMS AM50 simulation at 40 km/h (TH: THUMS, Imp: impactor simulations). I.e., for each IC, all values are normalised such that the darker green THUMS bar corresponds to 100%. The error bars show the range stemming from the two stances.

For THUMS, on average, the HIC₁₅ predicted the lowest AIS 2+ IR whereas the predicted IR was highest for the HIP (Figure 4.4). Notably, almost all vehicle–THUMS simulations with the AF05 resulted in IRs at or close to 100% whereas the AM50 and especially the AM95 predicted considerably lower IRs. Despite the tendency that the head impacted stiffer structures at 30 than at 40 km/h, the predicted IRs were lower at a vehicle speed of 30 km/h (light colours) compared with its equivalent 40 km/h case (dark colours) for all simulations and all ICs unless the IRs at 30 and 40 km/h were both 100%. All ICs reached a maximum during head–vehicle impact with two exceptions: In the AM50 simulations at 30 km/h, the maximum GAMBIT was reached during elbow–vehicle impact, 45 ms prior to first head–vehicle contact. In the AM95 simulations at 30 km/h, the maximum HIC₁₅ was also reached during elbow–vehicle impact, 50 ms prior to first head–vehicle contact.

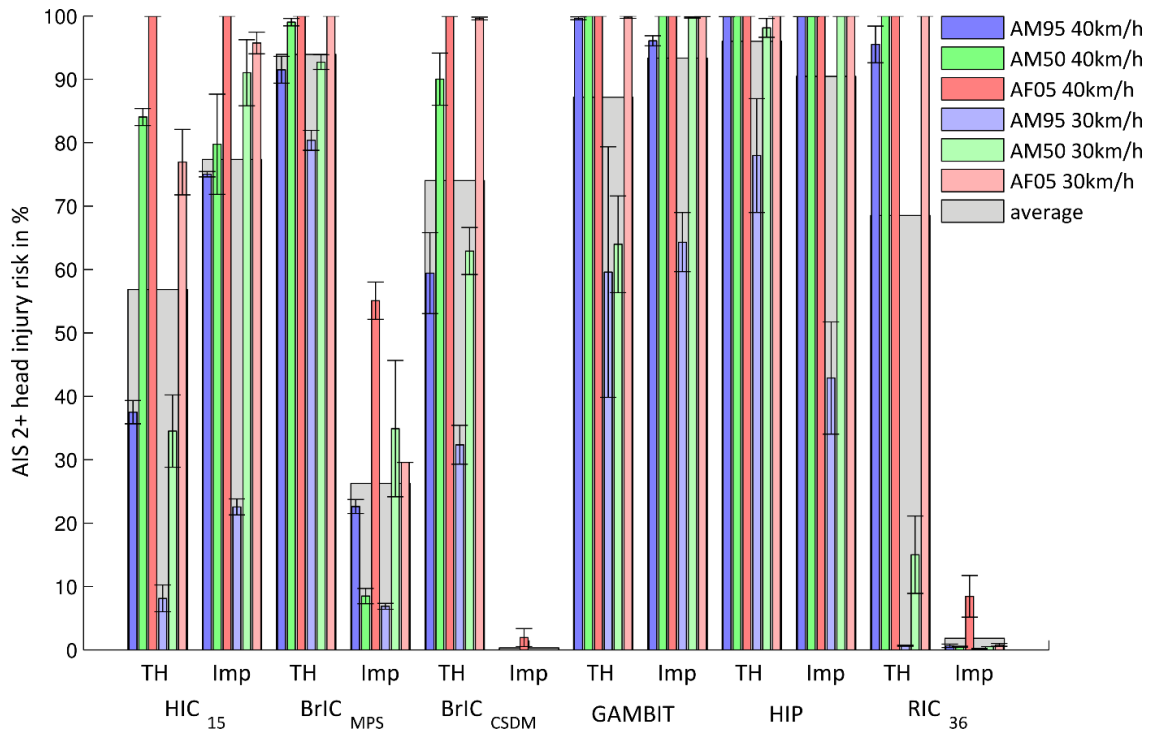


Figure 4.4: AIS 2+ head IRs in the THUMS (TH) and impactor (Imp) simulations.

For the impactor simulations, the average HIC₁₅, GAMBIT and HIP were greater than 75% (Figure 4.4). The two ICs that were calculated from head rotation only, BrIC and RIC, predicted comparatively low average IRs. The predicted IRs for HIC were similar or higher in the 30 km/h cases compared with their equivalent 40 km/h cases, especially for the AM50 and AM95 simulations. This trend was likely due to the aforementioned differences in stiffness for different impact locations.

Comparing the IRs predicted by the vehicle–THUMS with those of the impactor–vehicle simulations (Figure 4.4), the average HIC₁₅ IR predictions were lower for THUMS than for the impactor simulations. This result is unlikely due to differences in head impact velocity: The head impact velocities measured in THUMS were generally within 1 m/s of the initial vehicle speed and thus close to the head impactor speed. For the AF05 THUMS simulations, the differences were slightly greater; the head impact velocities were up to 1.7 m/s lower than vehicle speed at 40 km/h

and up to 1.5 m/s higher at 30 km/h. The two ICs based on rotation only, BrIC and RIC, predicted considerably lower IRs for the impactor compared with the THUMS simulations. The GAMBIT and HIP both predicted comparatively high IRs close to or at 100%.

4.4 Discussion

This pilot study has shown that full-scale THUMS simulations can provide additional head injury risk information to safety system developers. To increase pedestrian safety, full-scale pedestrian simulations should therefore complement impactor tests used in consumer ratings. However, in this study, the impacts were limited to the vehicle centreline. An updated test protocol should include a larger set of simulations which cover a much wider area of impact points on the vehicle.

Apart from HIC₁₅, the ICs and thresholds for IRs used in this Addendum were not specifically developed for vehicle–pedestrian crashes and should therefore be interpreted with care. In vehicle–pedestrian crashes, the duration of head rotation may be longer than during the load cases for which the ICs were originally developed. For instance, BrIC was developed and validated with head impacts during American football, frontal and side car crashes (Takhounts et al. 2013). The MPS- and CSDM-based IRs used for BrIC were derived from uniaxial rotations of FE models where the rotational velocity pulse was varied; the only duration explicitly mentioned was 25 ms (Takhounts et al. 2013). BrIC has not yet been validated for combined rotation in various directions such as those occurring in vehicle–pedestrian crashes. In addition, a previous study showed that BrIC, HIP and RIC did not correlate well with the tissue-level criteria CSDM and MPS in pedestrian simulations (Yanaoka et al. 2015). Another study showed no correlation ($R^2 < 0.1$) between BrIC and CSDM in pedestrian impacts prior to head impact; BrIC overestimated the head injury risk during this time period (Gabler et al. 2014). However, when including the head impact, the correlation improved considerably ($R^2 = 0.6$). In the present study, BrIC was highest during head impact in almost all simulations. Since CSDM correlates with brain injury risk (Kleiven 2007), the BrIC values in this studies would give a good indication of the actual brain injury risk due to rotation if the FE models and injury risk curves were perfect.

AIS 2+ was chosen as an injury limit mainly because previous studies provided more AIS 2 data for injury risk curve development on living humans than other injury levels. AIS 2 head injuries include closed, simple skull vault fractures, concussions with loss of consciousness for less than one hour, cranial nerve injuries and “tiny” brain haematoma (AAAM 2005). In Paper I, the majority of pedestrian crashes was maximum AIS 0–2 (all body regions) although the estimated average vehicle speed was only 29 km/h. A limit of AIS 2+ was therefore deemed appropriate for this study.

Some of the calculated IRs were high which may be a result of the combination of the FE models, the ICs and the injury risk curves used. In real-life pedestrian crashes with forward-moving Volvo passenger cars, 87 head and face AIS2+ injuries were registered in 207 pedestrian collisions (Lindman et al. 2011). Some of the pedestrians likely suffered from multiple head injuries; the risk of obtaining an AIS2+ head or face injury in a pedestrian collision with a Volvo was therefore lower than 42% for the data set although 85% of the vehicle speeds were below 40 km/h.

The IC values and the IRs generally decreased with increasing subject height for all ICs. Since the highest risks occurred during head impact, the head impact location was likely a major cause for this trend. Taller subjects experienced a head impact further up and often on the windscreen

while smaller subjects impacted the bonnet. For THUMS, the varying head masses also likely contributed to this trend. Whether the risk increases further for subjects shorter than the AF05 could not be studied within the scope of this Addendum, but should be further investigated in view of child pedestrians.

For the purely rotational criteria BrIC and RIC, the IRs predicted by the impactor and THUMS did not compare well. Previous studies already pointed out differences in angular kinematics between full-scale and impactor experiments (e.g., Kerrigan et al. 2008). Thus, measuring rotation in the head impactor without changing the test setup is unlikely to provide additional value for predicting real-life injury risk. However, measuring rotation would be recommended in dummy tests or full-body simulations although angular head kinematics in dummies and PMHSs also showed some differences (Kerrigan et al. 2012). As a possible alternative, simulations could be used to determine the boundary conditions for the head impact. The head impactor could be fitted with a neck and an upper body mass, and then be used to impact the vehicle with the boundary conditions determined in the full-body simulations. With this updated test setup, measuring head rotation might give a better prediction of real-life head IRs comprising head rotation. However, this possibility requires further investigation.

5 General Discussion

The main aim of this thesis has been pursued in four parts. Papers I and II examined the linear and angular displacements of the head, shoulder and spine in five new and two earlier full-scale pedestrian tests. From the five new tests, six-degrees-of-freedom kinematics were obtained for the head, several vertebrae, pelvis and scapulae. The epidemiology of shoulder impacts in real-life crashes was investigated in Paper I. In Paper III, the effect of shoulder impact on head kinematics was studied using volunteer and PMHS shoulder impact experiments to evaluate THUMS version 4. Subsequently, THUMS was used to study head response to shoulder impacts with boundary conditions being inspired by pedestrian impacts where the shoulder posture, the angle of the surface impacting the shoulder, and the impact velocity angle were varied. In Paper IV, pragmatic scaling of THUMS was studied as an alternative to morphing to ascertain which technique yielded the more accurate head impact conditions when compared with individual PMHS responses.

5.1 Methods and Analyses in the PMHS experiments

PMHSs can be assumed to be the most accurate available surrogate for humans in pedestrian full-scale tests (Kerrigan et al. 2008). Such tests can be considered ethical if they can be used to develop and validate test tools with the ultimate goal to save lives. However, subject preparation is a race against decay processes, which may alter subject response and reduce its biofidelity. In order to reduce this effect, embalming is sometimes used, although it is unknown how much this alters the subject's response. In the new experiment in Paper I and the experiments in Paper II, a combination of Winckler's embalming method (Winckler 1974), and storage at 4–6°C until the day of the test were used. The subjects all had increased joint stiffness, probably due to the effect of embalming, but the low temperature storage may also have contributed to increased stiffness. The joints were thus moved prior to the experiment in order to remove as much of the additional stiffness as possible. However, as the force necessary to achieve the full range of motion could have caused bone fractures, full removal of the excess stiffness was not possible. However, fresh or fresh-frozen PMHSs lack the body stiffness of a living human. Although the exact effect of the embalming is unknown, it can be argued that a certain amount of stiffness increase might be legitimate.

Subject positioning in pedestrian full-scale experiments with PMHSs is of concern due to lack of muscle activity, as highlighted by a number of previous studies (e.g., Kerrigan et al. 2005b, Subit et al. 2008) that found that it was virtually impossible to move the legs into a certain desired walking position. A final solution to PMHS positioning for pedestrian experiments has, to the best knowledge of the author, not yet been found. The lack of muscle activity also complicates the replication of realistic ground contact forces. The initial suggestion of adding thin wooden sticks to aid maintaining posture (Pritz et al. 1975) has not been in wide use, as this practice is believed to stiffen leg response unnaturally. Dropping the subject some time before the impact did not produce realistic ground force either (Kam et al. 2005). In the past different support systems have been used to hold the subject upright until the moment of impact. In Papers I and II, the installed dropping mechanism used a belt around the neck that was connected to an electromagnet by metal strings (Chalandon et al. 2007). Ishikawa et al. (1993) instead screwed the metal strings to the cranium. Subit et al. (2008) employed an under-shoulder belt around the thorax. However, each support system generated forces in places where they would not exist in a real pedestrian crash,

e.g., causing a slight extension of the neck or a raising of the shoulders. Thus both the support system and the lack of muscle activity limited control over the initial posture of subjects.

In the new experiments in Papers I and II, a new method of video analysis was used enabling the acquisition of 3D translations and 3D rotations of each body part with a single camera. For this film analysis, special photo targets, consisting of a large number of tracking points on a rigid surface had to be used. The coordinates of each tracking point relative to the point of interest, e.g., a head CG or a vertebral body CG, must be known in order for this point of interest to be tracked. If the number of points on each photo target is sufficient, the set of equations used in the film analysis is over-determined permitting error minimisation and improved accuracy. With the method used, the head WAD and lateral offset of the head impact point as measured post-test on the vehicle and when measured with the video analysis were within 1 cm of each other. Thus, it appeared that the accuracy of this new method of video analysis has the potential for considerable improvement in comparison with other video analysis approaches where only one camera is used.

5.2 Experimental Data in HBM Evaluations

Before an HBM can be used, its biofidelity must be evaluated for a load case similar to the intended load case. In the evaluation of the THUMS shoulder in Paper III, the model was evaluated against two lateral shoulder impact experiments with additional oblique anterior and posterior impacts in one of the studies in which spine and head kinematics were evaluated at the same time. Subsequently, based on the evaluation results, the model was used in a similar manner, but with different shoulder postures, angles of the impacting surface, and angles of the impact velocity.

Evaluation of HBMs in pedestrian full-scale simulations is challenging due to the scarcity of pedestrian experiments reported to date as well as the vast number of interdependent variables influencing pedestrian kinematics. Hardly any 6 DOF data on pedestrian kinematics are available, and even 3D translational data are scarce since most full-scale pedestrian studies concern 2D linear kinematics. In addition to Papers I and II, to the best of the author's knowledge, only Forman et al. (2015b) published 6 DOF data where three PMHSs were impacted by a generic sedan buck. For better prediction of TBI, more three-dimensional rotation data are required for the evaluation of head rotation in HBMs. Translational data out of the sagittal plane is needed to improve the prediction of the head impact lateral offset on the vehicle. For evaluation of HBMs and for a better understanding of the human in-crash response, it is obvious that there is an urgent need for detailed experimental data produced in controlled full-scale pedestrian accidents with detailed information on subject anthropometry, initial posture, vehicle model and test boundary conditions. Papers I and II aim to provide such data for use in HBM evaluation of pedestrian crashes.

Normalising experimental data and constructing kinematic corridors in pedestrian crashes is not straight forward. The pelvis–BLE height ratio and the upper arm response affect upper body kinematics considerably, as shown in Papers I, II and IV. These factors cannot be used in traditional normalisation methods. Normalisation methods for pedestrian trajectories during the primary impact have been proposed in several studies (Kerrigan et al. 2005b, Kerrigan et al. 2007, Yanaoka et al. in press). However, the method proposed by Kerrigan et al. (2005b) exhibited considerable limitations when applied to slightly different load cases (Kerrigan et al. 2007), and the method proposed by Yanaoka et al. (in press) remains to be evaluated for a range of test conditions. Both

normalisation methods have since been applied to develop trajectory corridors from normalised, averaged trajectories (SAE J2868 2010, Forman et al. 2015a). However, their corridor boundary calculation methods appear to be somewhat arbitrary and based on pragmatic rather than scientific reasoning. Nusholtz et al. (2010) showed that the average of multiple curves no longer necessarily captures the underlying physics and thus over-simplifies subject responses. If this is true, constructing corridors from averaged trajectories simplifies subject responses to an even greater degree and limit the potential to study the biomechanics in a pedestrian crash. To enable in-depth studies of the biomechanics, investigating the individual experimental data instead of normalised corridors is a more worthwhile approach. This approach allows for the HBM to be compared to and evaluated against individual responses that the author considers to be a valuable contribution to HBM evaluation.

If an HBM's biofidelity is optimised towards a specific load case of certain severity then, in other load cases and severities when linear, non-biological material models are used, the HBM might respond in a non-biofidelic manner. Biological materials are typically non-linear, anisotropic and rate-dependent. Thus, with linear material models, there would be a risk that optimising an HBM's response for low-severity impacts would make the HBM too soft in high-severity impacts, and vice versa. The material models in THUMS 4.0 are mostly non-linear. Most use a Poisson's ratio, Young's modulus, yield stress and tangent modulus to define material behaviour and stress-strain relations. Some use load curves or rate-dependent load curve tables to define material properties. However, the materials used in THUMS 4.0 are all isotropic. In the present work, THUMS was evaluated against impacts from various directions and at various severities. Its biofidelity was generally good in all simulations although the neck tended to be slightly too stiff in lateral bending, and arm abduction was not replicated for large abduction angles.

Compared with a full-scale pedestrian test, the load cases in the shoulder impact experiments used in Paper III were well defined. However, existing shoulder impact studies might not adequately mimic the shoulder impact in a pedestrian crash. The angles of the impacting surface and of the impact velocity in pedestrian shoulder impacts generally differ from those used in earlier shoulder impact studies. Additionally, a pedestrian shoulder may be in a raised posture after elbow–vehicle impact and thus not in a neutral position, such as those used in previous shoulder impact experiments. Although the simulations in Paper III attempted to mimic low severity pedestrian shoulder impacts and yielded reasonable results, these findings should be verified through additional experimental testing since such biomechanical data is currently not available.

Data sets not originally designed for HBM validation might lack important simulation input information. For the experimental data used for Paper III, it was possible to extract all the necessary information from video footage and photographs. In future experiments it would be of great value that all the measurements required for simulation were available. In particular, well-documented subject initial position and well-defined setups would increase the value of such studies.

Generally, additional detailed experimental data is required for HBM validation. Additional data would aid in further studying the biomechanics in pedestrian crashes and in impactor tests, and enable establishing response corridors of adequate statistical significance. While this is true for many load cases in traffic safety, new data is particularly important for pedestrian safety since there are so many factors influencing the kinematics.

5.3 PMHS vs. Volunteers Data in HBM Evaluations

With HBMs in general and with pedestrian HBMs in particular, the question can be raised whether the HBM should replicate a PMHS, a relaxed or a tensed living person, and how a transformation between different muscle activations could be implemented in the model. Ultimately, for real-life crash safety, the HBM should obviously replicate a living person. However, controlled crash testing with living pedestrians on an injurious level is not an option, and detailed in-crash kinematics of pedestrians in real-life crashes are impossible to obtain from accident reconstructions without the help of HBMs (Section 1.6) unless high-speed cameras had recorded such real-life crashes. Thus, full-scale pedestrian crash kinematics of human subjects can currently only be obtained from PMHSs. Two possible approaches can be taken to implement different muscle activations into HBMs. One approach is to estimate the general effect of passive and active musculature, and add it to the model as increased stiffness. This approach seems to have been taken in the development of THUMS (Section 1.7.1). Body-segment testing at low severity with volunteers aids in estimating the increased stiffness of volunteers compared with PMHSs. A second approach is to make the HBM match the PMHS responses and then add active muscles to the model. Active muscles have already been implemented in a previous version of the occupant THUMS (Östh et al. 2012). The second approach is more complex, but it would enable studying the responses of pedestrians whether they were aware or unaware of the imminent crash.

After pelvis impact against the vehicle, the pedestrian PMHSs all displayed neck bending away from the vehicle before the head began catching up with the upper torso. This response was observed in all PMHSs in Forman et al. (2015a), too. In THUMS version 4, no similar neck bending away from the vehicle was observed, indicating that the THUMS neck might be too stiff in lateral bending. However, THUMS should ultimately represent a living human with at least static muscle activation for posture maintenance. Thus, the question can be raised whether the increased neck bending stiffness in THUMS compared with PMHSs is actually biofidelic. Stenlund et al. (2015) exposed volunteers to a perturbation that was similar to a pedestrian pelvis impact, but much lower severity. They observed neck bending similar to the initial neck bending in the full-scale PMHS experiments, but at lower magnitude (Appendix F). This divergence might be partly due to the lack of muscle activation in the PMHSs although the severity in the volunteer tests was much lower than in a vehicle–pedestrian pelvis impact at 40 km/h. As the amount of head rotation increased with increasing severity in the volunteer experiments, a living pedestrian might display considerable head rotation away from the vehicle in the initial stages of the crash. This emphasizes that the THUMS neck is likely too stiff in lateral bending.

5.4 Prevalence of Elbow and Shoulder Impacts

Although the epidemiology presented in Paper I showed that elbow and shoulder impacts were documented in only a minority of the cases, these impacts did not always leave visible damage on the vehicle in the full-scale PMHS experiments in Papers I and II. The frequency of documented elbow and shoulder impacts might therefore not—due to underreporting—mirror the actual frequency, which might be higher. Elbow and shoulder impacts being linked to severe injuries (Paper I) therefore does not necessarily induce these impacts to cause severe injuries.

To further investigate the prevalence of elbow and shoulder impacts in actual car–pedestrian crashes, injury distributions of such crashes are studied. These distributions should be interpreted carefully since they do not normally specify whether a specific injury has occurred during the car–pedestrian impact or during the pedestrian–ground impact. In addition, even if considerable load is transferred, not all elbow and shoulder impacts lead to an injury, as seen in Paper II. However, injury distributions can still give an indication of elbow and shoulder impact prevalence that complements the crash data presented in Paper I. Injuries that might indicate an elbow or shoulder impact are fractures of the humerus, clavicle and scapula, shoulder dislocations and severe bruising.

In an early study (Kong et al. 1996), 273 hospitalised pedestrians, who had been struck by vehicles moving faster than 16 km/h and who had not died at the scene, were examined for injuries. Shoulder fractures were found in 15 (5%) of these pedestrians, and humerus fractures in 14 (5%). In a more recent study, upper extremity fractures in pedestrian–motor-vehicle crashes were specifically named as an underappreciated concern (Landy et al. 2010). The study included 336 adult hospitalised pedestrians of which 25% had sustained upper extremity injuries. A humerus fracture had been sustained by 38 pedestrians (11%). In a similar study, Siram et al. (2011) found upper extremity fractures in 12% of the 79 307 hospitalised adult pedestrians included in their study. In another study, a total of 13 655 adult pedestrians that had been hospitalised after a traffic accident were screened for upper extremity fractures (Rubin et al. 2015). In total, 2 615 (19%) of the pedestrians had sustained upper extremity fractures. Of these fractures, 32% were humerus, 17% were clavicle, 13% were scapula, and 38% were other upper extremity fractures related to the lower arms and hands. Multiple upper extremity fractures had occurred in 18% of the pedestrians suffering from an upper extremity fracture. Thus, between 10–12% of all pedestrians included in their study had experienced a fracture of the humerus, clavicle or scapula.

Previous studies show that a considerable percentage of the hospitalised pedestrians suffered from injuries that could be related to elbow and shoulder impacts with the vehicle. All of these studies excluded pedestrians who had died at the scene, although the accident reconstruction epidemiology (Section 3.2) indicated that both elbow and shoulder impacts were more likely in severe crashes. Overall, this analysis supports the hypothesis that elbow and shoulder impacts against the car may be more frequent than previously reported. Thus, more full-scale PMHS experiments should be made available in which the arms are allowed to move freely to reproduce elbow and shoulder impacts as in real-life pedestrian crashes. Elbow and shoulder impacts should also be reproduced by HBMs that are used to study pedestrian responses during car impacts.

5.5 Simulation Results

For the present work, an FE model was chosen instead of a MB model. Unlike MB models, FE models enable injury assessment by using tissue criteria. Tissue criteria provide more local and thus more accurate injury prediction. They will be especially useful when investigating long-term medical impairment due to brain injury in pedestrians in the future. However, as mentioned in Section 1.7, FE models used in pedestrian crashes have to be evaluated in terms of kinematics before tissue criteria can be applied. Therefore, this thesis focuses on the evaluation of model kinematics rather than on tissue criteria evaluation. The THUMS model was chosen as it was the only full-body FE pedestrian model commercially available at the time, and as it is widely used in industrial and academic environments (Yasuki 2006). Its version 4 was selected mainly because the

shoulder included more anatomical features such as a solid representation of the subscapularis muscle and the capsular ligament, both of which were not included in earlier THUMS versions. Without these features, the arm and shoulder responses could not have been studied in such detail. For instance, in shoulder impacts, the load path from the impact to the spine would likely have been different if the subscapularis would not have been represented as solid elements in the model.

In general, a decision has to be made at which point a human model is biofidelic. Wismans et al. (2005) have established a definition of human body validation as “the process of assessing the reliability of a simulation model in comparison to one or more reference tests with human subjects”, where the experiments used for the validation should not be the same tests that were used for the original model input. According to Shigeta et al. (2009), none of the experiments used for the current work appear to have been used for model input. In addition, well-defined criteria of when the HBM can be regarded as “biofidelic” in a certain load case should be established before the assessment. This was not within the scope of the present work, but should be included in future HBM validation. Establishing such criteria for biofidelity could be done, e.g. by setting a limit of a certain percentage of the simulation results matching the experimental corridors, or by setting minimum values in mathematical methods that compare the shapes of two curves. Applying different approaches, several rating methods attempt to calculate such measures (Rhule et al. 2002, Sprague and Geers 2004, Hovenga et al. 2005, Gehre et al. 2009) with varying results (Vavalle et al. 2013), underlining the difficulty in establishing one single rating method for the biofidelity assessment of HBMs. Furthermore, the question remains how well the corridors display the average responses and the associated spread of the living human population. While these are inherent limitations when discussing any attempts to validate HBMs, the validation process itself helps improve the understanding of human body responses by continuing to bring up new questions that can be addressed with new experimental setups.

5.5.1 Shoulder Impact Simulations

For the shoulder impact component validation in Paper III, the experimental data was not normalised and the THUMS model was not scaled. The THUMS model was designed to simulate a male of around 177 cm stature, around 77 kg weight and adult age (around 30–40 years). In Ono et al. (2005), the average subject standing height, weight, and age were 171 ± 7 cm, 64 ± 12 kg, and 24 ± 1 year. The standing height of the subjects in Bolte et al. (2003) was not given, but the average weight and age were 71 ± 12 kg and 74 ± 8 years. Normalisation can be used to reduce response variations between subjects in an attempt to obtain the response of an average subject (Mertz 1984). Attempts were made to normalise the experimental data from Ono et al. (2005) but an appropriate normalisation factor could not be found. For shoulder deflections, the subject’s shoulder width appeared at first to be a good normalisation factor candidate. In another attempt, scaling based on total subject mass was applied (Eppinger et al. 1984). However, response variation among the subjects was not considerably reduced, which led to both normalisation attempts being discarded. Another candidate could be the effective mass of the impacted subjects. A higher effective mass would lead to a higher contact force and thus generally greater shoulder deflections would be expected. However, since any general trend could not be observed when comparing maximum contact force and maximum shoulder deflection, this approach was as well discarded. Thus, other factors appeared to have influenced the shoulder deflections to a greater extent than the candidates

named above. Such other factors may be the individual size of the scapula, its distance from the spine or the coupling of the scapula to the thorax since the scapular motion over the thorax appears to govern the shoulder response, as discussed in Paper III. Normalising the spine and head kinematics was not attempted since the individual spread was rather small in the non-normalised data. Another approach would have been to scale the HBM to each subject's body proportions, although this would have contradicted the aim of evaluating the original HBM.

Information on the positioning of the subjects in experimental shoulder impact studies was scarce, especially in Bolte et al. (2003). For the simulations in Paper III, the model was positioned, as accurately as possible, according to photo and video footage. However, since there were no exact posture measurements in the experimental studies, it is unknown by how much the posture of the model actually deviated from those of the volunteers and the PMHSs. A study of the influence of posture was outside of the scope of this thesis, but it has been studied elsewhere. Poulard et al. (2014) studied the influence of spine posture on HBM responses in side impacts and compared the responses with previous PMHS tests. They noted some influence of spine posture on the onset and peak timing of spine kinematics. In addition, adjusting the spine posture individually to that of each PMHS improved injury prediction of the HBM. However, the effect of spine posture on response amplitudes was limited. In the experimental data used for the present work, the model was most likely positioned accurately enough for the response deviations to be of minor relevance considering the spread in the experimental data.

Since elbow impacts usually occur before shoulder impacts, the author believes that the elbow impact could reduce head impact velocity more than the shoulder impact. As discussed in Paper III, the time span between first impactor–shoulder contact and the onset of head movement was about 30–40 ms in the volunteer experiments and approximately 20 ms in the higher severity PMHS experiments. The time span in a vehicle–pedestrian crash from first shoulder–vehicle contact to first head–vehicle was 7–30 ms in Paper I and II as well as previous experiments (Kerrigan et al. 2007, Schroeder et al. 2008). With this timing, the author's hypothesis that shoulder impacts might mitigate skull fracture risk is probably incorrect. However, if this time span could be increased by future safety systems providing a similar mechanism, the head impact velocity could be reduced which would reduce head injury risk. After first head–vehicle contact resultant head linear accelerations remained high for a duration of 20 ms in Kerrigan et al. (2009). In Paper II, the time span from shoulder impact to deepest head intrusion was 24–30 ms, and the timespan from head first contact to the deepest intrusion into the windscreens was 7–23 ms. If the head impact is on the lower part of the windscreens then due to shoulder impact, a head–dashboard impact might be avoided or mitigated. Contrariwise, the head rebound might be increased by shoulder impact, increasing the overall head delta v (the velocity difference just before head first contact and just after head separation from the windscreens) and thus potentially increasing head injury risk. As pointed out by Watanabe et al. (2011), the velocity of head and chest varied greatly after shoulder impact in an SUV–pedestrian impact, which induces neck curvature and which might potentially increase neck injury risk.

In the shoulder impact simulations similar to pedestrian shoulder impacts, shoulder posture at the time of impact was shown to influence head kinematics. When the shoulder was elevated or anteriorly elevated, the maximum head displacement in the direction of impact increased by 50% compared with a neutral shoulder position. In vehicle–pedestrian crashes, the ipsilateral shoulder

is likely to be elevated after elbow impact against the vehicle. Thus, the effect of shoulder impacts on head injury risk discussed in the previous paragraph would be enhanced after elbow impacts. In contrast, changing the impactor orientation or the impact velocity direction from lateral to superolateral reduced the maximum head displacement. Thus, the vehicle speed and geometry are likely to change the effect of shoulder impacts on head injury risk. This effect requires further research.

Overall, it appears that shoulder impacts might increase the risk of injury to the head and neck in pedestrian accidents; however, a more accurate risk assessment depends on the load case, as discussed in Paper III. In contrast, elbow impacts might reduce head injury risk since the time span between elbow impact and first contact of the head and the vehicle may be long enough for the velocity difference between the head and the vehicle to be reduced. In Papers I and II, the time spans between elbow and head first contacts varied between 37 and 58 ms, thus considerably longer than the time span between shoulder and head contact. For one subject in Paper II, the elbow even prevented a typical head impact against the vehicle by strongly supporting the upper body.

5.5.2 Full-body Simulations

Pedestrian kinematics are complex and sensitive to initial posture and anthropometry. In Paper IV, the initial posture of each PMHS was reproduced with THUMS from pre-impact photographs and measurements. As detailed in Section 1.7.2, the most accurate method available today to match the anthropometry of an HBM to that of a test subject is morphing. Nevertheless, morphing is time-consuming and requires highly detailed data of the subject's anthropometry. For this reason, in Paper IV, pragmatic scaling methods which were fast to implement with a pre-processor and required only knowledge of the total stature and mass of the subjects were investigated. Due to the large variability between subject responses and since no accepted normalisation method for the experimental kinematics existed at the time of the study, assessment of the scaling method was interconnected with the biofidelity evaluation of THUMS. The THUMS model appeared to provide generally human-like responses. Thus, for this particular vehicle type, the answer to which scaling method provided the most accurate head impact conditions should be valid independent of THUMS biofidelity evaluations.

Between pragmatic scaling and morphing, several intermediate methods can be used to adapt HBMs to subject anthropometries. For instance, Watanabe et al. (2012) scaled THUMS body parts to all available anthropometric measurements provided in the experimental study they used to evaluate THUMS biofidelity. This method is certainly more accurate than pragmatic scaling in adapting THUMS to the subjects since it takes body proportions into account. Nevertheless, its implementation is also more complex. After scaling individual body parts, some further pre-processing may be required to ensure proper node connectivity and element quality. Hu et al. (2012) investigated methods to develop parametric whole-body human FE models to assess the effects of size, age, sex and obesity on injury risk of occupants in frontal crashes. Although they favoured morphing HBMs to individual PMHSs for HBM biofidelity validation, they recognised that PMHS experiments with full-body CT scans are scarce. As an intermediate solution, and for a statistical HBM anthropometry assessing injury risks for a wider range of the population, they proposed a method similar to morphing using statistical landmark data from bone geometry, outer body scans and posture data. Using this method, the shape of organs and other soft tissue inside the body is estimated. Thus, although more accurate in matching anthropometrical data than

pragmatic scaling or scaling of body parts, their proposed method is still less accurate than complete, full-body morphing. Although the importance of matching any HBM's anthropometry to individual subjects has been widely acknowledged, particularly in pedestrian–car crash simulations, little is known about how accurately anthropometry be matched in order to obtain accurate kinematics and injury predictions. Future research into more complex scaling and morphing techniques is expected to provide further insight into this matter.

THUMS was generally numerically stable. Some premature terminations due to numerical issues were encountered during and after positioning of the model. These terminations were caused mainly by negative volumes in the ankle ligaments, where the positioning resulted in highly skewed elements. The elements were probably skewed because these particular parts did not get enough simulation time to relax during the positioning. Thus, increasing the simulation time from 150 ms to 300 ms for soft tissue stabilisation would probably have prevented these numerical issues. Poulard et al. (2015) developed a framework for adjusting the THUMS spine posture and found that matching the posture was achieved after 150 ms of simulation time whereas the soft tissue stabilised after 300 ms. In the present work, where their method had not yet been adopted, the numerical issues no longer occurred after the skewed elements in the ankle ligaments were straightened manually. The final simulations usually terminated normally. In four simulations, negative volumes occurred in the soft tissue around the contralateral shoulder, causing premature error terminations. This issue was resolved by adding an internal contact to the affected soft tissue.

In the Addendum to this thesis (Chapter 4), it was shown that full-scale THUMS simulations can provide additional head injury risk information to pedestrian safety system developers which is not covered by head impactor testing or simulations. The BrIC and the RIC₃₆ recorded with THUMS were not replicated by the impactor simulations. In addition, a reduction of HIC₁₅-values was not associated with an equally large reduction of BrIC.

5.6 Implications for HBM Development and Physical Testing

The pelvis, spine, upper arm and shoulder responses appeared to influence head kinematics considerably in full-scale pedestrian crashes (Section 3.1). This influence has implications for the development of HBMs, future PMHS testing and regulatory testing.

In Paper III, it was found that THUMS 4.0 is a suitable tool for studying head linear and angular kinematics following shoulder impact in pedestrian accidents. However, head twist was considerably higher in the model compared with the volunteers. Neck stiffness with respect to neck axial rotation should therefore be adjusted in THUMS version 4. The model compared better with tensed than with relaxed volunteers, indicating that a certain amount of muscle tension had been added to the stiffness of the model during development. These observations should be taken into account if, in the future, THUMS will be fitted with active musculature.

The scapular motion over the thorax governed shoulder response and load transfer from the surface impacting the shoulder to the upper body in the model (Paper III). The motion of the scapula over the thorax was influenced by impact direction and shoulder posture. Scapula size and geometry are expected to play a role in different individuals as well. In posterior impacts, the scapula was mainly pushed against the ribs with reduced ability to slide over the rib cage. Lateral and anterior impacts, in contrast, allowed the scapula to slide medially over the thorax, increasing

shoulder deflections. Supero-lateral impacts did not produce significant variations in shoulder deflection as long as the scapular movement engaged the thorax and spine. However, when both the angle of the impacting surface and the impact velocity angle were changed to 30° and 45°, respectively, the scapula moved and rotated mainly downwards, reducing the scapula–thorax and scapula–spine coupling. With elevated shoulders, the medial edge of the scapula was rather close to the spine, which led to enhanced coupling between the scapula and the spine. Thus, measuring scapula geometry and orientation in neutral and elevated postures in future shoulder impact tests is recommended. Additional shoulder impact experiments with elevated as well as elevated and anteriorly displaced shoulders are suggested to experimentally corroborate the simulation findings in Paper III, since shoulder posture had considerable influence on head linear displacements.

Peak head velocity relative to the vehicle often occurs before head impact (Section 1.6). To date, to the best knowledge of the author, a thorough explanation has not been found for this phenomenon. One implication from the findings in Papers I, II and III is that elbow and shoulder impacts contribute to the head reducing its velocity relative to the vehicle while at the same time limiting the downward motion of the upper body.

For future full-scale pedestrian experiments, the implications of this work are, that although binding the hands together reduces variability, the resulting kinematics might not represent those in actual car–pedestrian crashes. Binding the hands together restrains upper arm movement and is thereby likely to prevent elbow impacts in which the upper arm provides considerable support to the upper torso, thus affecting head kinematics and head impact velocity.

For HBM development, this work implies that the biofidelic kinematics of the spine, especially the neck, the arm and the shoulder are important to accurately assess head kinematics and, ultimately, head injuries.

Current test protocols in Euro NCAP use only one impact speed (11.1 m/s) and one impact angle (65° to ground for the adult head impactor) and do not measure head rotation. The author believes that head injury risk cannot be fully assessed with this method. Upper body kinematics varied considerably with different vehicles used, although vehicle speeds were consistently about 11 m/s (e.g., Kerrigan et al. 2005a, Kerrigan et al. 2005b, Subit et al. 2008, Watanabe et al. 2012). As a result, head impact velocities and head impact angles with respect to ground varied considerably between different vehicles. Resultant head velocities relative the vehicle immediately before head impact were lowest in impacts with a SUV type vehicle (Kerrigan et al. 2005b), around 7–9 m/s. In impacts with a medium sized sedan (Subit et al. 2008), a small city car, (Subit et al. 2008) or a small sedan (Kerrigan et al. 2005a), head impact velocities of around 11–14 m/s had been measured in previous studies. In Paper II, head impact velocities ranged between 8.7 and 14.5 m/s. However, the exact value was dependent on the method used to calculate head impact velocity, i.e., on filtering as well as on whether and for which time span head velocity was averaged. A longer time span for averaging generally led to higher head impact velocities since the head velocity relative to the vehicle generally peaked 10–25 ms before first head–vehicle contact and then decreased. Head impact angles with respect to ground appeared to be similar in impacts with the SUV type vehicle and the medium size sedan, nearly 90°. In contrast, the head trajectory was much flatter in an impact with the small sedan or the small city car, where the head impact angle with respect to ground was much lower and estimated at around 30–45°. Head impactor testing

should therefore at least take into account a larger range of head impact velocities and angles, ideally based on full-scale experiments or full-scale simulations with a similar vehicle front. A risk of at least mild TBI even prior to head–vehicle impact is present, as shown in Paper II. In future regulatory testing, head rotation should therefore be measured. Since head rotation before head impact might contribute to TBI and since the current head impactor testing would not capture this rotation, full-scale testing or simulation is recommended.

5.7 Implications for Safety Systems

The findings from this work can also be applied to develop new, or to enhance existing pedestrian safety systems. The reasoning in this section is valid for adult pedestrians. For children and shorter persons, lower pelvis to BLE height ratios may lead to different kinematics, and thus to different conclusions.

From the head impact velocities mentioned in Section 5.6, the conclusion that an SUV vehicle type provides the lowest risk for fatal injuries in pedestrians should not be drawn. The pelvis kinematics presented in Kerrigan et al. (2005b) indicate that the pelvis might be at a high risk of injury, followed by a presumably high load on the thorax during contact with the BLE. As mentioned in Section 1.1, thoracic injuries alone would have been the principal cause of fatalities in nearly 50% of the fatal cases in Lau et al. (1998), although they may not appear in other statistics because they often coincide with fatal head injuries. Thus, the slightly reduced head impact velocity observed in experiments with SUVs might, all things considered, not be as beneficial if it is accompanied by a considerably higher thoracic injury risk. Several studies have attempted to optimise vehicle front geometries for pedestrian protection. Kausalyah et al. (2014) used an adult and a child MB model and minimised HIC while excluding front shapes that caused run-overs. The optimum front for the child model was similar to an SUV shape. However, considering that they did not use any other injury criterion apart from HIC, this result is hardly surprising. Zhao et al. (2010) also optimised the vehicle front for HIC only, but used four sizes of pedestrian MB models and found the vehicle shape with the optimal HIC trade-off for all pedestrian sizes. Their optimised shape had a low, horizontal bonnet reminiscent of a sedan-type vehicle. Carter et al. (2005) conducted a similar study in which they used HIC and a maximum thorax centre of gravity acceleration of 60 g for 3 ms or longer. However, the thoracic injury criterion was given a lower weight compared with the HIC. As a result, the optimised shape had a BLE which was at shoulder height for a 6 year-old child and at lower ribcage height for a 5th percentile female model, both of which exceeded the thoracic injury criterion. While previous studies appear to be inconclusive in terms of which is the optimum vehicle front shape for pedestrian protection, they clearly show that the resulting optimum shape depends on the optimisation input and the injury criteria used. The author of this thesis believes that a sedan type of vehicle or a sports car would be most beneficial in terms of overall pedestrian injury risk. The front shapes of these vehicles appear to result in the longest time span from first contact to head impact so that by deploying safety systems enough time might be available for the head velocity difference relative the vehicle to be reduced.

Furthermore, the present study has shown that impacts of the upper extremities, i.e., elbow and shoulder impacts, considerably influence head kinematics. Elbow impacts appear to be a factor in reducing the velocity difference between the head and the vehicle prior to head impact. In contrast, with a given relative head–vehicle velocity, shoulder impacts appear to occur too close in

time to head–vehicle first contact for them to reduce the head–vehicle velocity. Instead, shoulder impacts might even increase injury risk as the head rotational velocity appears to increase. The observations from elbow and shoulder impacts have implications for the design of pedestrian safety systems. The author believes that increasing the time span between elbow/shoulder–vehicle contact and head contact would be beneficial since the increased time span would allow for a reduction of the velocity difference between head and vehicle prior to head impact. Such an earlier impact could be achieved by raising the pop-up bonnet even further or by pedestrian airbags that are thicker and cover a larger bonnet area than those currently available. Such systems would even be beneficial for smaller pedestrians who might not experience an elbow impact that would considerably support the upper torso. In such cases, the systems would mimic an elbow impact and initiate load transfer to the head at an earlier stage.

5.8 Contributions

This work contributes to pedestrian safety in several ways. The kinematics and biomechanics of car–pedestrian crashes have been studied in depth with particular focus on the effect of pelvis, spine, upper arm and shoulder responses on head kinematics.

Novel 6DOF kinematics of the head, spine, shoulders and pelvis of five subjects were published together with detailed information on subject anthropometry, initial posture and test boundary conditions. To the best knowledge of the author, to date, this is the only data set with more than three subjects, 6DOF kinematics and detailed subject information. This data set can be used by other researchers and industry for HBM evaluation.

One HBM, the THUMS version 4, was evaluated against this data set. Other researchers and industry can use this information to improve THUMS. In the process of this work, an FE vehicle model was developed and validated. This vehicle model can be used as is or further developed to study a bigger range of load cases.

The THUMS model in pure shoulder impacts was evaluated against volunteer and PMHS data, and compared with functional biomechanics. The importance of biofidelic scapula motion over the thorax and of biofidelic spine motion for human-like head kinematics was highlighted. This knowledge can be used to evaluate other models, not only for pedestrian safety but also for occupant safety in side impacts. THUMS was then used to investigate how shoulder impacts similar to those in full-scale pedestrian crashes influenced head kinematics.

The influence of varying pedestrian anthropometry and minor variations in initial posture, pelvic sliding over the bonnet, spine bending and the arm–shoulder complex interaction with the vehicle on head kinematics was assessed. Various implications for future studies arose from this work. In full-scale testing, anthropometry and initial posture should be documented in detail. Arm movement should not be constrained, e.g., by binding the hands together. Ipsilateral upper arm kinematics should also be recorded.

Full-scale pedestrian experiments and THUMS were used to evaluate pragmatic scaling techniques with respect to their ability to predict head impact conditions. This assessment enables other researchers and industry to quickly adapt their HBMs to experimental subjects without the need for morphing, although the limitations of this assessment must be taken into account.

6 Conclusions

The main aim of this thesis has been to enhance the understanding of six-dimensional head translational and rotational kinematics in car–pedestrian crashes prior to head impact against a vehicle. Particular focus was put on the influence of pelvic sliding over the bonnet, spine bending and arm–shoulder-complex interaction on head kinematics. Furthermore, varying pedestrian anthropometries and minor variations in pedestrian initial posture were studied.

Six-dimensional kinematics of the head, spine, pelvis and shoulders were quantified in five new full-scale pedestrian PMHS experiments. Since detailed subject anthropometry, initial posture and test boundary conditions are reported, this data set is highly useful for HBM evaluation. Varying anthropometry and minor variations in initial posture influenced pelvic sliding over the bonnet and ipsilateral upper arm responses which, in turn, changed the head kinematics. Pelvic sliding over the bonnet appeared to be governed by the pelvis–BLE height ratio and tended to increase the WAD and peak head velocity. The ipsilateral upper arm response determined the amount of support the upper arm provided to the upper torso after elbow–vehicle impact. With an increase in upper arm support head impact velocity was generally reduced.

In real-life pedestrian crashes, elbow and shoulder impacts were documented in only a minority of the cases. However, analysis of pedestrian upper extremity injuries indicated that elbow and shoulder impacts might be more common than previously reported. These findings support the hypothesis that elbow and shoulder impacts are important to take into account in pedestrian safety.

THUMS version 4 was, in general, biofidelic compared with volunteer and PMHS experiments in pure shoulder impacts. The model generally compared better with tensed than with relaxed volunteers. Elevating the THUMS shoulder increased head linear displacement compared with the neutral shoulder posture. Changing the impact direction or the impactor orientation from lateral to supero-lateral generally reduced head linear displacements. In full-scale pedestrian simulations, THUMS showed generally biofidelic responses although the upper arm abduction can be improved to better replicate large abductions. THUMS biofidelity was assessed in combination with pragmatic scaling methods in terms of their ability to predict head impact conditions. The results showed that upper arm response considerably influenced head kinematics and head impact conditions. Both in pure shoulder impacts and in full-scale pedestrian simulations, the THUMS neck appeared to be slightly too stiff in lateral bending. Nevertheless, THUMS was a good tool to study biomechanics and kinematics in car–pedestrian crashes.

Overall, the findings in this thesis increase the knowledge on how pedestrian upper-body 6DOF kinematics influence head kinematics. They highlight the importance of elbow and shoulder impacts and will thereby contribute to increase the quality of testing and simulating. This work hopes to serve as inspiration for novel pedestrian safety systems that will decrease pedestrian fatalities and mitigate pedestrian injuries.

7 Future Work

As detailed in Section 1.8, many areas of pedestrian crash safety still remain unaddressed. Further detailed experimental full-scale pedestrian PMHS 6DOF kinematics including detailed information on pedestrian anthropometry, initial stance and test boundary conditions should be made publicly available for HBM and dummy evaluation. Pelvis, upper arm and spine kinematics should be closely monitored in these tests. In order to cover a wider range of real-life crashes and to ultimately develop appropriate normalisation techniques and kinematic corridors the tests should include variations in pedestrian size and vehicle model.

Pedestrian kinematics after head–vehicle contact in full-scale PMHS experiments have still not been published, to the best knowledge of the author. Although recording such kinematics is technically challenging since, in the flight phase, the PMHSs tend to rotate around multiple axes much more than during impact against the vehicle, post-vehicle-impact kinematics are much needed for the evaluation of all kinds of pedestrian HBMs. Validating HBMs for the flight phase and secondary impact would help to assess injury risk during secondary impact and enable development of pedestrian safety systems for secondary impact.

Other experimental pedestrian kinematics that are not yet publicly available include those in impacts against other areas of a vehicle such as the front corners or the vehicle rear side. Various other vehicle geometries have not been experimentally tested with full-scale pedestrian PMHSs, such as busses and trucks, or future vehicle geometries.

If THUMS is used to further improve pedestrian safety, the next steps are to improve THUMS to better capture arm abduction and spine motion, particularly neck lateral bending. THUMS can then be used to investigate how current regulatory testing could be improved to facilitate a more detailed assessment of head injury risk. When combined with a detailed brain model, THUMS can be used to evaluate global head injury criteria.

Another area where knowledge is lacking is child pedestrian safety. Ethical concerns and availability severely limit the possibilities to conduct full-scale PMHS experiments with children. However, simulations with future pedestrian child HBMs could considerably improve pedestrian safety for children.

Equally, other population groups might not be adequately represented by current testing and simulation methods. Among these are the obese, the elderly, pregnant and other groups with body proportions that considerably deviate from the average male.

In the future, a larger vehicle speed range should also be addressed, including both higher and lower speeds than currently tested. At lower vehicle speeds, pedestrian muscle activity is expected to play an increasingly important role. Thus, implementation of active muscles in pedestrian HBMs is an additional goal for the future.

References

- AAAM (2005) "The Abbreviated Injury Scale 2005. Update 2008.". American Association for Automotive Medicine (AAAM), Des Plaines, IL,
- Akiyama, A., M. Okamoto and N. Rangarajan (2001). "Development and application of the new pedestrian dummy". International Technical Conference on the Enhanced Safety of Vehicles (ESV), Amsterdam, The Netherlands.
- Akiyama, A., S. Yoshida, T. Matsuhashi, N. Rangarajan, T. Shams, H. Ishikawa and A. Konosu (1999). "Development of Simulation Model and Pedestrian Dummy", SAE Technical Paper.
- Antona-Makoshi, J., J. Davidsson, S. Ejima and K. Ono (2015). "Development of a comprehensive injury criterion for moderate and mild traumatic brain injuries". JSAE Annual Congress (Spring), Pacifico Yokohama, Japan.
- Arregui-Dalmases, C., F. J. Lopez-Valdes and M. Segui-Gomez (2010) "Pedestrian injuries in eight European countries: An analysis of hospital discharge data". Accident Analysis and Prevention 42: 1164-1171.
- Ashton, S. J., D. Césari and J. van Wijk (1983) "Experimental Reconstruction and Mathematical Modelling of Real World Pedestrian Accidents".
- Badea-Romero, A. and J. Lenard (2013) "Source of head injury for pedestrians and pedal cyclists: Striking vehicle or road?". Accident Analysis and Prevention 50: 1140-1150.
- Baker, M. (2006). "W(t) in terms of matrices." Retrieved November 02, 2015, from <http://www.euclideanspace.com/physics/kinematics/angularvelocity/mark.htm>.
- Bernstein, J. (2003). "Musculoskeletal Medicine". Rosemont, IL, American Academy of Orthopaedic Surgeons.
- Bolte, J. H., M. H. Hines, R. G. Herriott, J. D. McFadden and B. R. Donnelly (2003) "Shoulder impact response and injury due to lateral and oblique loading". Stapp Car Crash Journal 47: 35-53.
- Bolte, J. H., M. H. Hines, J. D. McFadden and R. A. Saul (2000) "Shoulder response characteristics and injury due to lateral glenohumeral joint impacts". Stapp Car Crash Journal 44: 261-280.
- Brach, R. M. (2015) "Reconstruction of Vehicle-Pedestrian Collisions Including an Unknown Point of Impact". SAE Technical Paper 2015-01-1419.
- Breen, J. (2002). "European Priorities for Pedestrian Safety". Pedestrian Safety Seminar, Sydney, Australia.
- Brun-Cassan, F., J. C. Vincent, C. Tarrière, A. Fayon, D. Césari, C. Cavallero and G. Mauron (1984) "Comparison of Experimental Car-Pedestrian Collisions Performed with Various Modified Side-Impact Dummies and Cadavers".
- Carter, E., S. Ebdon and C. Neal-Sturgess (2005). "Optimization of Passenger Car Design for the Mitigation of Pedestrian Head Injury Using a Genetic Algorithm". The Genetic and Evolutionary Computation Conference (GECCO), Washington DC, ACM Press.
- Carter, E. L., C. E. Neal-Sturgess and R. N. Hardy (2008) "APROSYS in-depth database of serious pedestrian and cyclist impacts with vehicles". International Journal of Crashworthiness 13(6): 629-642.
- Cavallero, C., D. Césari, M. Ramet, P. Billault, J. F. Farisse, B. Seriat-Gautier and J. Bonnoit (1983) "Improvement of Pedestrian Safety: Influence of Shape of Passenger Car-Front Structures Upon Pedestrian Kinematics and Injuries: Evaluation Based on 50 Cadaver Tests".

- Cavanaugh, J. M., T. Walliko, A. Malhotra, Y. Zhu and A. I. King (1990) "Biomechanical Response and Injury Tolerance of the Pelvis in Twelve Sled Side Impacts". SAE Technical Paper.
- Césari, D., M. Ramet, C. Cavallero, P. Billault, J. Gambarelli, G. Guérinel, J. F. Farisse and P. Bourret (1980). "Experimental Study of Pedestrian Kinematics and Injuries". International Research Council on the Biomechanics of Impact (IRCOBI), Birmingham, England.
- Chalandon, S., T. Serre, C. Masson, F. Minne, P.-J. Arnoux, C. Perrin, P. Borde, C. Cotte, C. H. Brunet and D. Césari (2007). "A Comparative Study Between Subsystem and Global Approaches for the Pedestrian Impact". Enhanced Safety of Vehicles (ESV), Lyon, France.
- Chang, D. (2008) "National Pedestrian Crash Report". National Highway Traffic Safety Administration (NHTSA), Washington,
- Chawla, A., S. Mukherjee, D. Mohan and A. Parihar (2005). "Validation of the cervical spine model in THUMS". Enhanced Safety of Vehicles (ESV), Washington D.C., USA.
- Cheng, H., L. Obergefell and A. Rizer (1996). "The development of the GEBOB program". 15th Southern Biomedical Engineering Conference, Dayton, OH.
- Compigne, S., Y. Caire, T. Quesnel and J.-P. Verriest (2004) "Non-injurious and injurious impact response of the human shoulder three-dimensional analysis of kinematics and determination of injury threshold". Stapp Car Crash Journal 48: 89-123.
- Depriester, J.-P., C. Perrin, T. Serre and S. Chandalon (2005). "Comparison of several methods for real pedestrian accident reconstruction". Enhanced Safety of Vehicles (ESV), Washington D.C. .
- Desai, C., G. Sharma, P. Shah, C. Ageorges, C. Mayer and D. Fressmann (2012). "A generic positioning tool for human body FE models". International Research Council on the Biomechanics of Injury (IRCOBI), Dublin, Ireland.
- Elemance. (2015). "Elemance Services & Specialties." Retrieved November 02, 2015, from <http://www.elemance.com/services>.
- Elliott, J. R., C. K. Simms and D. P. Wood (2012b) "Pedestrian head translation, rotation and impact velocity: The influence of vehicle speed, pedestrian speed and pedestrian gait". Accident Analysis and Prevention 45: 342-353.
- Eppinger, R. H., J. H. Marcus and R. M. Morgan (1984) "Development of Dummy and Injury Index for NHTSA's Thoracic Side Impact Protection Research Program". SAE Technical Paper 840885.
- Eppinger, R. H., E. Sun, F. Bandak, M. Haffner, N. Khaewpong, M. Maltese, S. Kuppa, T. Nguyen, E. G. Takhounts, R. Tannous, A. Zhang and R. Saul (1999) "Development of Improved Injury Criteria for the Assessment of Advanced Automotive Restraint Systems - II". National Highway Traffic Safety Administration (NHTSA),
- Euro NCAP (2014a) "Pedestrian Testing Protocol". European New Car Assessment Programme (Euro NCAP),
- Farisse, J. F., B. Seriat-Gautier, J. Dalmas, N. Daou, P. Bourret, C. Cavallero, D. Césari, M. Ramet, P. Billault and M. Berthommier (1981). "Anatomical and Biomechanical Study of Injuries Observed During Experimental Pedestrian-Car Collisions". International Research Council on the Biomechanics of Impact (IRCOBI), Salon de Provence, France.
- Fildes, B., C. H. Gabler, D. Otte, A. Linder and L. Sparke (2004). "Pedestrian Impact Priorities Using Real-World Crash Data and Harm". International Research Council on the Biomechanics of Injury (IRCOBI), Graz, Austria.

- Forman, J. L., H. Joodaki, A. Forghani, P. Riley, V. Bollapragada, D. Lessley, B. Overby, S. Heltzel and J. Crandall (2015a). "Biofidelity Corridors for Whole-Body Pedestrian Impact with a Generic Buck". International Research Council on the Biomechanics of Injury (IRCOBI), Lyon, France.
- Forman, J. L., H. Joodaki, A. Forghani, P. O. Riley, V. Bollapragada, D. J. Lessley, B. Overby, S. Heltzel, J. R. Kerrigan and J. R. Crandall (2015b) "Whole-body response for pedestrian impact with a generic sedan buck". *Stapp Car Crash Journal* 59.
- Fredriksson, R., E. Rosén and A. Kullgren (2010) "Priorities of Pedestrian Protection—A Real-Life Study of Severe Injuries and Car Sources". *Accident Analysis and Prevention* 42(6): 1672-1681.
- Gabler, L. F., M. B. Panzer and J. R. Crandall (2014). "On the Application of BrIC to the Biomechanics of Various Automotive Impact Scenarios". Proceedings of the Forty Second International Workshop on Human Subjects for Biomechanical Research, San Diego, CA.
- Gehre, C., H. Gades and P. Wernicke (2009). "Objective Rating of Signals using Test and Simulation Responses". Enhanced Safety of Vehicles (ESV), Stuttgart, Germany.
- Gennarelli, T. A., A. K. Ommaya and L. E. Thibault (1971). "Comparison of Translational and Rotational Head Motions in Experimental Cerebral Concussion". 15th Stapp Car Crash Conference, Coronado, CA.
- Gennarelli, T. A., L. E. Thibault and A. K. Ommaya (1972). "Pathophysiologic Responses to Rotational and Translational Accelerations of the Head". 16th Stapp Car Crash Conference, Detroit, MI.
- Goldstein, H. (2000). "Classical Mechanics, 3rd ed.". Reading, MA, Addison-Wesley.
- Gray, H. (2008). "Gray's Anatomy". Edinburgh, Churchill Livingstone-Elsevier
- Haddon, W. J. (1980) "Options for the prevention of motor vehicle crash injury". *Israeli Journal of Medical Sciences*(16): 45-65.
- Hamacher, M., L. Eckstein and R. Paas (2012). "Vehicle related influence of post-car impact pedestrian kinematics on secondary impact". International Research Council on the Biomechanics of Injury (IRCOBI), Dublin, Ireland.
- Hardy, R. (2009) "APROSYS - Final Report for the Work on "Pedestrian and Pedal Cyclist Accidents" (SP3)". Cranfield Impact Centre, AP-90-0003
- Harruff, R. C., A. Avery and A. S. Alter-Pandya (1998) "Analysis of Circumstances and Injuries in 217 Pedestrian Traffic Fatalities". *Accident Analysis and Prevention* 30(1): 11-20.
- Haug, E., H.-Y. Choi, S. Robin and M. Beaugonin (2004). "Human Models for Crash and Impact Simulation". In *Handbook of Numerical Analysis, Special Volume: Computational Models for the Human Body*. N. Ayache. Amsterdam, The Netherlands, Elsevier. XII.
- Hirsch, A. E. and A. K. Ommaya (1970). "Protection from Brain Injury: THE Relative Significance of Translational and Rotational Motions of the Head after Impact". 14th Stapp Car Crash Conference, New York.
- Holbourn, A. H. S. (1943) "The mechanics of head injuries". *The Lancet* 2(6267): 438-441.
- Hovenga, P., H. Spit, M. Uijldert and A. Dalenoort (2005) "Improved Prediction of Hybrid-III Injury Values Using Advanced Multibody Techniques and Objective Rating".
- Hu, J., J. D. Rupp and M. P. Reed (2012) "Focusing on Vulnerable Populations in Crashes: Recent Advances in Finite Element Human Models for Injury Biomechanics Research". *Journal of Automotive Safety and Energy* 3(4): 295-307.
- Humanetics Innovative Solutions. (2013). "Hybrid III 50th Pedestrian." Retrieved October 2, 2013, from <http://www.humaneticsatd.com/crash-test-dummies/pedestrian/hybrid-iii-50th>.

- IRTAD (2014) "Road Safety Annual Report 2014". International Traffic Safety Data and Analysis Group (IRTAD), Organisation for Economic Co-operation and Development (OECD),
- Irwin, A. L., T. J. Walilko, J. M. Cavanaugh, Y. Zhu and A. I. King (1993). "Displacement Responses of the Shoulder and Thorax in Lateral Sled Impacts". Stapp Car Crash Conference, Warrendale, PA, USA.
- Ishikawa, H., J. Kajzer and G. Schroeder (1993). "Computer Simulation of Impact Response of the Human Body in Car-Pedestrian Accidents". Stapp Car Crash Conference, San Antonio, US.
- Iwamoto, M., Y. Kisanuki, I. Watanabe, K. Furusu, K. Miki and J. Hasegawa (2002). "Development of a finite element model of the total human model for safety (THUMS) and application to injury reconstruction". International Research Council on the Biomechanics of Injury (IRCOBI), Munich, Germany.
- Jakobsson, L., T. Broberg, H. Karlsson, A. Fredriksson, N. Gråberg, C. Gullander and M. Lindman (2013). "Pedestrian Airbag Technology – A Production System". Enhanced Safety of Vehicles (ESV), Seoul, Republic of Korea.
- Jani, D., A. Chawla, S. Mukherjee, R. Goyal and V. Nataraju (2009a) "Repositioning human body lower extremity FE model". SAE Technical Paper 2009-01-0922.
- Jani, D., A. Chawla, S. Mukherjee, R. Goyal and V. Nataraju (2009b). "Human body FE model repositioning: A step towards posture specific - human body models (PS-HBM)". International Research Council on the Biomechanics of Injury (IRCOBI), York, UK.
- Jarrett, K. L. and R. A. Saul (1998). "Pedestrian Injury - Analysis of the PCDS Field Collision Data". International Technical Conference on the Enhanced Safety of Vehicles (ESV), Windsor, Ontario, Canada.
- Kallieris, D. and G. Schmidt (1988) "New Aspects of Pedestrian Protection Loading and Injury Pattern in Simulated Pedestrian Accidents". SAE Technical Paper 881725.
- Kam, C. Y., J. Kerrigan, M. Meissner, C. Drinkwater, D. Murphy, J. Bolton, C. Arregui, R. Kendall, J. Ivarsson, J. Crandall, B. Deng, J. T. Wang, C. Kerkeling and W. Hahn (2005). "Design of a Full-Scale Impact System for Analysis of Vehicle Pedestrian Collisions". SAE World Congress, Detroit, Michigan.
- Kausalyah, V., S. Shasthri, K. A. Abdullah, M. M. Idres, Q. H. Shah and S. V. Wong (2014) "Optimisation of vehicle front-end geometry for adult and pediatric pedestrian protection". International Journal of Crashworthiness 19(2): 153-160.
- Kebaetse, M., P. McClure and N. A. Pratt (1999) "Thoracic Position Effect on Shoulder Range of Motion, Strength, and Three-Dimensional Scapular Kinematics". Archives of Physical Medicine and Rehabilitation 80: 945-950.
- Kerrigan, J. R., C. Arregui-Dalmases and J. R. Crandall (2012) "Assessment of pedestrian head impact dynamics in small sedan and large SUV collisions". International Journal of Crashworthiness 17(3): 243-258.
- Kerrigan, J. R., C. Arregui and J. R. Crandall (2009). "Pedestrian Head Impact Dynamics: Comparison of Dummy and PMHS in Small Sedan and Large SUV Impacts". International Technical Conference on the Enhanced Safety of Vehicles (ESV), Stuttgart, Germany.
- Kerrigan, J. R., J. R. Crandall and B. Deng (2007) "Pedestrian kinematic response to mid-sized vehicle impact". International Journal of Vehicle Safety 2(3): 221-240.
- Kerrigan, J. R., J. R. Crandall and B. Deng (2008) "A Comparative Analysis of the Pedestrian Injury Risk Predicted by Mechanical Impactors and Post Mortem Human Surrogates". Stapp Car Crash Journal 52: 527-567.

- Kerrigan, J. R., C. Y. Kam, D. Drinkwater, D. Murphy, D. Bose, J. Ivarsson and J. R. Crandall (2005b). "Kinematic Comparison of the Polar II and PMHS in Pedestrian Impact Tests with a Sport-Utility Vehicle". International Research Council on the Biomechanics of Injury (IRCOBI), Prague, Czech Republic.
- Kerrigan, J. R., D. B. Murphy, D. C. Drinkwater, C. Y. Kam, D. Bose and J. R. Crandall (2005a). "Kinematic Corridors for PMHS Tested in Full-Scale Pedestrian Impact Tests". International Technical Conference on the Enhanced Safety of Vehicles (ESV), Washington D.C., US.
- Kimpara, H. and M. Iwamoto (2012) "Mild Traumatic Brain Injury Predictors Based on Angular Accelerations During Impacts". *Annals of Biomedical Engineering* 40(1): 114-126.
- Kleiven, S. (2007) "Predictors for traumatic brain injuries evaluated through accident reconstructions". *Stapp Car Crash Journal*(51): 81-114.
- Koh, S. W., J. M. Cavanaugh and J. Zhu (2001) "Injury and Response of the Shoulder in Lateral Sled Tests". *Stapp Car Crash Journal* 45: 101-141.
- Kong, L. B., M. Lekawa, R. A. Navarro, J. McGrath, M. Cohen, D. R. Margulies and J. R. Hiatt (1996) "Pedestrian-motor vehicle trauma: an analysis of injury profiles by age". *Journal of the American College of Surgeons* 182(1): 17-23.
- Kramer, M., K. Burow and A. Heger (1973) "Fracture Mechanism of Lower Legs Under Impact Load".
- Krieger, K. W., A. J. Padgaonkar and A. I. King (1976) "Full-Scale Experimental Simulation of Pedestrian-Vehicle Impacts".
- Landy, D. C., R. A. Norton, J. A. Barkin, S. Henriques, P. Owens and R. A. Miki (2010) "Upper extremity fractures in pedestrian versus motor vehicle accidents: an underappreciated concern". *Iowa Orthopaedic Journal* 30: 99-102.
- Lau, G., E. Seow and E. S. Lim (1998) "A review of pedestrian fatalities in Singapore from 1990 to 1994". *Annals of the Academy of Medicine, Singapore* 27(6): 830-837.
- Leijdesdorff, H. A., J. T. J. M. van Dijck, P. Krijnen, C. L. A. M. Vleggeert-Lankamp and I. B. Schipper (2014) "Injury Pattern, Hospital Triage, and Mortality of 1250 Patients with Severe Traumatic Brain Injury Caused by Road Traffic Accidents". *Journal of Neurotrauma* 31: 459-465.
- Lindman, M., L. Jakobsson and S. Jonsson (2011). "Pedestrians interacting with a passenger car; a study of real world accidents". International Research Council on the Biomechanics of Injury (IRCOBI), Krakow (Poland).
- Lindman, M., A. Ödblom, E. Bergvall, A. Eidehall, B. Svanberg and T. Lukaszewicz (2010). "Benefit Estimation Model for Pedestrian Auto Brake Functionality". 4th International ESAR Conference, Hanover, Germany.
- Longhitano, D. (2009). "Protecting Pedestrians Through Vehicle Design - Advancements Can Reduce Pedestrian Injury in Collisions." Retrieved October 02, 2013, from <http://www.edmunds.com/car-safety/protecting-pedestrians-through-vehicle-design.html>.
- Longhitano, D., B. Henary, K. Bhalla, J. Ivarsson and J. Crandall (2005) "Influence of Vehicle Body Type on Pedestrian Injury Distribution". SAE Technical Paper 2005-01-1876.
- LSTC Inc. (2014a). "LS-Dyna R7.1.1". Livermore, CA.
- LSTC Inc. (2014b). "LS-Prepost 4.2". Livermore, CA.
- Maeno, T. and J. Hasegawa (2001). "Development of a finite element model of the total human model for safety (THUMS) and application to car-pedestrian impacts". Enhanced Safety of Vehicles (ESV), Amsterdam, The Netherlands.

- Maki, T., T. Asai and J. Kajzer (2003b). "Development of future pedestrian protection technologies". Enhanced Safety of Vehicles (ESV), Nagoya, Japan.
- Maki, T., J. Kajzer, K. Mizuno and Y. Sekine (2003a) "Comparative analysis of vehicle-bicyclist and vehicle-pedestrian accidents in Japan". Accident Analysis and Prevention 35(6): 927-940.
- Mallory, A., R. Fredriksson, E. Rosén and B. Donnelly (2012) "Pedestrian Injuries By Source: Serious and Disabling Injuries in US and European Cases". Annals of Advances in Automotive Medicine 56: 13-24.
- Marieb, E. N. and K. Hoehn (2010). "Human Anatomy and Physiology". San Francisco, CA, USA, Pearson Benjamin Cummings.
- Marth, D. R. (2002) "Biomechanics of the shoulder in lateral impact" Ph.D. thesis, Wayne State University.
- Mathworks, T. (2012). "MATLAB R2012b". Natick, MA.
- Melvin, J. W. and K. Weber (1985) "Review of Biomechanical Impact Response and Injury in the Automotive Environment, Task B Final Report". National Highway Traffic Safety Administration, Washington, D.C., DOT HS 807 042
- Mertz, H. J. (1984) "A Procedure for Normalizing Impact Response Data".
- Mizuno, Y. (2003). "Summary of IHRA Pedestrian Safety WG Activities (2003) - Proposed Test Methods to Evaluate Pedestrian Protection Afforded by Passenger Cars". Enhanced Safety of Vehicles (ESV), Nagoya, Japan.
- Mizuno, Y. (2005). "Summary of IHRA Pedestrian Safety WG Activities (2005) - Proposed Test Methods to Evaluate Pedestrian Protection Afforded by Passenger Cars". International Technical Conference on the Enhanced Safety of Vehicles (ESV), Washington D.C., USA.
- Newman, J. A. (1985). "A Generalized Acceleration Model for Brain Injury Tolerance". Winterlude Head Injury Workshop. Ottawa.
- Newman, J. A. (1986). "A generalized acceleration model for brain injury threshold (GAMBIT)". International Research Council on the Biomechanics of Impact (IRCOBI), Zurich, Switzerland.
- Newman, J. A., C. Barr, M. Beusenberg, E. Fournier, N. Shewchenko, E. Welbourne and C. Withnall (2000). "A New Biomechanical Assessment of Mild Traumatic Brain Injury Part 2 - Results and Conclusions". International Research Council on the Biomechanics of Injury (IRCOBI), Montpellier, France.
- NHTSA. (2000). "Injury risk curves and protection reference values." Retrieved November 02, 2015, from <http://www.nhtsa.gov/cars/rules/rulings/80g/80gii.html>.
- Nusholtz, G. S., T. P. Hsu, M. A. Gracián Luna, L. Di Domenico and S. B. Kochekseraii (2010) "The Consequences of Average Curve Generation: Implications for Biomechanics Data". Stapp Car Crash Journal 54: 1-18, Paper No. 2010-2022-0001.
- OECD (1998) "Safety of vulnerable road users". Organisation for Economic Co-operation and Development (OECD), Scientific Expert Group on the Safety of Vulnerable Road Users (RS7),
- Olver, J. H., J. L. Ponsford and C. A. Curran (1996) "Outcome following traumatic brain injury: a comparison between 2 and 5 years after injury". Brain Injury 10(11): 841-848.
- Ommaya, A. K. (1995) "Head injury mechanisms and the concept of preventive management - a review and critical synthesis". Journal of Neurotrauma 12(4): 527-546.
- Ono, K., S. Ejima, K. Kaneoka, M. Fukushima, S. Yamada, S. Ujihashi and S. Compigne (2005). "Biomechanical responses of head / neck / torso to lateral impact loading on shoulders of male and female volunteers". International Research Council on the Biomechanics of Injury (IRCOBI), Prague, Czech Republic.

- Ono, K., A. Kikuchi, M. Nakamura and H. Kobayashi (1980). "Human Head Tolerance to Sagittal Impact Reliable Estimation Deduced from Experimental Head Injury Using Subhuman Primates and Human Cadaver Skulls". 24th Stapp Car Crash Conference, Troy, MI.
- Otte, D. (1999). "Severity and Mechanism of Head Impacts in Car to Pedestrian Accidents". International Research Council on the Biomechanics of Injury (IRCOBI), Sitges, Spain.
- Otte, D., C. Krettek, H. Brunner and H. Zwipp (2003). "Scientific Approach and Methodology of a New In-Depth-Investigation Study in Germany so called GIDAS". Enhanced Safety of Vehicles (ESV), Nagoya, Japan.
- Paas, R., J. Davidsson, C. Masson, U. Sander, K. Brolin and J. K. Yang (2012). "Pedestrian shoulder and spine kinematics in full-scale PMHS tests for human body model evaluation". International Research Council on the Biomechanics of Injury (IRCOBI), Dublin, Ireland.
- Paye, J. (2002). "Vehicle hood deployment device for pedestrian protection". US6439330 B1.
- Pearl, M. L., S. Jackins, S. B. Lippitt, J. A. Sidles and F. A. Matsen III (1992) "Humeroscapular positions in a shoulder range-of-motion-examination". Journal of Shoulder and Elbow Surgery 1(6): 296-305.
- PIPER. (2015). "The PIPER Project - Position and Personalize Advanced Human Body Models for Injury Prediction." Retrieved Sept. 04, 2015, from <http://www.piper-project.eu/>.
- Pipkorn, B., R. Fredriksson and J. Olsson (2007). "Bumper bag for SUV to passenger vehicle compatibility and pedestrian protection". Enhanced Safety of Vehicles (ESV), Lyon, France.
- Pipkorn, B. and K. Mroz (2009) "Validation of a Human Body Model for Frontal Crash and its Use for Chest Injury Prediction". SAE Int. J. Passeng. Cars - Mech. Syst. 1(1): 1094-1117.
- Plaga, J. A., C. Albery, M. Boehmer, C. Goodyear and G. Thomas (2005) "Design and Development of Anthropometrically Correct Head Forms for Joint Strike Fighter Ejection Seat Testing". Air Force Research Laboratory, Springfield, VA, AFRL-HE-WP-TR-2005-0044
- Poulard, D., D. Subit, J.-P. Donlon and R. W. Kent (2015) "Development of a computational framework to adjust the pre-impact spine posture of a whole-body model based on cadaver tests data". Journal of Biomechanics 48: 636-643.
- Poulard, D., D. Subit, J.-P. Donlon, D. J. Lessley, T. Kim, G. Park and R. W. Kent (2014) "The Contribution of Pre-impact Spine Posture on Human Body Model Response in Whole-body Side Impact". Stapp Car Crash Journal 58: 385-422.
- Pritz, H. B., E. B. Weis and J. T. Herridge (1975) "Body-vehicle interaction: experimental study, Volume I". National Highway Traffic Safety Administration (NHTSA), Washington, D.C., USA,
- Reed, M. P. and M. B. Parkinson (2008). "Modeling variability in torso shape for chair and seat design". ASME 2008 International Design Engineering Technical Conferences and Computers and Information in Engineering Conference, New York, USA.
- Rhule, H. H., M. R. Maltese, B. R. Donnelly, R. H. Eppinger, J. K. Brunner and J. H. Bolte (2002) "Development of a new biofidelity ranking system for anthropomorphic test devices". Stapp Car Crash Journal 46: 477-512.
- Rosén, E. and U. Sander (2009) "Pedestrian fatality risk as a function of car impact speed". Accident Analysis and Prevention 41: 536-542.
- Roudsari, B. S., C. N. Mock and R. Kaufman (2005) "An evaluation of the association between vehicle type and the source and severity of pedestrian injuries". Traffic Injury Prevention 6(2): 185-192.

- Rubin, G., K. Peleg, A. Givon and N. Rozen (2015) "Upper extremity fractures among hospitalized road traffic accident adults". *American Journal of Emergency Medicine* 33: 250-253.
- SAE (1994) "J1733 - Sign Convention for Vehicle Crash Testing. Issued DEC94". Society of Automotive Engineers, Inc. (SAE), Warrendale, PA,
- SAE J2868 (2010) "Pedestrian Dummy Full Scale Test Results and Resource Materials, Surface Vehicle Information Report J2868".
- Sahoo, D., C. Deck and R. Willinger (2014) "Development and validation of an advanced anisotropic visco-hyperelastic human brain FE model". *Journal of the Mechanical Behaviour of Biomedical Materials* 33: 24-42.
- Schroeder, G., K. Fukuyama, K. Yamazaki, K. Kamiji and T. Yasuki (2008). "Injury Mechanism of Pedestrians Impact Test with a Sport-Utility Vehicle and Mini-Van". International Research Council on the Biomechanics of Injury (IRCOBI), Bern, Switzerland.
- Schroeder, G., A. Konosu, H. Ishikawa and J. Kajzer (1999). "Verletzungsmechanismen des Fußgängers bei Kollisionen mit einer modernen Fahrzeugfront - eine experimentelle Studie". Kongressbericht der Deutschen Gesellschaft für Verkehrsmedizin e.V., Berlin.
- Schuster, P. J. (2006) "Current Trends in Bumper Design for Pedestrian Impact". SAE Technical Paper 2006-01-0464.
- Serre, T., C. Brunet, K. Bruyere, J. P. Verriest, D. Mitton, S. Bertrand and W. Skalli (2006) "HUMOS (Human Model for Safety) Geometry: From One Specimen to the 5th and 95th Percentile". SAE Technical Paper 2006-01-2324.
- Shi, X., L. Cao, M. P. Reed, J. D. Rupp and J. Hu (2015) "Effects of obesity on occupant responses in frontal crashes: a simulation analysis using human body models". *Computer Methods in Biomechanics and Biomedical Engineering* 18(12): 1280-1292.
- Shigeta, K., Y. Kitagawa and T. Yasuki (2009). "Development of next generation Human FE Model capable of Organ Injury Prediction". International Technical Conference on the Enhanced Safety of Vehicles (ESV), Stuttgart, Germany.
- Simms, C. and D. Wood (2009). "Pedestrian and Cyclist Impact - A Biomechanical Perspective". Dordrecht, Heidelberg, London, New York, Springer.
- Siram, S. M., V. Sonaike, O. B. Bolorunduro, W. R. Greene, S. Z. Gerald, D. C. Chang, E. E. r. Cornwell and T. A. Oyetunji (2011) "Does the Pattern of Injury in Elderly Pedestrian Trauma Mirror That of The Younger Pedestrian?". *Journal of Surgical Research* 167: 14-18.
- Sprague, M. A. and T. L. Geers (2004) "A spectral-element method for modelling cavitation in transient fluid-structure interaction". *International Journal of Numerical Methods in Engineering* 60(15): 2467-2499.
- Stenlund, T. C., R. Lundström, O. Lindroos, C. K. Häger, L. Burström, G. Neely and B. Rehn (2015) "Seated postural neck and trunk reactions to sideways perturbations with or without a cognitive task". *Journal of Electromyography and Kinesiology* 25(3): 548-556.
- Subit, D., S. Duprey, S. Lau, H. Guillemot, D. Lessley and R. Kent (2010) "Response of the Human Torso to Lateral and Oblique Constant-Velocity Impacts". *Ann Adv Automot Med (AAAM)* 54: 27-40.
- Subit, D., J. Kerrigan, J. Crandall, K. Fukuyama, K. Yamazaki, K. Kamiji and T. Yasuki (2008). "Pedestrian-Vehicle Interaction: Kinematics and Injury Analysis of Four Full-Scale Tests". International Research Council on the Biomechanics of Injury (IRCOBI), Bern, Switzerland.
- Sugimoto, T. and K. Yamazaki (2005). "First results from the JAMA human body model project". Enhanced Safety of Vehicles (ESV), Washington, D.C.

- Takhounts, E. G., M. J. Craig, K. M. Moorhouse, J. McFadden and V. Hasija (2013) "Development of Brain Injury Criteria (BrIC)". *Stapp Car Crash Journal* 57: 243-266.
- Takhounts, E. G., V. Hasija, S. A. Ridella, S. Rowson and S. M. Duma (2011). "Kinematic Rotational Brain Injury Criterion (BRIC)". Enhanced Safety of Vehicles (ESV), Washington, D.C.
- Thollon, L. (2001) "Modélisation du membre thoracique dans le cadre d'un choc latéral: Approche expérimentale et numérique" Ph.D. thesis, Université de la Méditerranée Aix-Marseille-II.
- Thollon, L., C. Jammes, M. Behr, P. J. Arnoux, C. Cavallero and C. Brunet (2007) "How to Decrease Pedestrian Injuries - Conceptual Evolutions Starting From 137 Crash Tests". *The Journal of Trauma - Injury, Infection, and Critical Care* 62(2): 512-519.
- Timmel, M., S. Kolling, P. Osterrieder and P. A. Du Bois (2007) "A finite element model for impact simulation with laminated glass". *International Journal of Impact Engineering* 34: 1465-1478.
- TMC (2011). "THUMS User Manual, AM50 Pedestrian/Occupant Model, Academic Version 4.0_20111003", TOYOTA MOTOR CORPORATION.
- Untario, C., J. Shin, J. Ivarsson, J. R. Crandall, D. Subit, Y. Takahashi, A. Akiyama and Y. Kikuchi (2008) "A study of the pedestrian impact kinematics using finite element dummy models: the corridors and dimensional analysis scaling of upper-body trajectories". *International Journal of Crashworthiness* 13(5): 469-478.
- Watanabe, R., T. Katsuhara, H. Miyazaki, Y. Kitagawa and T. Yasuki (2012) "Research of the Relationship of Pedestrian Injury to Collision Speed, Car-type, Impact Location and Pedestrian Sizes using Human FE model (THUMS Version 4)". *Stapp Car Crash J* 56 (October 2012): 269-321.
- Watanabe, R., H. Miyazaki, Y. Kitagawa and T. Yasuki (2011). "Research of Collision Speed Dependency of Pedestrian Head and Chest Injuries using Human FE Model (THUMS Version 4)". International Technical Conference on the Enhanced Safety of Vehicles (ESV), Washington, D.C.
- Vavalle, N. A., B. C. Jelen, D. P. Moreno, J. D. Stitzel and F. S. Gayzik (2013) "An Evaluation of Objective Rating Methods for Full-Body Finite Element Model Comparison to PMHS Tests". *Traffic Injury Prevention* 14(sup1): S87-S94.
- Versace, J. (1971). "A Review of the Severity Index". *Stapp Car Crash Conference*, Coronado, California.
- Vezen, P. and J. P. Verriest (2005). "Development of a set of numerical human models for safety". Enhanced Safety of Vehicles (ESV), Washington D.C.
- White, R. P., N. Rangarajan and M. Haffner (1996). "Development of the THOR advanced frontal crash test dummy". SAFE Association Annual Symposium.
- WHO (2006) "Road traffic injury prevention training manual, Unit 2: Risk factors for road traffic injuries". World Health Organisation, New Delhi, India,
- WHO (2013a) "Global Status Report on Road Safety 2013: Supporting a Decade of Action". World Health Organization (WHO), Geneva, Switzerland,
- WHO (2013b) "Pedestrian safety: a road safety manual for decision-makers and practitioners". World Health Organization (WHO), Geneva, Switzerland, ISBN: 978 92 4 150535 2
- Viano, D. C. (1989). "Biomechanical Responses and Injuries in Blunt Lateral Impact". *Stapp Car Crash Conference*, Washington, DC, SAE Technical Paper No. 892432.
- Wikimedia Commons. (2014). "File: Blausen_0019_AnatomicalDirectionalReferences.png." Retrieved July 8, 2015, from

- https://en.wikipedia.org/wiki/Anatomical_terms_of_location#/media/File:Blausen_0019_AnatomicalDirectionalReferences.png.
- Winckler, G. (1974). "Manuel d'anatomie topographique et fonctionnelle". Paris, France, Masson.
- Wismans, J., R. Happee and J. A. W. van Dommelen (2005). "Computational Human Body Models". IUTAM Symposium on Impact Biomechanics: From Fundamental Insights to Applications, Dublin, Ireland, Springer.
- Yanaoka, T., Y. Dokko and Y. Takahashi (2015) "Investigation on an Injury Criterion Related to Traumatic Brain Injury Primarily Induced by Head Rotation". SAE Technical Paper 2015-01-1439.
- Yanaoka, T., K. Torikai, M. Ikeda and Y. Takahashi (in press) "Investigation of the influence of the aligned height on the scaled whole body trajectories in car-to-pedestrian collisions". International Journal of Automotive Engineering.
- Yao, J. F., J. K. Yang and R. Fredriksson (2006) "Reconstruction of head-to-hood impact in an automobile-to-child-pedestrian collision". International Journal of Crashworthiness 11(4): 387-395.
- Yao, J. F., J. K. Yang and D. Otte (2008) "Investigation of head injuries by reconstructions of real-world vehicle-versus-adult-pedestrian accidents". Safety Science 46: 1103-1114.
- Yasuki, T. (2006) "Using THUMS for pedestrian safety simulations". ATZ Auto Technology 6(4): 44-47.
- Zhang, G., L. Cao, J. Hu and K. H. Yang (2008) "A field data analysis of risk factors affecting the injury risks in vehicle-to-pedestrian crashes". Annals of Advances in Automotive Medicine 52: 199-214.
- Zhao, Y., G. F. Rosala, I. F. Campean and A. J. Day (2010) "A response surface approach to front-car optimisation for minimising pedestrian head injury levels". International Journal of Crashworthiness 15(2): 143-150.
- Öman, M., R. Fredriksson, P.-O. Bylund and U. Björnstad (2015) "Analysis of the mechanism of injury in non-fatal vehicle-to-pedestrian and vehicle-to-bicyclist frontal crashes in Sweden". International Journal of Injury Control and Safety Promotion (in press).
- Östh, J., K. Brolin, S. Carlsson, J. Wismans and J. Davidsson (2012) "The Occupant Response to Autonomous Braking: A Modeling Approach That Accounts for Active Musculature". Traffic Injury Prevention 13(3): 265-277.

Appendix

Appendix A: Anatomy and Physiology

Here, human shoulder and spine anatomy and physiology are described. Understanding the motions of the joints involved is important for the interpretation of how upper body and arm responses influence the head kinematics in car–pedestrian crashes. Further insight into the motions of the shoulder and spine can be gained from functional biomechanics, but functional biomechanics will not be further discussed in this chapter.

Appendix A1: Shoulder Anatomy and Physiology

The human shoulder consists of three bones, the humerus or upper arm bone, the scapula or shoulder blade, and the clavicle or collarbone, as well as muscles, tendons and ligaments (Marieb and Hoehn 2010), see Figure A1. Five articulations contribute to the motion of the shoulder, three of which are anatomical joints and two of which are false, or physiological, joints.

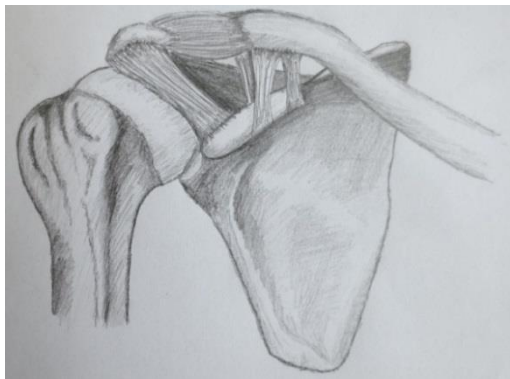


Figure A1: The bones of the shoulder, anterior view: humerus (left), clavicle (top/right) and scapula (mid/bottom). Including the glenohumeral capsule, the coracoacromial ligament (left ligament), the acromioclavicular ligament (top ligament), and the coracoclavicular ligament (right ligament in two parts, left: trapezoid, right: conoid). Image combined and redrawn from several sources (Bernstein 2003, Gray 2008, Marieb and Hoehn 2010)

The major anatomical joint in the shoulder is the glenohumeral joint which is a multiaxial synovial ball and socket joint connecting the humerus to the glenoid fossa of the scapula. This joint is commonly referred to as the shoulder joint. Due to limited interaction between bony surfaces, it is the most flexible joint in the body and allows for a major part of the upper arm range of motion (Marieb and Hoehn 2010). The acromioclavicular joint is the articulation between the acromion, i.e. a part of the scapula, and the clavicle. It is a gliding synovial joint, functioning as a pivot which allows for greater arm rotation. The third anatomical joint of the shoulder is the sternoclavicular joint which forms the articulation between clavicle and sternum. This synovial double-plane joint makes movement of the clavicle possible in three planes, enlarging the range of motion of the shoulder even more.

In addition to these three anatomical joints, two physiological joints are part of the pectoral girdle

and thus contribute to shoulder motion. The suprhumeral joint is an articulation of the head of the humerus and the coracoacromial ligament, supporting the glenohumeral joint in providing a greater range of motion. The scapulothoracic joint is the articulation between the anterior face of the scapula and the posterior rib cage where muscles and tendons allow the scapula to slide over the rib cage and thus allow one rotational and two translational degrees of freedom of scapular motion.

These five articulations combine to form the human joint with the largest range of motion and also the most complex joint in the human body (Marieb and Hoehn 2010). Measuring the range of motion of single articulations of the shoulder has been attempted several times in the past (e.g., Pearl et al. 1992, Kebaetse et al. 1999), but has proven to be difficult since various articulations contribute to each movement. The overall response of the shoulder to direct impact has been studied in various previous publications (Section 1.5.2). However, the author has not found any evidence that the mechanism of energy transfer through the shoulder into the upper torso and spine has been studied in detail.

Appendix A2: Spine Anatomy and Physiology

The human spine normally consists of 24 vertebrae which form the articulations of the spinal column, and of two bones in the lower part, the sacrum and the coccyx (Marieb and Hoehn 2010). The upper seven vertebrae (C1-C7) form the cervical spine. C1 (also called atlas) and C2 (also called axis) contribute to the head's range of motion to a large extent. The atlanto-occipital joint allows a nodding kind of motion whereas the atlanto-axial joint allows rotating the head to the left and the right (Marieb and Hoehn 2010). The other cervical vertebrae (C3-C7) allow for flexion, extension, lateral flexion and rotation of the neck. Below the cervical vertebrae there are twelve thoracic vertebrae (T1-T12) which all connect to the ribs. This section of the spine enables rotation in the thoracic region plus a limited amount of lateral flexion, limited by the ribs, and limited flexion and extension. Further down there are five lumbar vertebrae (L1-L5) which carry the most weight of all vertebrae and are therefore larger and with a more robust structure. The lumbar spine allows for flexion and extension as well as a limited amount of lateral flexion, but rotation is prevented (Marieb and Hoehn 2010). The sacrum itself does not contribute to the spinal range of motion although limited motion might be possible in the articulation between the sacrum and L5. The sacrum is laterally connected to the pelvic girdle. While all humans have the same number of cervical vertebrae, the number of vertebrae in other regions varies in about 5% of the population (Marieb and Hoehn 2010). In an average adult, the vertebral column has a length of about 70 cm. From a lateral perspective, the spine describes an S shape with posteriorly concave parts in the cervical and lumbar sections and posteriorly convex parts in the thoracic and sacral sections. From an anterior perspective, the spine in healthy humans is generally straight.

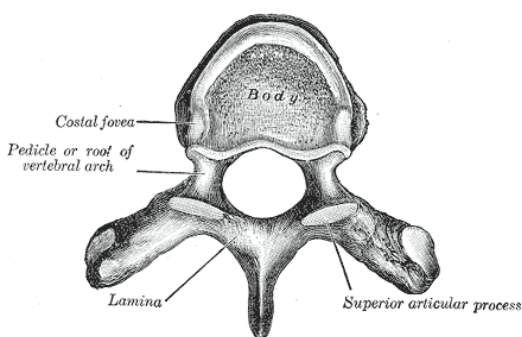


Figure A2: A typical thoracic vertebra from a superior perspective; the anterior side of the vertebra is at the top of the picture (adapted from Gray 2008).

Typical vertebrae (Figure A2) consist of an oval body at the anterior side, a vertebral arch to which the transverse processes, the articular facets, and the spinous process are attached at the posterior side, and the vertebral foramen, a hole in the vertebrae where the spinal cord is situated and which is mostly triangular for the cervical and lumbar vertebrae but rather circular for the thoracic vertebrae (Figure A2). All articulate vertebrae, apart from between the atlas and the axis, have intervertebral discs between them. They consist of an inner nucleus pulposus providing the disk with elasticity and compressibility and thus

contributing to the spine range of motion, and the collagenous annulus fibrosus on the outside, providing stability to the disk.

Appendix B: Crash Test Dummies and Impactors

Pedestrian crash test dummies have been in continuous development for several decades. Honda developed the Polar-II and the updated version, Polar-III (Akiyama et al. 1999, Akiyama et al. 2001), based on the frontal crash test dummy Thor (White et al. 1996). In addition, a pedestrian version of the Hybrid II and the updated version Hybrid III (Humanetics Innovative Solutions 2013) have been developed. Together with HBMs (Section 1.7) and PMHSs (Section 1.5.1), crash test dummies are to date the only available tools for evaluating passive safety systems in full-body testing prior to entering the market. However, designing a robust dummy strong enough to tolerate severe impacts without breaking may be a goal conflicting with the goal of developing a biofidelic dummy. Pedestrian trajectories in PMHS experiments generally display a considerable amount of spread (Ashton et al. 1983) which presents a problem in the evaluation process of passive safety systems. Therefore, pedestrian crash test dummies are designed to facilitate repeatable trajectories although pedestrian dummies that are too simplified will most likely not predict biofidelic trajectories or realistic head impact conditions (Akiyama et al. 2001). This issue of over-simplification became apparent in non-biofidelic kinematic results of early simplified pedestrian dummies (Simms and Wood 2009). Later versions of the pedestrian crash test dummies, such as the Polar II, were more comparable with the PMHS experiments (Kerrigan et al. 2005b) while the head trajectory remained to be addressed in more detail (see also Section 1.5.1). Nevertheless, physical full-scale pedestrian testing with standardized subjects and a real vehicle is considered a valuable complement to numerical simulations.

Subsystem impactors have been developed to simplify testing and increase test result repeatability. Current pedestrian Euro-NCAP safety assessments include using adult and child headform, upper legform and legform impactors to assess car front ends (Euro NCAP 2014a). While repeatable results are an obvious goal especially in regulatory testing, a number of shortcomings have been identified regarding subsystem impactors. Pedestrian Euro-NCAP tests are based on relatively simple boundary conditions. The adult head impactor, for example, impacts several points on the vehicle at only one impact speed (11.1 m/s) and one angle (65° to ground level). These boundary conditions do not cover a wide range of potential head impact conditions, whereas head impact velocities and angles vary in PMHS experiments (Kerrigan et al. 2008) and full-body simulations (Elliott et al. 2012b). The sensors used in the head impactors measure 3-dimensional force/acceleration in the head impactor centre of gravity (Euro NCAP 2014a). To date, head rotation, neck load, or spine curvature are not assessed although they all pose a pedestrian injury risk (Section 1.4). Thus, while regulative testing provides necessary motivation towards improved pedestrian safety, the usage of impactors might not address all of the safety issues present in real-life accidents.

Appendix C: Three-Dimensional Rotations

The three-dimensional angular displacements in Papers I, II and IV are presented as successive Euler angles, or strictly speaking, as Tait-Bryan-angles with the order conventions z-y'-x" (Paper I) and x-y'-z" (Papers II and IV). E.g., the order convention x-y'-z" means that rotations

are first carried out about the global x-axis, then about the new y-axis, then about the newest z-axis.

In the experiments in Papers I and II, the Euler angles were calculated automatically by the video analysis software. In the simulations in Paper IV, the Euler angles were calculated as follows: Prior to the simulation, four extra nodes were defined for each body part which rotated with that body part. These nodes formed a rigid body and were tracked throughout the simulation. From the position of each node over time, the overall translation of the rigid body was first removed. Then, for each time step, a rotation matrix R was calculated (Eq. C1).

$$\begin{aligned} & \begin{bmatrix} n_{1,x}(t) & n_{2,x}(t) & n_{3,x}(t) & n_{4,x}(t) \\ n_{1,y}(t) & n_{2,y}(t) & n_{3,y}(t) & n_{4,y}(t) \\ n_{1,z}(t) & n_{2,z}(t) & n_{3,z}(t) & n_{4,z}(t) \end{bmatrix} \\ &= R(t) \cdot \begin{bmatrix} n_{1,x}(0) & n_{2,x}(0) & n_{3,x}(0) & n_{4,x}(0) \\ n_{1,y}(0) & n_{2,y}(0) & n_{3,y}(0) & n_{4,y}(0) \\ n_{1,z}(0) & n_{2,z}(0) & n_{3,z}(0) & n_{4,z}(0) \end{bmatrix} \end{aligned} \quad (\text{C1})$$

where n_{ij} are the three-dimensional coordinates of the four nodes after subtracting the overall translation of the rigid body. For the order convention x-y'-z'', the rotation matrix R takes the form of Eq. C2 (Goldstein 2000).

$$R(t) = \begin{bmatrix} c_2 c_3 & -c_2 s_3 & s_2 \\ c_1 s_3 + s_1 s_2 c_3 & c_1 c_3 - s_1 s_2 s_3 & -s_1 c_2 \\ s_1 s_3 - c_1 s_2 c_3 & s_1 c_3 + c_1 s_2 s_3 & c_1 c_2 \end{bmatrix} \quad (\text{C2})$$

where s represents sine, c represents cosine, and the indices 1, 2, 3 represent the Euler angles α, β, γ about the axes x, y, z, respectively. Thus, s_1 represents $\sin(\alpha)$, c_2 represents $\cos(\beta)$ and so on. From the elements of the rotation matrix, the Euler angles can easily be calculated. Gimbal lock occurs when the solution to C1 is not unique, i.e., when $\sin(\beta) = 0$. This was checked throughout all calculations and did not occur.

To obtain angular velocities $\omega_x, \omega_y, \omega_z$, the rotation matrix must be differentiated according to Eq. C3 (Baker 2006).

$$\omega(t) = \begin{bmatrix} 0 & -\omega_z & \omega_y \\ \omega_z & 0 & -\omega_x \\ -\omega_y & \omega_x & 0 \end{bmatrix} = \frac{dR}{dt} R^T \quad (\text{C3})$$

Appendix D: Head Injury Criteria and their Injury Risk Curves

Several injury criteria are available for the head. Generally, injury criteria can be divided into global and local criteria. Both use a measurable variable to calculate a value which can be used to determine the risk of injury. For global head injury criteria, the measurable variables used to date are time histories of linear and angular accelerations as well as time histories of linear and angular velocities. This section provides an overview over the global head injury criteria available to date.

Appendix D1: HIC

The criterion most commonly used for the head in pedestrian safety to date is the Head Injury Criterion (HIC) which is a global criterion (Versace 1971). The HIC is the only head injury criterion used in the Euro-NCAP consumer rating to date (Euro NCAP 2014a). It is calculated from linear acceleration a , measured in multiples of gravity, and duration $t_2 - t_1$ (Eq. D1). Currently, HIC_{15} with a time interval of 15 ms and HIC_{36} with an interval of 36 ms are used with skull fracture probabilities of 31% at $HIC_{15} = 700$ and 48% at $HIC_{36} = 1000$ (Eppinger et al. 1999). Rotation and directional effects are not considered in the HIC.

$$HIC = \left\{ \left(\frac{1}{t_2 - t_1} \int_{t_1}^{t_2} a(t) dt \right)^{2.5} (t_2 - t_1) \right\}_{max} \quad (D1)$$

The AIS2+ head injury risk based on HIC is then given by Eq. D2 (NHTSA 2000).

$$p(MAIS2) = \frac{1}{1 + e^{2.49 + \frac{200}{HIC} - 0.00483 \cdot HIC}} \quad (D2)$$

Appendix D2: RIC

The Rotational Injury Criterion RIC (Eq. D3) was developed based on a brain finite element (FE) model where local injury criteria were correlated with the proposed RIC (Kimpara and Iwamoto 2012). RIC was evaluated over a time period of 36 ms and the proposed threshold was 10 300 000 for RIC_{36} . While RIC appeared to predict mild TBI, it does not take into account possible directional effects. RIC does not take into account linear accelerations. For a complete analysis of head injuries, the criterion should therefore be combined with a criterion that takes linear acceleration into account, such as the HIC.

$$RIC_{36} = \left\{ \left(\frac{1}{t_2 - t_1} \int_{t_1}^{t_2} \alpha(t) dt \right)^{2.5} (t_2 - t_1) \right\}_{max} \quad (D3)$$

where α is resultant angular acceleration in rad/s^2 , and $t_2 - t_1 = 36 \text{ ms}$.

The AIS2+ head injury risk based on GAMBIT is then given by Eq. D4 (Kimpara and Iwamoto 2012).

$$p(MAIS2) = \frac{1}{1 + e^{7.036 - 0.000000679 \left(\frac{s^{6.5}}{\text{rad}^{2.5}} \right) \cdot RIC}} \quad (D4)$$

Appendix D3: GAMBIT

The generalized acceleration model for brain injury threshold (GAMBIT) was first proposed by Newman (1985) and later revised by Newman (1986) with GAMBIT = 1 corresponding to a 50% risk of AIS 3+ head injuries (Eq. D5). The development was based on experimental monkey head kinematics and trauma as well as on PMHS head impacts. GAMBIT was later revised to Eq. (6). Directional effects and time dependency were proposed but not taken into account since the data available at the time was not detailed enough for developing thresholds for directional and time dependencies.

$$GAMBIT_{rev} = \frac{a_{max}}{250g} + \frac{\alpha_{max}}{10000 \frac{rad}{s^2}} \quad (D5)$$

where a is resultant linear acceleration and α is resultant angular acceleration.

The AIS2+ head injury risk based on GAMBIT is then given by Eq. D6 (Newman et al. 2000).

$$p(MAIS2) = \frac{1}{1 + e^{6.777 - 17.26 \cdot GAMBIT}} \quad (D6)$$

Appendix D4: HIP

The head impact power (HIP) was developed from reconstructions of helmeted head impacts with Hybrid-III dummies (Newman et al. 2000). Directional linear and directional angular effects as well as durations are taken into account (Eq. D7), where a HIP of 12.5 kW corresponds to a risk for concussion of 50%.

$$HIP = \sum_{i=1}^3 m a_i \int a_i dt + \sum_{i=1}^3 I_{ii} \alpha_i \int \alpha_i dt \quad (D7)$$

where a_i is the linear acceleration in direction i , α_i is resultant angular acceleration in direction i , I_{ii} is the ii -th component of the inertial tensor of a Hybrid-III headform, m is the mass of a Hybrid-III headform, and $t_2 - t_1 = 36$ ms. The values for the Hybrid-III headform are given as $m = 4.5$ kg, $I_{xx} = 0.016$ Nms 2 , $I_{yy} = 0.024$ Nms 2 , and $I_{zz} = 0.022$ Nms 2 .

The AIS2+ head injury risk based on HIP is then given by Eq. D8 (Newman et al. 2000).

$$p(MAIS2) = \frac{1}{1 + e^{4.682 - 0.0003655 \frac{1}{W} HIP}} \quad (D8)$$

Appendix D5: BrIC

The brain rotational injury criterion (BrIC, Eq. D9) was developed mainly for rotational loading (Takhounts et al. 2011, Takhounts et al. 2013). The authors therefore recommended combining BrIC with HIC. Further, they stated that the criterion was derived from diffuse axonal injury (DAI) and may not be directly applicable to other types of head or brain injuries. Time dependency was not included. In the development of the BrIC, data from FE simulations, animal testing and

football concussion injuries were combined. The critical values for three-dimensional angular velocities were chosen such that a BrIC value of 1.0 corresponded to a risk of 50% for AIS4+ brain injury. Based on critical values derived from CSDM and maximum principal strain (MPS), the suggested angular velocity thresholds $\omega_{i,crit}$ were $\omega_{x,crit} = 66.25$ rad/s, $\omega_{y,crit} = 56.45$ rad/s and $\omega_{z,crit} = 42.87$ rad/s.

$$BrIC = \sqrt{\left(\frac{\omega_x}{\omega_{x,crit}}\right)^2 + \left(\frac{\omega_y}{\omega_{y,crit}}\right)^2 + \left(\frac{\omega_z}{\omega_{z,crit}}\right)^2} \quad (D9)$$

The AIS2+ head injury risk based on BrIC is then given by Eq. D10 for the MPS-based development and Eq. D11 for the CSDM-based development (Takhounts et al. 2013).

$$p_{BrIC,MPS}(MAIS2) = 1 - \frac{1}{e^{\left(\frac{BrIC}{0.602}\right)^{2.84}}} \quad (D10)$$

$$p_{BrIC,CSDM}(MAIS2) = 1 - \frac{1}{e^{\left(\frac{BrIC - 0.523}{0.324}\right)^{1.8}}} \quad (D11)$$

Appendix D6: BITS and RVCi

Recently, the Brain Injury Threshold Surface (BITS, Eq. D12) has been proposed as another criterion combining linear acceleration, angular velocity and time (Antona-Makoshi et al. 2015). The BITS was developed based on monkey head trauma experiments which were simulated with a monkey head-neck FE model. Scaling the critical thresholds from monkeys to humans was still on-going at the time this thesis was submitted.

$$BITS = \left(\frac{\alpha}{a_{crit}}\right)^2 + \left(\frac{\alpha}{\alpha_{crit}}\right)^2 - \left(\frac{\Delta t_{crit}}{\Delta t}\right)^2 \quad (D12)$$

Also recently, the Rotational Velocity Change Index (RVCi, Eq. D13) was developed with the aim to establish good correlation with the tissue-level criteria MPS and CSDM for both occupant and pedestrian impacts (Yanaoka et al. 2015). The maximum time difference $t_1 - t_2$ needed for the calculation of the RVCi was derived from maximising the correlation between RVCi and the tissue-level criteria for each of their simulations separately. Thus, to date, RVCi cannot be calculated from global measurements only.

$$RVCi = \sqrt{R_x \left(\int_{t_1}^{t_2} a_x dt \right)^2 + R_y \left(\int_{t_1}^{t_2} a_y dt \right)^2 + R_z \left(\int_{t_1}^{t_2} a_z dt \right)^2} \quad (D13)$$

Appendix E: Additional Results from the Addendum

In this section head impact velocities in the vehicle–THUMS simulations (Table E1) as well as head injury criteria from the vehicle–THUMS (Table E2) and impactor–vehicle (Table E3) simulations are presented.

Table E1: Head impact velocities in the vehicle–THUMS simulations. RLF: right (ipsilateral) leg forward, LLF: left (contralateral) leg forward.

THUMS head impact vel. (m/s)	AM50, 40 km/h	AM95, 40 km/h	AF05, 40 km/h	AM50, 30 km/h	AM95, 30 km/h	AF05, 30 km/h
RLF	11.5	11.8	9.8	8.0	8.4	9.4
LLF	11.0	11.9	8.4	8.6	N/A	9.8

Table E2: Head injury criteria in the vehicle–THUMS simulations. AM50/AM95/AF05: THUMS sizes, RLF: right (ipsilateral) leg forward, LLF: left (contralateral) leg forward, 40/30: car speed (km/h).

Vehicle– THUMS	HIC ₁₅ (g ^{2.5} *s)	HIC ₃₆ (g ^{2.5} *s)	BrIC (di- mensionless)	GAMBIT (dimen- sionless)	HIP (kW)	RIC ₃₆ $10^6 \cdot (\text{rad/s}^2)^{2.5} \cdot \text{s}$
AM50RLF40	926	1343	0.994	1.538	106	30.4
AM50LLF40	886	1332	1.101	1.417	83	44.7
AM95RLF40	480	618	0.800	0.771	33	10.1
AM95LLF40	507	750	0.860	0.690	31	16.4
AF05RLF40	2198	1558	1.555	2.787	145	166.8
AF05LLF40	2761	1744	1.631	3.322	180	198.6
AM50RLF30	514	634	0.828	0.446	22	6.9
AM50LLF30	426	567	0.864	0.407	28	8.4
AM95RLF30	179	364	0.471	0.471	18	2.8
AM95LLF30	239	355	0.728	0.396	15	3.1
AF05RLF30	763	799	0.718	0.718	43	47.0
AF05LLF30	878	873	0.892	0.892	54	42.4

Table E3: Head injury criteria in the impactor–vehicle simulations. Impact locations according to head impact in the THUMS simulations, impactor velocities according to car velocities in THUMS simulations.

Impactor– Vehicle	HIC ₁₅ (g ^{2.5*} s)	HIC ₃₆ (g ^{2.5*} s)	BrIC (di- mensionless)	GAMBIT (dimen- sionless)	HIP (kW)	RIC ₃₆ $10^6*(\text{rad}/\text{s}^2)^{2.5}*s$
AM50RLF40	965	462	0.269	1.007	38	2.7
AM50LLF40	764	379	0.242	1.025	32	2.2
AM95RLF40	800	890	0.380	0.592	32	3.5
AM95LLF40	791	688	0.365	0.567	36	2.1
AF05RLF40	2750	1589	0.541	1.089	60	6.1
AF05LLF40	2662	1543	0.573	1.339	70	7.4
AM50RLF30	1222	1417	0.506	0.781	54	2.6
AM50LLF30	933	827	0.383	0.729	35	2.6
AM95RLF30	383	192	0.232	0.439	13	1.0
AM95LLF30	360	237	0.243	0.415	11	1.4
AF05RLF30	1302	1054	0.416	0.789	43	3.6
AF05LLF30	1124	884	0.416	0.826	40	2.7

Appendix F: Initial Neck Lateral Bending away from the Vehicle

All PMHSs in Papers I and II as well as in Forman et al. (2015a) displayed neck lateral bending away from the vehicle shortly after pelvis impact. Since PMHSs lack active muscles, their neck lateral bending stiffness might be lower than for living pedestrians. In THUMS, this initial neck lateral bending was not observed. Therefore, in this section, a recent volunteer study using low-severity perturbations at pelvis level was compared with the PMHS and the THUMS responses.

Stenlund et al. (2015) exposed 20 healthy, young, male volunteers to lateral accelerations from the right side at two severity levels while restrained to a flat chair without a backrest. When assessing upper torso and head kinematics, their test setup can be considered comparable to full-scale pedestrian testing in the time period between pelvis–vehicle and arm–vehicle impact since the upper torso and head kinematics are largely governed by inertia. However, their experiment was at low severity compared with a PMHS pedestrian test at a 40 km/h car speed. Stenlund et al. (2015) found that the neck initially flexed to the left, i.e., away from the perturbation. In the initial stages of the high severity acceleration (peak 13.2 m/s², duration 0.8 s), the head rotated to the left up to a mean maximum of 1°±1°, although this movement was not observed in all of their volunteers. Head rotation to the left was greater in high severity acceleration than in low severity acceleration (peak 5.1 m/s², duration 1.2 s). Lower spine bending was to the left from the beginning of the acceleration whereas the upper spine and head lagged behind and caught up only gradually. Qualitatively, between pelvis–vehicle and arm–vehicle contact, the spine and head kinematics of the average volunteer in their study compare well with the PMHS full-scale pedestrian spine and head kinematics. Quantitatively, the pedestrian PMHSs displayed greater maximum head rotation (8–20°) away from the vehicle in the initial stages than what the volunteers experienced in rotations away from the perturbation in the high severity setup. This

divergence might be partly due to the lack of muscle activation in the PMHSs. However, for the volunteers, the chair moved only 24 cm. Thus, the severity was much lower than in a vehicle–pedestrian pelvis impact at 40 km/h. As the amount of head rotation increased with increasing severity in the volunteer experiments, a living pedestrian might display considerable head rotation away from the vehicle in the initial stages of the crash.

Paper I

Paas R, Davidsson J, Masson C, Sander U, Brolin K, Yang JK (2012) *Pedestrian Shoulder and Spine Kinematics in Full-Scale PMHS Tests for Human Body Model Evaluation*. Proceedings of IRCOBI Conference, Dublin, Ireland, pp. 730-750.

Paper II

Paas R, Masson C, Davidsson J (2015) Head boundary conditions in pedestrian crashes with passenger cars: six-degrees-of-freedom post-mortem human subject responses, *International Journal of Crashworthiness*, 20:6, 547-559.

Paper III

Paas R, Davidsson J, Brolin K (2015) Head Kinematics and Shoulder Biomechanics in Shoulder Impacts Similar to Pedestrian Crashes—A THUMS Study. *Traffic Injury Prevention*, 16:5, 498-506.

Paper IV

Paas R, Östh J, Davidsson J *Which Pragmatic Finite Element Human Body Model Scaling Technique Can Most Accurately Predict Head Impact Conditions in Pedestrian–Car Crashes?* Proceedings of IRCOBI conference 2015, Lyon, France.